Hemodynamics in the Thoracic Aorta using OpenFOAM: 4D PCMRI versus CFD

J. Casacuberta
E. Soudah
P. J. Gamez-Montero
G. Raush
R. Castilla
J.S. Perez

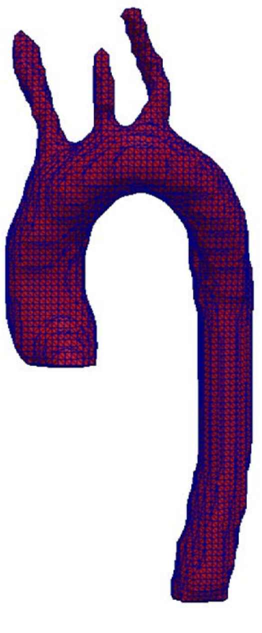

Monograph CIMNE Nº-154, March 2015

Hemodynamics in the Thoracic Aorta using OpenFOAM: 4D PCMRI versus CFD

J. Casacuberta[1]
E. Soudah[2]
P. J. Gamez-Montero[1]
G. Raush[1]
R. Castilla[1]
J.S. Pérez[2]

1. School of Industrial and Aeronautic Engineering of Terrassa. Department of Fluid Mechanics, LABSON, Universitat Politècnica de Catalunya, Campus Terrassa, Terrassa, Spain
2. International Center for Numerical Methods in Engineering (CIMNE)
Computational Engineering Group, Universitat Politècnica de Catalunya, Barcelona, Spain

Monograph CIMNE Nº-154, March 2015

International Center for Numerical Methods in Engineering
Gran Capitán s/n, 08034 Barcelona, Spain

INTERNATIONAL CENTER FOR NUMERICAL METHODS IN ENGINEERING
Edificio C1, Campus Norte UPC
Gran Capitán s/n
08034 Barcelona, Spain
www.cimne.com

First edition: March 2015

HEMODYNAMICS IN THE THORACIC AORTA USING OPENFOAM: 4D PCMRI versus CFD
Monograph CIMNE M154
© Los autores

ISBN: 978-84-943928-0-1
Depósito legal: B-9283-2015

Content

1. Introduction

1.1 Aim of the work

The aim of this work is the study of fluid dynamics models using the CFD software OpenFOAM, an open source software allowing meshing, manipulation, simulation and post-processing of many problems involving fluid mechanics.

The work consists of a study with OpenFOAM of a real engineering problem, namely to analyze hemodynamics in the thoracic aorta in collaboration with CIMNE (Centre Internacional de Mdes Numcs en Enginyeria) and LABSON-UPC (Laboratorio de Sistemas Oleohidricos y Neumcos). Specifically, the study aims to compute the shear stress that blood causes to aorta walls.

1.2 Justification of the work

OpenFOAM allows operation and manipulation of fields, and, more specifically, fluid fields. As an open source software, OpenFOAM offers users complete freedom to customize and extend its existing functionality. However, there does not exist any freely available official document with examples for the main utilities and explanations of how to deal with the great amount of possibilities that OpenFOAM can offer. The users guide provided by OpenFOAM contains information about the main controls and solvers, but without showing clear cases allowing users to understand how to set them. By way of example, the OpenFOAM users guide enumerates the resolution codes that exist to simulate a flow depending on its nature (incompressible laminar, incompressible turbulent) but it does not show how to program them. Users have to use examples done by others in order to configure their own cases and take profit of the OpenFOAM forums created by the community.

This makes it difficult for beginners to introduce themselves to the software, understand its controls, and figure out how to set cases properly depending on their nature. Consequently, the guide developed in this work is conceived to show clear-cut examples of representative cases, help understanding how to program the required steps, and present useful tools for pre-processing, resolution and post-processing. As the author has recently been introduced to OpenFOAM himself, in the appendix section will count with the point of view of a fresh beginner, thus reflecting his understanding of what kind of problems arise in the first steps of an OpenFOAM user and how to deal with them. This section pretends to become a starting point for new learners.

The aorta is the main artery in the human body, distributing blood directly from the heart. As a consequence, there is much medical interest in understanding the dynamics of blood passing through it. The increasing amount of available techniques and CFD software allows enhanced treatment and simulation, attempting to analyze the influence of hemodynamics on medical diseases.

CIMNE has carried out studies with medical images obtained from patients by magnetic resonance techniques. However, it is necessary to validate their data, as well as to determine how noise affects measurements. The study with OpenFOAM will provide contrast data. Comparison between real measures and numerical simulation will offer an interesting approach and relevant conclusions.

The main goal of the study is to determine the shear stress that blood causes to aorta walls. This is a direct factor in the accumulation of atheroma plates in vessels, which may cause detachments and therefore embolism. Since it is very difficult to obtain wall shear stress values experimentally, CFD analysis will contribute to its assessment, and therefore to a better understanding of the human body.

1.3 Scope of the work

- Simulate the hemodynamics of blood in a real aorta geometry
- Obtain with OpenFOAM an accurate distribution of the wall shear stress that blood causes to aorta walls
- Compare and contrast medical images with OpenFOAM simulations

1.4 Requirements of the work

- Simulate blood flow through a real aorta geometry in steady state conditions
- Simulate the most critical conditions regarding wall shear stress during a cardiac cycle (peak systolic conditions)

- Consider blood as an incompressible Newtonian fluid
- Consider a static aorta geometry with rigid and blood-impermeable walls
- Consider laminar flow conditions
- Use a real aorta geometry, including the three supra-aortic branches but without the coronary arteries

1.5 Objectives

The main objectives are to:

Solve with OpenFOAM the fluid dynamics in a real aorta geometry

Compute accurately wall shear stress caused by blood to aorta walls using OpenFOAM and its meshing tool (*snappyHexMesh*)

Determine interesting flow variables from the point of view of medical analysis

Compare OpenFOAM results with real medical images, especially focusing on their wall shear stress distribution

2. Theoretical foundations

2.1 About fluid mechanics

The main ideas used to introduce the fluid mechanics field in this project are extracted from [1], a very useful article explaining the evolution with time of fluid mechanics.

The art of fluid mechanics arguably has its roots in prehistoric times when streamlined spears, sicke-shaped boomerangs and fin-stabilized arrows evolved empirically. The Greek mathematician Archimedes (287–212 BC) provided an exact solution to the fluid-at-rest problem, long before calculus or the modern laws of mechanics were known. Leonardo da Vinci (1452–1519) correctly deduced the conservation of mass equation for incompressible, one-dimensional flows and also pioneered flow visualization. Little more than a century and half after Newton's *Principia Mathematica* was published in 1687, the first principles of viscous fluid flows were affirmed in the form of the Navier-Stokes equations. With very few exceptions, the Navier-Stokes equations provide an excellent model for both laminar and turbulent flows.

Each of the fundamental laws of fluid mechanics, conservation of mass, momentum and energy, are presented next. At every point in space-time and in Cartesian tensor notation, the three conservation laws read as follows:

$$\frac{\partial \rho}{\partial t} + \frac{\partial}{\partial x_k}(\rho u_k) = 0 \tag{2.1}$$

$$\rho\left(\frac{\partial u_i}{\partial t} + u_k \frac{\partial u_i}{\partial x_k}\right) = \frac{\partial \sum k_i}{\partial x_k} + \rho g_i \tag{2.2}$$

$$\rho\left(\frac{\partial e}{\partial t} + u_k \frac{\partial e}{\partial x_k}\right) = -\frac{q_k}{\partial x_i} + \sum k_i \frac{\partial u_i}{\partial x_k} \tag{2.3}$$

where ρ is the fluid density, u_k is an instantaneous velocity component $(u,\ v,\ w)$, $\sum k_i$ is the second order stress tensor (surface force per unit area), g_i is the body force per unit mass, e is the internal energy per unit mass, and q_k is the sum of heat flux vectors due to conduction and radiation. The independent variables are time t and the three spatial variables x, y and z.

The fundamental laws of fluid mechanics are listed in their *raw form*, i.e., assuming only that the speeds involved are non-relativistic and that the fluid is continuum. The latter assumption implies that the derivatives of all the dependent variables exist in some reasonable sense. In other words, local properties such as density and velocity are defined as averages over elements large compared with the microscopic structure of the fluid but small enough in comparison with the scale of the macroscopic phenomena to permit the use of differential calculus to describe them.

Equations 2.1, 2.2 and 2.3 constitute five differential equations for the 17 unknowns ρ, u_i, $\sum k_i$, e and q_k. Absent any body couples, the stress tensor is symmetric having only six independent components, which reduces the number of unknowns to 14. To close the conservation equations, relation between the stress tensor and deformation rate, relation between the heat flux vector and the temperature field, and appropriate equations of state, relating the different thermodynamic properties are needed. For a Newtonian, isotropic, Fourier, ideal gas, for example, these relations read:

$$\sum k_i = -p\delta_{ki} + \mu\left(\frac{\partial u_i}{\partial x_k} + \frac{\partial u_k}{\partial x_i}\right) + \lambda\left(\frac{\partial u_j}{\partial x_j}\right)\delta_{ki} \tag{2.4}$$

$$q_i = -\kappa\frac{\partial T}{\partial x_i} + \text{Heat flux due to radiation} \tag{2.5}$$

$$de = c_v dT \quad \text{and} \quad p = \rho R T \tag{2.6}$$

where p is the thermodynamic pressure, μ and λ are the first and second coefficient of viscosity, respectively, δ_{ki} is the unit second-order tensor (Kronecker delta), κ is the thermal conductivity, T is the temperature field, c_v is the specific heat at constant volume, and R is the gas constant. Newtonian implies a linear relation between the stress tensor and the symmetric part of the deformation tensor. The isotropy assumption reduces the 81 constants of proportionality in that linear relation to 2 constants.

The Stokes' hypothesis relates the first and second coefficients of viscosity, $\lambda + \frac{2}{3}\mu = 0$. With the above constitutive relations and neglecting the radiative heat transfer, Equations 2.1, 2.2 and 2.3 respectively read:

$$\frac{\partial \rho}{\partial t} + \frac{\partial}{\partial x_k}(\rho u_k) = 0 \tag{2.7}$$

$$\rho\left(\frac{\partial u_i}{\partial t}+u_k\frac{\partial u_i}{\partial x_k}\right)=-\frac{\partial p}{\partial x_i}+\rho g_i+\frac{\partial}{\partial x_x}\left[\mu\left(\frac{\partial u_i}{\partial x_k}+\frac{\partial u_k}{\partial x_i}\right)+\delta_{ki}\lambda\frac{\partial u_j}{\partial x_j}\right] \tag{2.8}$$

$$\rho c_v\left(\frac{\partial T}{\partial t}+u_k\frac{\partial T}{\partial x_k}\right)=\frac{\partial}{\partial x_k}\left(\kappa\frac{\partial T}{\partial x_k}\right)-p\frac{\partial u_k}{\partial x_k}+\phi \tag{2.9}$$

The three components of the vector equation 2.8 are the Navier-Stokes equations expressing the conservation of momentum for a Newtonian fluid. In the thermal energy Equation 2.9, ϕ is the dissipation function and is always positive. For a Newtonian, isotropic fluid, the viscous dissipation rate can be experessed as a function of the coefficients of viscosity and the derivatives of the velocity.

There are now six unknowns, ρ, u_i, p and T, and the five coupled Equations (2.7), (2.8) and (2.9) plus the equation of state relating pressure, density and temperature. These six equations together with sufficient number of initial and boundary conditions constitute a well-posed, albeit formidable, problem.

As for playing a relevant role in this work, it is important to add information regarding the shear stress. For a Newtonian fluid, the viscosity, by definition, depends only on temperature and pressure, not on the forces acting upon it. If the fluid is incompressible the equation governing the viscous stress (in Cartesian coordinates) is

$$\tau_{ij}=\mu\left(\frac{\partial v_i}{\partial x_j}+\frac{\partial v_j}{\partial x_i}\right) \tag{2.10}$$

Finally, because of its great importance in the field of fluid mechanics and because the solved cases in the guide are sorted according to it, the Reynolds number is presented:

$$Re=\frac{\text{inertia force}}{\text{viscous force}}=\frac{\rho UL}{\mu} \tag{2.11}$$

The relative importance of the ratio of the inertial forces to the viscous forces to determine the flow conditions is quantified by taking L as the characteristic scale of flow and U as characteristic velocity flow. Re represents a dimensionless number that can also be obtained when the Navier-Stokes equation is converted to a dimensionless form.

2.2 About numerical methods

As the theoretical fundamentals of the numerical methods and the finite volume method in particular are complex and difficult to widely explain, only the most revelant ideas are exposed. The scheme shown in [2] has been used as a model.

The equations of conservation of mass and momentum exposed above are difficult to solve in general. They are non-linear and coupled, which makes it difficult to treat them with the existing mathematical tools. An analytical solution is only feasible in very simple problems without much relevance. Even in some cases where simplifications of the equations are possible, the resolution remains complex.

To achieve a solution using numerical methods, a discretization of the domain is required, whose quality is determinant for the validity of the results. Numerical solutions are always approximations due to the existence of sources of errors: the discretization process, modified differential equations, iterative resolution methods, etc. It is possible to reduce the error of the discretization using more precise approximations, but it then negatively impacts on the cost and time of the simulations.

Numerical methods are mathematical tools, mainly used to easily achieve solutions which may be extremely complex. As mathematical schemes, they must meet specific criteria, ensuring that the solution is coherent and valid. For instance, the discretization must be such that when geometrical and/or temporal spacing tend to zero, the discretized equation and the exact equation coincide.

Moreover, the method must not diverge. This is to ensure that the error is being reduced while the iterative method proceeds.

Something important to be kept in mind is that nice and colorful results do not necessary have a real physical meaning. It is necessary to contrast the results and figure out if they are within an appropriate range. Furthermore, it is compulsory to develop laboratory methodologies to carry out experimental work in order to compare and contrast numerical results with *in-lab*, *in-vitro* and *in-vivo* tests.

2.3 Description of OpenFOAM

OpenFOAM is first and foremost a *C++ library*, used primarily to create executables, known as *applications*. The applications fall into two categories: *solvers*, that are each designed to solve a specific problem in continuum mechanics; and *utilities*, that are designed to perform tasks that involve data manipulation. The OpenFOAM distribution contains numerous solvers and utilities covering a wide range of problems.

One of the strengths of OpenFOAM is that new solvers and utilities can be created by its users with some pre-requisite knowledge of the underlying method, physics and programming techniques involved.

OpenFOAM is supplied with pre- and post-processing environments. The interface to the pre- and post- processing are themselves OpenFOAM utilities, thereby ensuring consistent data handling across all environments. The overall structure of OpenFOAM is shown in Figure **??**:

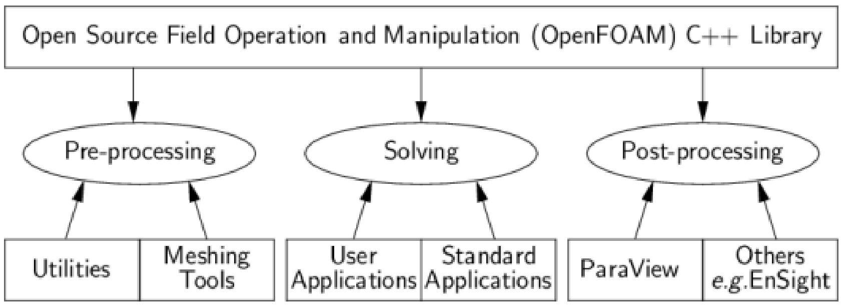

Figure 2.1: Overview of OpenFOAM structure, extracted from [3]

In this project, Version 2.2.1 of OpenFOAM has been used.

2.4 Overview of characteristics of the thoracic aorta

2.4.1 The circulatory system

The circulatory system in humans include three important parts: a heart, blood and blood vessels. The heart pumps the blood through the vessels in a loop, and the system is able to adapt to a large number of inputs as the demand on circulation varies throughout the body, day and life.

During systole, the left ventricle in the heart contracts and ejects the blood volume into the aorta. The blood pressure in aorta increases and the arterial wall is distended. After the left ventricle has relaxed, the aortic valve closes and maintains the pressure in the aorta while the blood flows throughout the body. The blood continues to flow through smaller and smaller arteries, until it reaches the capillary bed where water, oxygen and other nutrients and waste products are being exchanged, and is then transported back to the right side of the heart through the venous system. The right side of the heart pumps the blood to the lungs for oxygenation, which then enters the left side of the heart again, closing the loop [4].

2.4.2 Anatomy of the aorta

The blood leaves the left ventricle of the heart during systole and is ejected through the aortic valve into the ascending aorta. After the ascending aorta the blood deflects into three larger branching vessels in the aortic arch which supplies the arms and head, or makes a 180 turn and continues through the descending and thoracic aorta towards the abdomen.

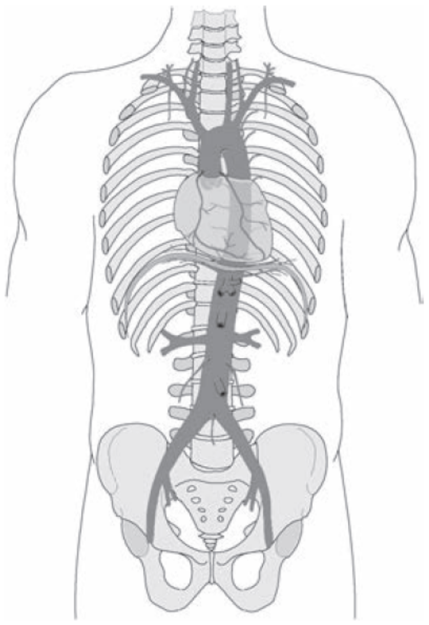

Figure 2.2: Scheme of the aorta in the human body, extracted from [4]

The parts of the aorta all have differents shapes, in terms of benching, branching and tapering, creating different flow fields. The flow behaviour in the ascending aorta is characterized by the flow through the aortic vale, and the curvature can create a skewed velocity profile. The flow in the arch is highly three-dimensional, with helical flow patterns developing due to the curvature. The flow patterns that are created in the ascending aorta and arch are still present in the descending aorta, where local recirculation regions may appear as a result of the curvature and bending of the arch.

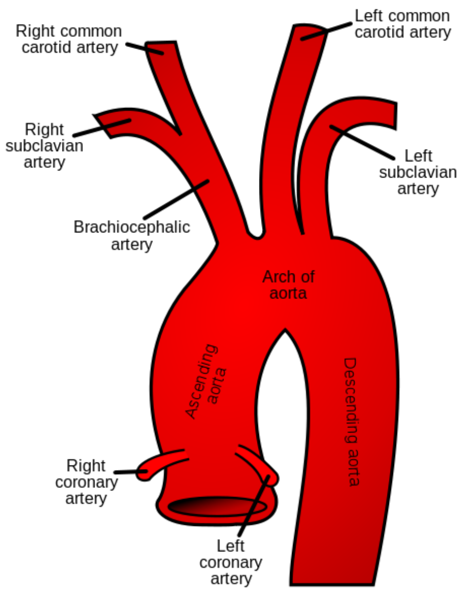

Figure 2.3: Main parts of a healthy thoracic aorta, extracted from [5]

The aortic wall is elastic in its healthy state, and will deform due to the increase or decrease in blood pressure [4].

2.4.3 Blood as a fluid

From the point of view of fluid mechanics, the main physical properties of blood required to prepare the OpenFOAM simulations are the following:

- **Viscosity:** $\mu = 3.5 \times 10^{-3} \, \dfrac{kg}{m \cdot s}$
- **Density:** $\rho = 1040 \, \dfrac{kg}{m^3}$

A controversial issue is whether to consider blood as a Newtonian or non-Newtonian flow. According to [6], in large arteries, the shear stress exerted on blood elements is linear with the rate of shear, and blood behaves as a Newtonian fluid, as Equation 2.10 shows. However, in the smaller arteries, the shear stress acting on blood elements is not linear with shear rate, and the blood exhibits a non-Newtonian behavior. Then, different models as the *power law* model or the *Carreau* model should be used.

In this work, and for modelling blood through a large artery as the aorta, blood has been considered a Newtonian fluid.

2.5 Relevance of the wall shear stress in medical research

There are two main forces applied to the arterial wall by blood, shown in the following Figure:

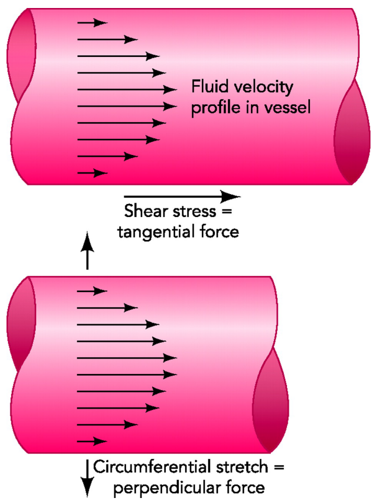

Figure 2.4: Forces applied by blood to the walls of a vessel, extracted from [7]

Blood pressure is a force that is directed perpendicular to the wall and is responsible for the cyclical distension of the vessel wall. As the blood pressure changes during the cardiac cycle, so the vessel wall extends then distends. The second force is the wall shear stress. This is the force acting on the inner lining of the artery wall, the endothelium, and is a frictional force resulting from the viscous drag of blood on the wall. Typically, wall shear stress has values of 0.5-20 Pa in a healthy artery, compared with the 10000 Pa blood pressure. As OpenFOAM works with kinematic pressure ($\frac{p}{\rho}$), this range of the wall shear stress becomes 4.8×10^{-4} to 0.02 m^2/s^2. The stretching of the artery during the cardiac cycle induces stress or tension within the artery wall. In health the increased stress acts to return the arterial wall to its *resting* position in a same way that a string will return to its resting position once the stretching force is released. This *tissue stress*, like blood pressure, is a large force in comparison with wall shear stress. It is high *tissue stress* caused by blood pressure that is responsible for the eventual rupture of both atherosclerotic plaque [1]

[1]**atherosclerotic plaque**: a deposit of fat and other substances that accumulate in the lining of the artery wall. Its rupture triggers a cascade of events that leads to clot enlargement, which may quickly obstruct the flow of blood. A complete blockage leads to ischemia of the myocardial (heart) muscle and damage

and aneurysms [2], not wall shear stress, which is a relatively tiny force incapable of producing the stresses required for rupture.

The wall shear stress plays an important role in the long-term pathology of cardiovascular disease. Studies have shown that changes in wall shear stress result in a host of cell sigalling events which give rise to effects over different timescales, from seconds (release of nitric oxide) to hours (alignment of endothelial cells [3] with the wall shear stress direction) to weeks (change in diameter of arteries).

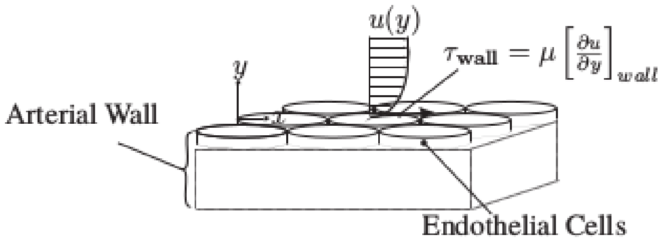

$u(y)$
y
x
$\tau_{\text{wall}} = \mu \left[\frac{\partial u}{\partial y}\right]_{wall}$
Arterial Wall
Endothelial Cells

Figure 2.5: Scheme of the wall shear stress on the endothelial cells, extracted from [8]

It is increasingly recognised that disease progression is a complex interplay between local biology and local mechanical forces, including both wall shear stress and *tissue stress*. In atherosclerosis [4], initiation of disease has long been recognised as occuring at regions of low wall shear stress. Reviews of the role of wall shear stress in disease development have emphasised the importance of low wall shear stress in disease initiation. Studies noted an inverse relation between intima-media thickness (IMT) [5] and wall shear stress.

It was hypothesised that high wall shear stress stimulates macrophage activity, leading to thinning of fibrous cap (or arterial lumen, the space inside the artery), which is then at risk of rupture through high tissue stress. The role of wall shear stress in stimulating the inflammatory process has been detected, with an atheroprotective (that protects against the formation of atherosclerosis) effect on high wall shear stress [9].

[2]**aneurysm:** localized, blood-filled balloon-like bulge in the wall of a blood vessel

[3]**endothelial cells:** cells forming the endothelium, which is the thin layer that lines the interior surface of blood vessels and lymphatic vessels, forming an interface between circulating blood or lymph in the lumen and the rest of the vessel wall

[4]**atherosclerosis:** specific form of arteriosclerosis in which an artery wall thickens as a result of invasion and accumulation of white blood cells

[5]**intima-media thickness:** is a measurement of the thickness of tunica intima and tunica media, the innermost two layers of the wall of an artery. IMT is used to detect the presence of atherosclerotic disease in humans

2.6 4D flow visualization method used for comparison

Thanks to the new medical techniques, such as MRI and CT scanning, it is possible to obtain a lot of information non-invasively and to visualize complex geometry of the patients. The comparison with the OpenFOAM simulations presented in this work will be done according to the results obtained with DiPPo, a tool able to integrate the velocity profile determined by 4D phase-contrast magnetic resonance in computational fluid dynamics, developed by the authors of [10].

One of the most important parts for the data acquisition is the magnetic resonance. For the aorta exposed in this work, measurements were carried out using a 3 T MR system (Magneton TRIO; Siemens, Erlangen, Germany) time-resolved, 3-dimensional MR velocity mapping based on an RF-spoiled gradient-echo sequence with inlerleaved 3-directional velocity encoding (predefined fixed velocity sensitivity = 150 cm/s for all measurements). Data were acquired in a sagittal-oblique, 3-dimensional volume that included the entire thoracic aorta and the proximal parts of the supra-aortic branches. Each 3-dimensional volume was carefully planned and adapted to the individual anatomy (spatial resolution, 2.1 × 3.2-3.5 × 3.5-5 mm^3).

In the in vivo situation, measurements may be compromised by the active cyclic motion of the heart (cardiac contraction and dilation) and the passive motion of the heart due to respiration. These motion components may lead to image artifacts and uncertainties about the exact measurement site in the aorta. Only if the breathing state was within a predefined window data was accepted for the geometrical reconstruction. To resolve the temporal evolution of vascular geometry and blood flow, measurements were synchronized with the cardiac cycle. The velocity data was recorder in intervals of Temporal Resolution (TeR) throughout the cardiac starting after the R-wave of the ECG. The initial delay after R-wave detection was required for execution of the navigator pulse and processing of the navigator signal. Two-fold acquisition (k-space segmentation factor = 2) of reference and 3-directional velocity sensitive scans for each cine time frame resulted in a temporal resolution of 8 repetition time = 45 to 49 milliseconds. To minimize breathing artifacts and image blurring, respiration control was performed based on combined adaptive k-space reordering and navigator gating. Further imaging parameters were as follows: rectangular field of view = 400 × (267-300) mm^2, flip angle = 15 degrees, time to echo = 3.5 to 3.7 milliseconds, repetition time = 5.6 to 6.1 milliseconds, and bandwidth = 480 to 650 Hz per pixel. For velocity measurements a voluntary healthy, male subject underwent MR examinations; written informed consent was obtained from the subject [10].

Another relevant issue of the image treatment is blood flow velocity decoding. Blood flow velocity in each voxel depends on acquisition velocity and gray scale. In general the velocities are encoded in the phase difference images such that there is a linear relationship between the gray scale value and the underlying velocity:

$$Velocity = \frac{PixelValue - GrayScale}{GrayScale} \cdot V_{enc} \tag{2.12}$$

where V_{enc} is the velocity sensitivity in cm/s (in the current case, $V_{enc} = 150$ cm/s), *GrayScale* depends of the DICOM (2048 in the current case) and *PixelValue* is the value of the gray color of the phase contrast image [10].

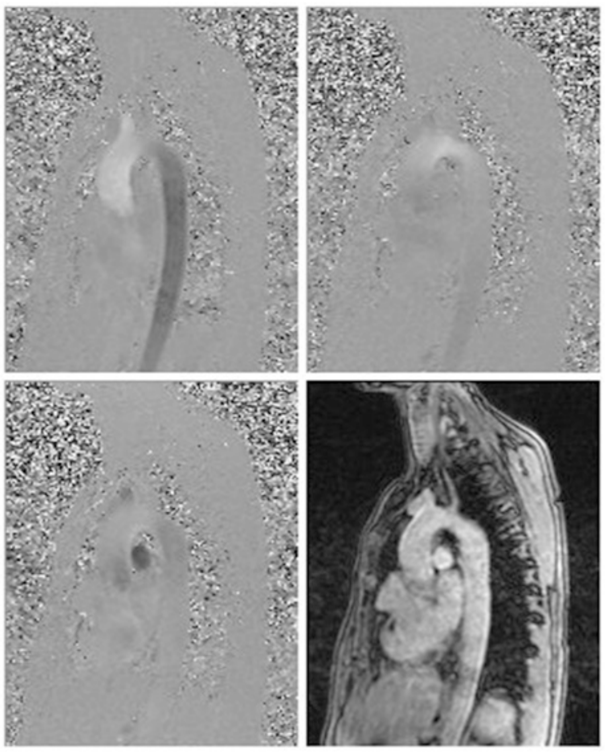

Figure 2.6: Phase contrast image (through plane velocity encoding) in Vx, Vy, Vz and magnitude image at the third iteration

2.7 State of the art

2.7.1 Learning OpenFOAM

OpenFOAM (named FOAM in its origins) was developed in the late 1980s at Imperial College (London), being sold some years later by UK company Nabla Ltd. In 2004, this company ceased operation and released FOAM as open source under GNU General Public License, under the name *OpenFOAM*. At this moment, two independent companies were created:

- OpenCFD Ltd.
- Wikki Ltd.

Both of these companies were started by some of FOAM's original developers and have nothing to do with one another. Each company mantains their own variation of OpenFOAM [11].

The Official OpenFOAM project is mantained by OpenCFD Ltd., whose variation is likely the most installed. On September 2012, the ESI Group announced the acquisition of OpenFOAM Ltd. from SGI.

This report explains at several places the difficulties found by new users to learn OpenFOAM due to the lack of maintained documentation. The main (and only) official tutorials freely provided by OpenCFD are:

- **User Guide:** is the main documentation for initiating with OpenFOAM. It contains information about its general running, as for instance data structures, compilation, applications, libraries, mesh generation, post-processing and more
- **Programmer's Guide:** contains more exhaustive explanations about the OpenFOAM programming issues
- **Example cases**: OpenFOAM cases with pre-prepared codes to be run

In spite of the fact that these documents show a very complete description of the OpenFOAM possibilities, they only offer an initial idea of the enormous potential of OpenFOAM. This is the reason why there has been an increasing use of Internet forums, most of them managed by other CFD learners. There, it is possible to expose personal problems, ask for existing functionalities, provide new utilities, and much more. There are intense debates where it is possible to participate and contribute with new ideas and solutions.

Moreover, one of the main contributions to expand the OpenFOAM knowledge has been the creation of websites containing solved cases, showing how to program specific utilities, explaining more deeply the different kinds of OpenFOAM solvers, etc. However, in the majority of websites, all the cases done by other users are basically academic or particular projects. It implies that the contents are based on the analysis of the results rather than exposing how the OpenFOAM simulations were carried out. Examples of very interesting works developed with OpenFOAM as university theses are [12], [13], [14], [15].

Consequently, these contents are very useful to contrast programing techniques and to extract main ideas, but are not adequate to introduce or improve the OpenFOAM skills, as it would be done with a guide in which the users can learn step by step. Although in most of them the OpenFOAM codes used to program the simulations are included, it is rarely possible to find accurate teaching explanations of its OpenFOAM simulations.

On the other hand, it would be unfair to say that there are no tutorials selflessly distributed by OpenFOAM users. Some examples are the following, encompassing different kinds of topics:

Filling of a tank

Airflow over a car

A comprehensive tour of snappyHexMesh

Airfoil simulation using gmsh

Dynamic meshes

These and many more tutorials are complete and allow an understanding of the OpenFOAM parameters involved in those simulations. The only handicap is that some of them develop and explain advanced tools, as for instance dynamic meshing. As a consequence, there is a gap between completing the first tutorial (explained in the official User Guide [3]) and accessing these complex tutorials. It is commonly accepted that the *Cavity tutorial* exposed in [3] is perfect to start with OpenFOAM and learn its basic fundamentals. However, other simple cases like this one, focusing on different OpenFOAM aspects, would be needed before moving to advanced tutorials and/or websites.

In conclusion, the OpenFOAM guide developed in this work allows new users to establish and extend their OpenFOAM background once the main tutorial of the official guide is done. Then, with the current guide it would be possible to improve the comprehension of the OpenFOAM structure, learn programming techniques, understand how to mesh different kind of geometries (2D and 3D), familiarize with the main pre- and post-processing OpenFOAM and ParaView capabilities, figure out which solvers and physical models are more adequate for each kind of fluid mechanics problem and many more. With it, it would be then much easier to use complex utilities found in internet and follow specific tutorials focused on advanced tools. Moreover, while most of the internet tutorials are each focused on one specific case, the current guide offers five different solved fluid mechanics problems with high applicability and all included in the same document. It has been conceived to guide the user through several cases, starting by simple ones and then following an increasing degree of difficulty. As all of them will be explained following the same schemes, structure and approach, the learning process may be simpler.

2.7.2 Thoracic aorta studies and hemodynamics CFD simulations

The use of CFD techniques in simulating blood patterns and modelling cardiovascular systems has become widespread within bioengineering and medical research in the past few decades. There are several advantages in using CFD to characterize the cardiovascular system (called *in silico* models), instead of the traditional *in vivo* experimental studies [16]:

- The relatively low costs associated with *in silico* models
- The less invasive nature of numerical simulations, since only minimal measurements from the patient are needed
- The ability to precisely control boundary conditions in the models
- The ability to accurately compute quantities that are difficult to measure *in vivo*, such as the wall shear stress

Coupling medical imaging and CFD allows to calculate highly resolved blood flow patterns in anatomically realistic models of the thoracic aorta, thus obtaining the distribution of WSS at the luminal surface. However, the increasing reliance on CFD for hemodynamic simulations requires a close look at the various assumptions required by the modeling activity. In particular, much effort has been spent in the past to assess the sensitivity to assumptions regarding boundary conditions [17].

Regarding the geometry, description of the arterial geometry used in CFD simulations is very important and essential for the results. Local arterial geometry components as curvature and smoothness will highly influence the results. The resolution of human aortas will also be influenced by the general geometry or topology of the number and location of branches [8].

Regarding the boundary conditions, an accurate and validated mechanical model would be required for the description of vessel movements during the cardiac cycle. There is a debate in the literature on the validity of currently proposed models for this purpose [8]. If instantaneous wall shear stress is important, it is necessary to consider a fluid-structure interaction simulation that can account for the deformation of the arterial wall [18]. On the other hand, the assumption of rigid wall geometry is commonly accepted in computational hemodynamics [8]. It is recommended to prescribe outflow boundary conditions based on *in vivo* accurate measurements. Depending on its location and type, the inlet velocity profile seems to influence both bulk flow and wall shear stress distribution [17][19].

The inlet flow profile was measured with MRI and prescribed in the ascending aorta, while an impedance pressure boundary condition was set in the thoracic aorta. Velocity contours in the descending aorta were found to be in very good agreement with MRI measurements, with prediction of flow reversal on the inner side in the descending aorta [18].

The average peak Reynolds number was higher in the ascending ($\approx$ 4500) and descending aorta ($\approx$ 4200) than in the aortic arch ($\approx$ 3400). Thirty young healthy volunteers were examinated by MRI. According to the calculated critical Reynolds numbers, flow instabilities were prominent in the ascending (14 out of 30 volunteers) and descending aorta (22 out of 30 volunteers) but not in the aortic arch (3 out of 30 volunteers). The supracritial Reynolds number, indicating flow instabilities, is significantly correlated with body weight, aortic diameter and cardiac output. While the findings might suggest the presence of flow instabilities in the healthy aorta at rest, this does not involve fully turbulent flow [20].

2.8 Hypotheses used for aorta simulation

The hypotheses assumed for the aorta simulation are the following:

Peak systolic conditions

Incompressible flow

Laminar flow

Newtonian flow

Rigid, blood-impermeable and smooth aorta walls

Static aorta geometry

Uniform inlet velocity profile

Right and left coronary arteries are not included

It is important to remark that the simulations will be carried out for a particular time instant, in peak systolic. It represents the time with higher inlet flow speed and therefore maximum values of wall shear stress. As one of the main goals of the work is to determine wall shear stress that blood causes in order to prevent medical diseases, the more critical conditions are simulated. As a consequence, the simulations are not going to be transitory, with constant boundary conditions, and thus the results must be analyzed accordingly.

3. Pre-processing of the aorta with OpenFOAM

The explanations contained in this Chapter detailing how the case was prepared for the simulations have four main purposes:

Expose the methodology used for the pre-processing of the OpenFOAM simulations of the aorta in case it would be necessary to repeat it in future studies

Show the progression of the work itself, encompassing programming of the OpenFOAM codes, development of tools used to improve the computation of the fluid dynamics parameters and adequacy of the initial aorta geometries for a suitable study

Expose the main steps and key factors when simulating internal laminar flow with OpenFOAM. Although the study of hemodynamics presented in this work focuses on a particular case to be solved (the aorta), the pre-processing of the case shown below can be used for simulations encompassing similar fluid mechanics characteristics

Expose the main steps and key factors when treating with OpenFOAM imported irregular geometries. As the geometry of the aorta used in this work has been obtained from the images of a real human body, one of the main difficulties of the case resolution has been to adapt this irregular geometry while making it suitable to be simulated with OpenFOAM

When exposing the methodology used for computer simulations, it is somewhat difficult to explain which steps were more determinant and complex to overcome before achieving the final results. This is the reason why in each one of the Sections of the current Chapter a brief text is included exposing the main difficulties found during the development of each part.

The OpenFOAM case (named AortaFoam) for the aorta simulations presents a structure of directories and subdirectories similar to the aircraft case exposed in the guide.

The process of segmentation by which the current aorta geometry was obtained (done with DiPPo [10]) is explained as follows: An n-phase 4D (spatio-temporal) image can be viewed as a discrete set of n volumetric images defined at n different time instants. The 4D aortic surface can also be viewed as a sequence of surfaces. During the segmentation stage, the 4D segmentation algorithm consists of the following steps:

- Aortic surface pre-segmentation: a 4D fast marching level set method simultaneously yields approximate 4D aortic surfaces
- Centerline extraction: aortic centerlines are determined from each approximate surface by skeletonization
- Accurate aortic surface segmentation: an accurate 4D aortic surface is obtained simultaneously with the application of a novel 4D optimal surface detection algorithm

In order to improve the aorta segmentation, a new step was added. It consists in introducing an optimization of Dijkstra's shortest path algorithm. Thanks to this algorithm, the region of interest is more precise, the tubular structures are improved and it is possible to select the branches of the aorta according to some values.

To understand the capabilities offered by the 4D method, a figure showing the module of the velocity field in peak systolic conditions is shown next:

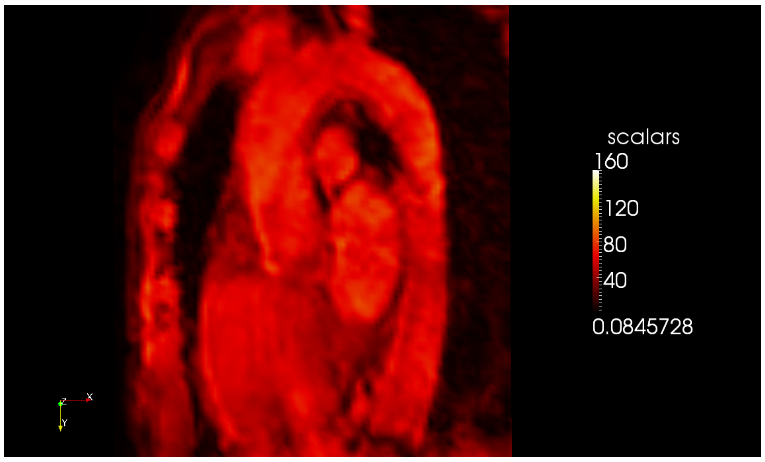

Figure 3.1: $|\mathbf{U}|$ in a longitudinal slice of the aorta obtained from the 4D method (cm/s)

Figure 3.1 shows the behaviour of blood through the aorta obtained by using MRI techniques, containing both the aorta and other human tissues. The figures below show the shape of the aorta (superposed to the medical image) used for the computation of the wall shear stress and obtained applying the segmentation process exposed above. It is the same geometry used for the OpenFOAM simulations:

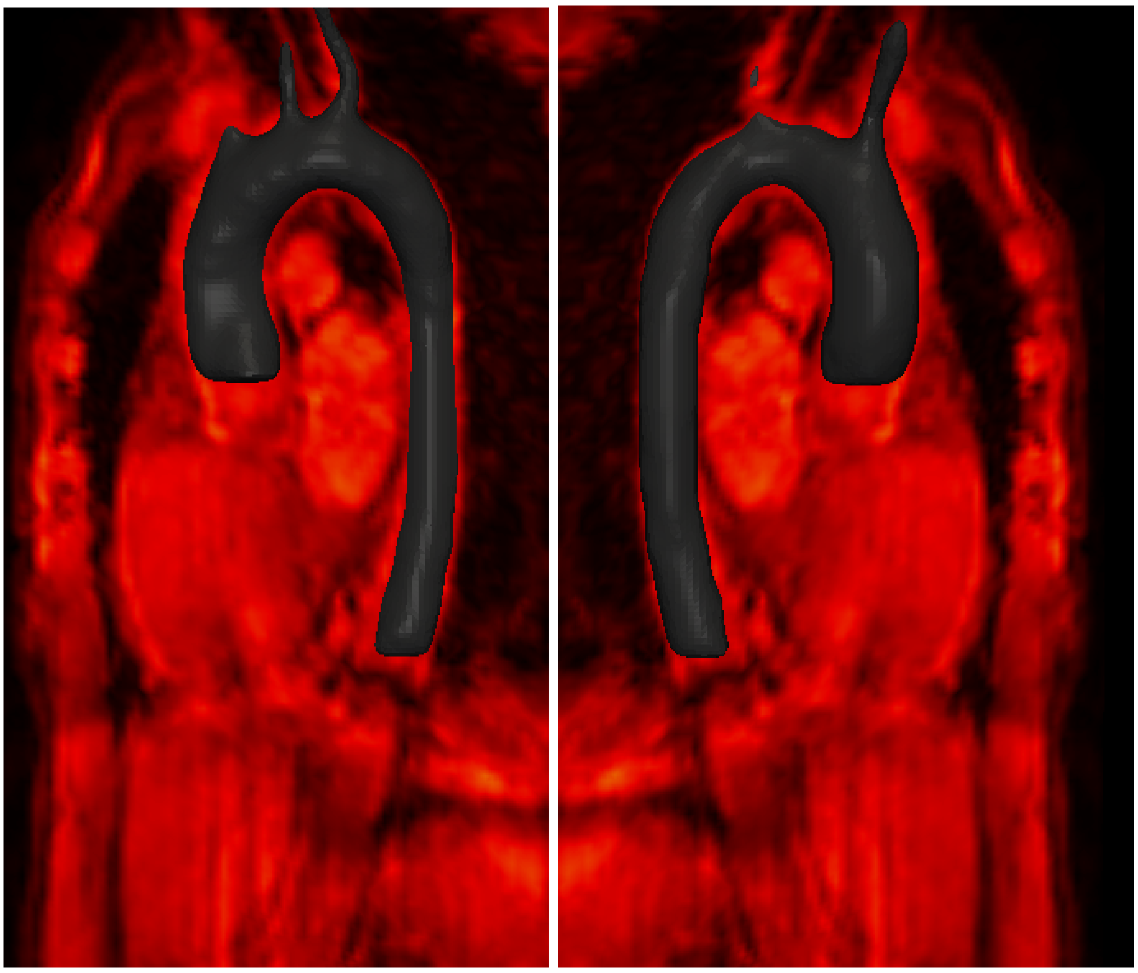

Images used for the segmentation process with the shape of the aorta geometry used for the OpenFOAM simulations

The segmentation has been done during the maximum systole.

3.1 Preparing the geometry

3.1.1 The 3 simulated geometries

Aim of the task: in order to investigate the fluid dynamics in the aorta, 3 different models have been used. Only the third (Figure 3.3) represents a real geometry, while the others are simplifications used for an easiest treatment of the case until the most complex steps of the pre-processing were fulfilled.

Main characteristics of each model:

3 models of study

First model:	primitive geometry with approximate inlet and outlet and without any supra-aortic vessel
Second model:	more realistic but with only two of the three supar-aortic vessels
Third model:	real geometry with the main inlet, the main outlet and the three supra-aortic vessels

Pictures of some models:

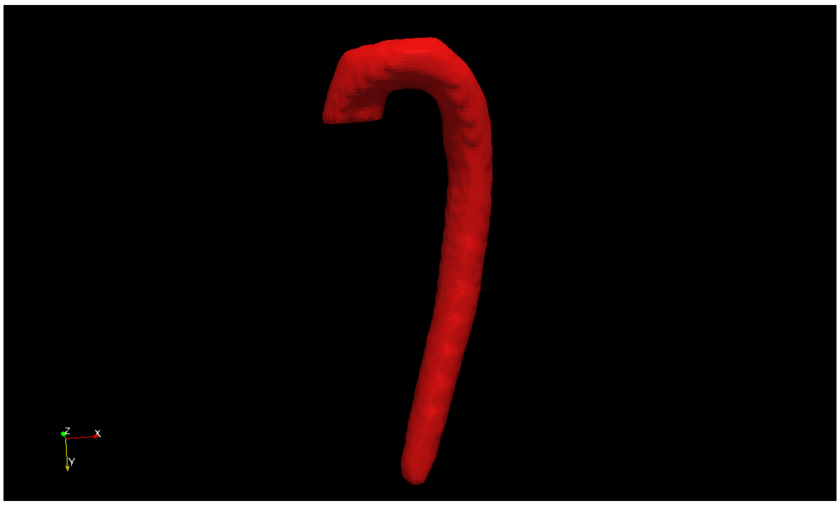

Figure 3.2: First model of aorta used in the simulations

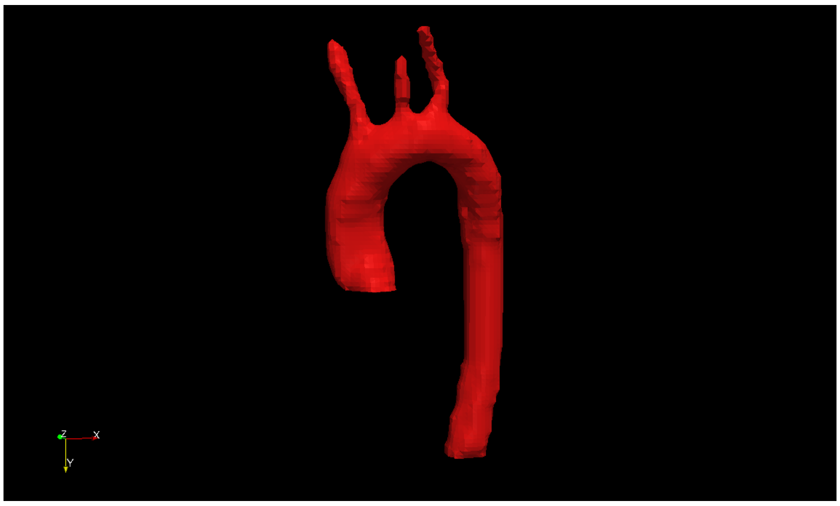

Figure 3.3: Third model of aorta used in the simulations

Working scheme:

Each one of the models has been used to study and test specific features of the pre-processing:

1. **First model** → as it is a very simple version of a real aorta, it has been used in the first steps of the investigation, especially with the preparation of the geometry. With this model, it has been possible to:
   - investigate how to smooth the surface
   - understand how to adapt external irregular geometry to OpenFOAM standards
   - find an adequate mesh for the case
   - develop a method to define the patches where the boundary conditions are applied
   - study how to obtain a high cell refinement at the walls of the aorta to compute an accurate value of wall shear stress
2. **Second model** → it presents a more realistic geometry of aorta. With the above questions being faced, it has been very important to investigate which boundary conditions would provide the more physically realistic flow conditions [21]. These tests have been done with model 2. This issue is further explained in Section 3.2, but the fact is that the boundary conditions imposed in the supra-aortic vessels are crucial for the mass flow rate distribution and the global behaviour of the fluid.

3. **Third model** → it represents a real geometry, being the one used for the final simulations and for the analysis of the results once the main programming difficulties had been overcome with models 1 and 2. This is the reason why the pre-processing explanations and the methodology presented in the current section are going to be entirely done using the third geometry.

Main difficulties:

– Each time a new model was introduced, it was necessary to readapt all the pre-processing parameters

– The instructions of Section 3.1.6, which are laborious, had to be computed for each one of the models

– Since geometries were simplified and despite simulating properly, the results of models 1 and 2 might not be physically realistic

3.1.2 Smoothing the surface

Aim of the task: as can be seen in Figure 3.3, the surface of the initial aorta geometry is irregular, rough and in some regions with a bad cell definition. If it were directly meshed, these flaws might lead to misleading conclusions regarding the wall shear stress. As could be seen in the first tests, a marked irregularity on the surface is a stress concentrator and therefore the wall shear stress in these areas grows with no physical reason.

Work methodology: a laplacian smoother was applied to the initial STL surface. The surfaceSmooth OpenFOAM utility was used, and although most of the irregularities on the surface could not be erased but only smoothed, this tool highly helped in adapting the geometry for the simulation.

This utility is included in the OpenFOAM surface mesh tools and no dictionaries are needed to run it. To use the utility, once the STL file containing the aorta geometry (named aortaGeometry.stl) has been saved within *constant/triSurface*, it is necessary to type:

```
surfaceSmooth aortaGeometry.stl 0.5 10 lastAortaSmooth10It.stl
```

where the inputs are as follows:

```
< utility > < originalFileName > < relaxationFactor > < numberOfIterations > < outputFileName >
```

Results: the differences between the surfaces of the aorta with or without smoothing can be observed in the following figures:

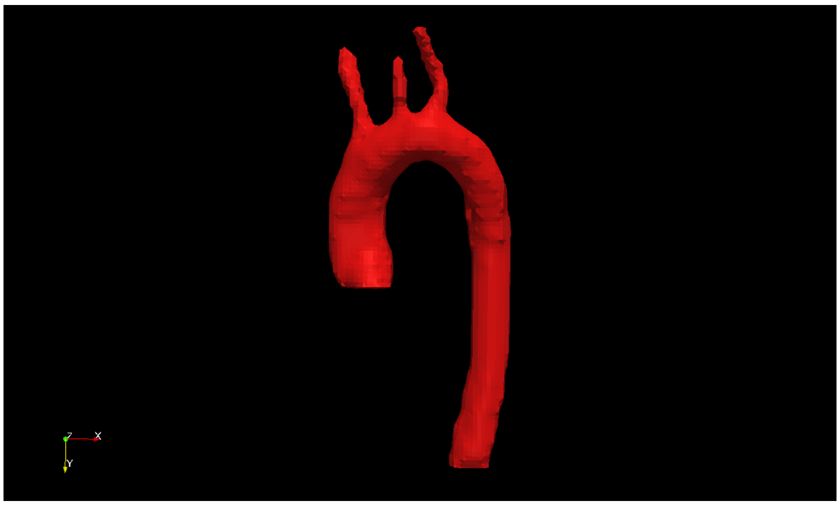

Figure 3.4: Surface of the aorta without smoothing

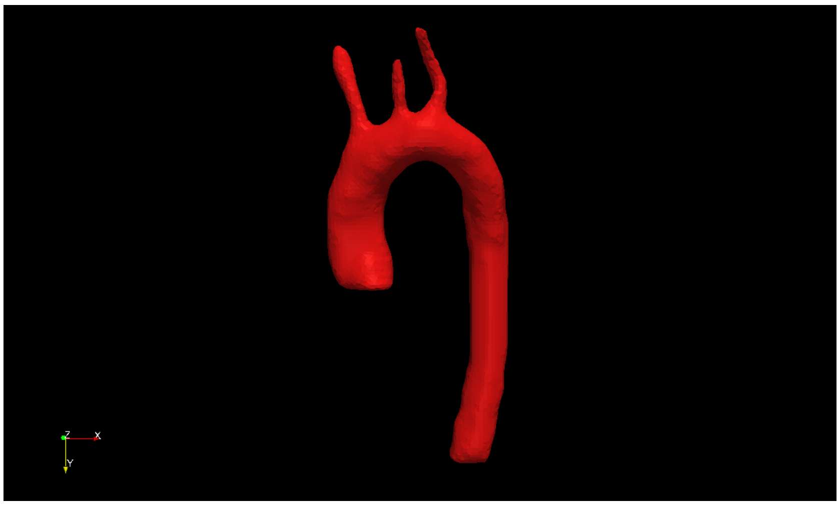

Figure 3.5: Surface of the aorta with smoothing

The differences between the surfaces with edges of the aorta with or without smoothing are the following:

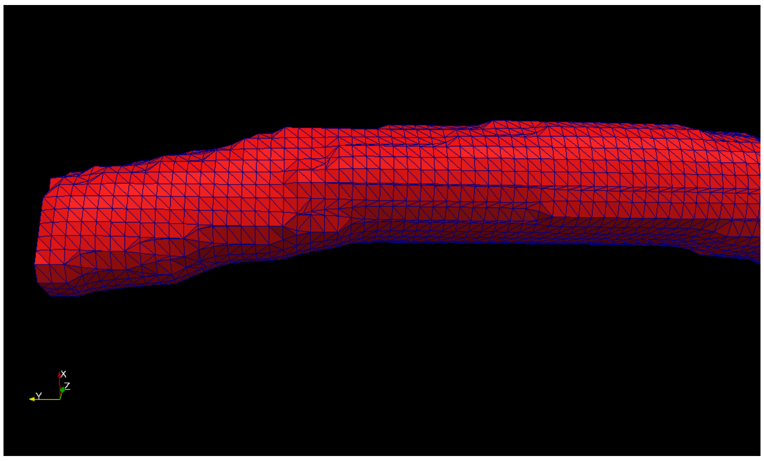

Figure 3.6: Surface with edges of the descending aorta without smoothing

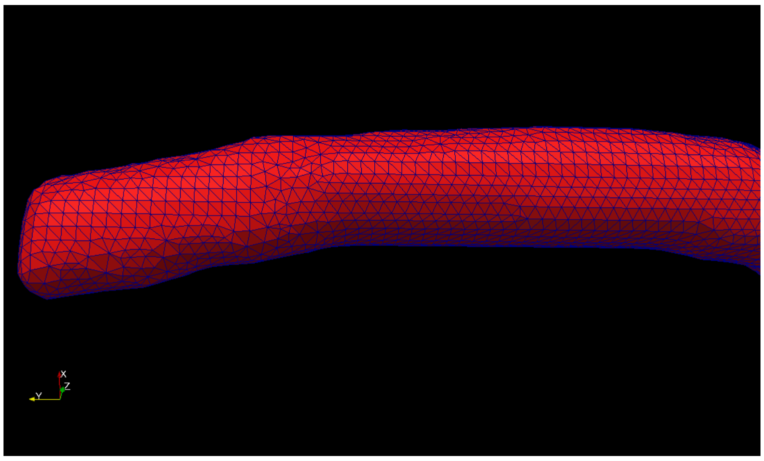

Figure 3.7: Surface with edges of the descending aorta with smoothing

Main difficulties:

- Understand, considering the time it takes for simulating, how many iterations were required to obtain good results
- The surfaceSmooth utility is not commonly used and it took time to investigate its functionality
- Althoug the utility is very useful, some parts of the geometry could not be completely smoothed

3.1.3 Surface feature extracting

Aim of the task: with the improved geometry, the next step was to use the surfaceFeaturesExtract utility, which extracts feature edges from tri-surfaces (as explained in the sixth chapter of the guide). It is not a tool to improve neither the geometry nor the computation of the fluid dynamics parameters, but it is required when simulating cases using the snappyHexMesh utility.

Work methodology: to execute this utility, it is first necessary to edit a dictionary (*surfaceFeatureExtractDict*) located within system. It contains the code shown in Appendix A.1.

Once it is prepared, it is necessary to type:

```
surfaceFeatureExtract
```

3.1.4 Meshing the geometry

Aim of the task: the meshing process is one of the main steps when preprocessing the case, mainly because the quality of the mesh is directly related to the accuracy of the results. In fact, the boundary layer can only be adequately solved if a very high cell refinement is obtained at the walls of the aorta. Furthermore, as one of the main objectives of this work is to determine the wall shear stress, this issue becomes even more crucial.

Work methodology: different kinds of meshes were tested, analyzing the influence of the number of cells and the cell refinements at the walls with the results and the convergence time. This analysis is described in Section 3.5, where the mesh used for the main simulations and exposed in this Section is justified.

The snappyHexMesh meshing utility used in the AortaFoam case is shown in the sixth chapter of the guide. Once the parameters of the final mesh had been chosen, the main meshing steps were:

1. **Creation of a background mesh:** it is necessary to generate a structured mesh, whose cells will be divided in smaller cubes to mesh the aorta geometry:

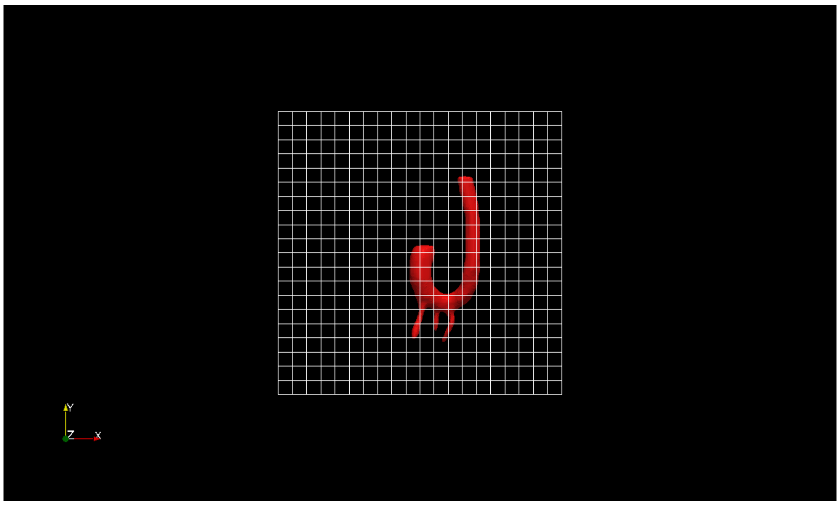

Figure 3.8: Surface of the aorta with the background mesh

This background mesh can be created by using blockMesh, whose dictionary is shown in Appendix A.2. The *boundary* file with the results of this process is shown in Appendix A.3.

2. **First meshing process of snappyHexMesh (castellatedMesh):** it creates a first and rudimentary cube-based mesh. As can be seen in Figure 3.9, the geometry of the aorta has been divided in small cubes but with a bad surface resolution:

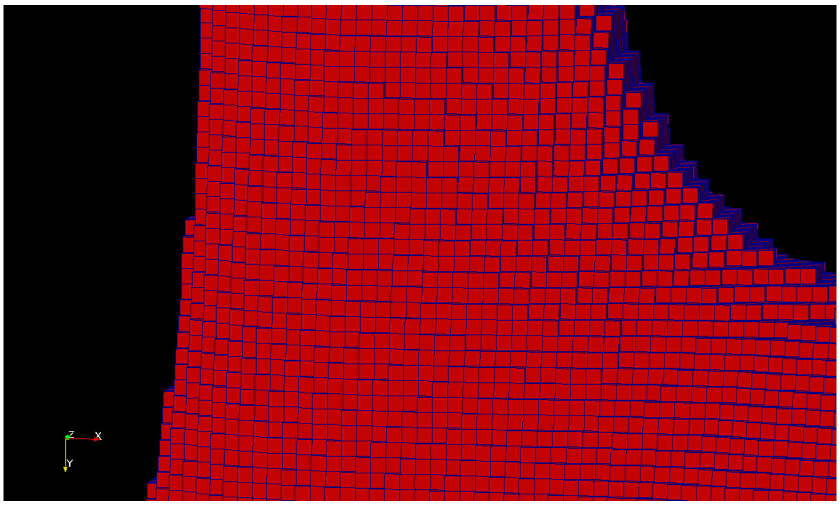

Figure 3.9: Mesh of the aorta after the first process of snappyHexMesh

3. **Second meshing process of snappyHexMesh (snap):** it works on the cells at the walls to adapt their vertices to the initial geometry in order to obtain a smooth and realistic mesh surface:

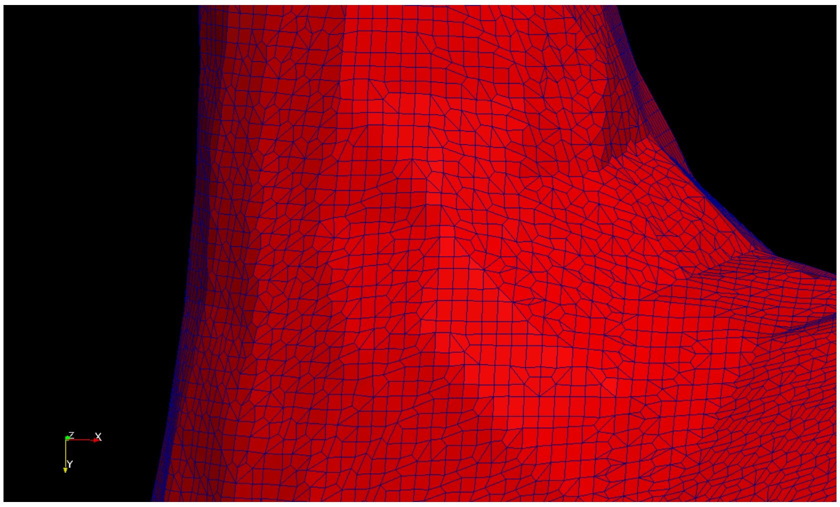

Figure 3.10: Mesh of the aorta after the second process of snappyHexMesh

The differences between the aorta mesh after and before this second meshing process:

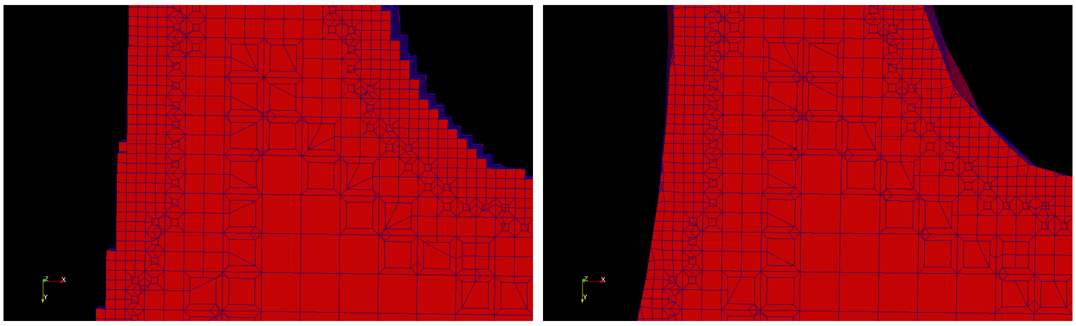

Comparative between the mesh after each one of the processes carried out to mesh the geometry with snappyHexMesh

The dictionary to run the previous meshing processes is shown in Appendix A.4.

Results: among all the meshes, the chosen one presents a uniform core of cell level 4. The refinement level indicates how many times the initial cubes have been divided until the required refinement is achieved. Near the walls, and for a proper computation of the wall shear stress, the mesh is being refined up to level 6, with transition layers of level 5. This configuration is commonly used; a higher refinement would imply extremely slow iterations. The cell refinement can be observed in the following figures:

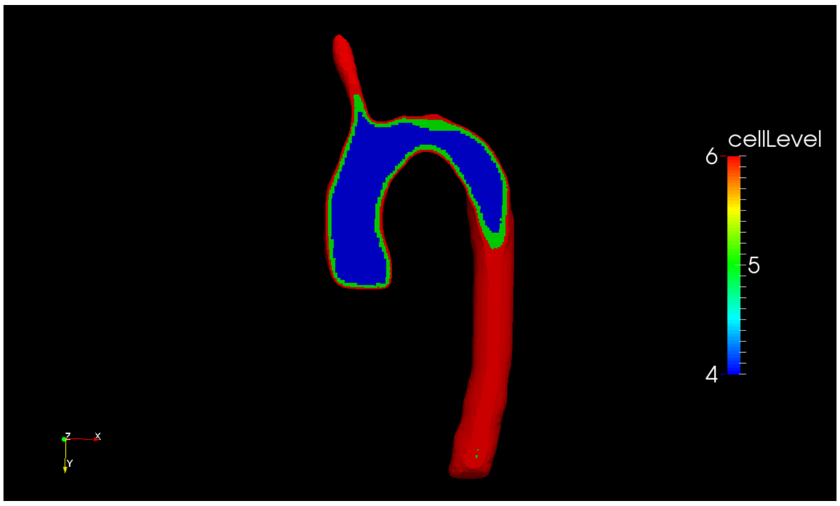

Figure 3.11: Cell level at the aortic arch of the initial mesh

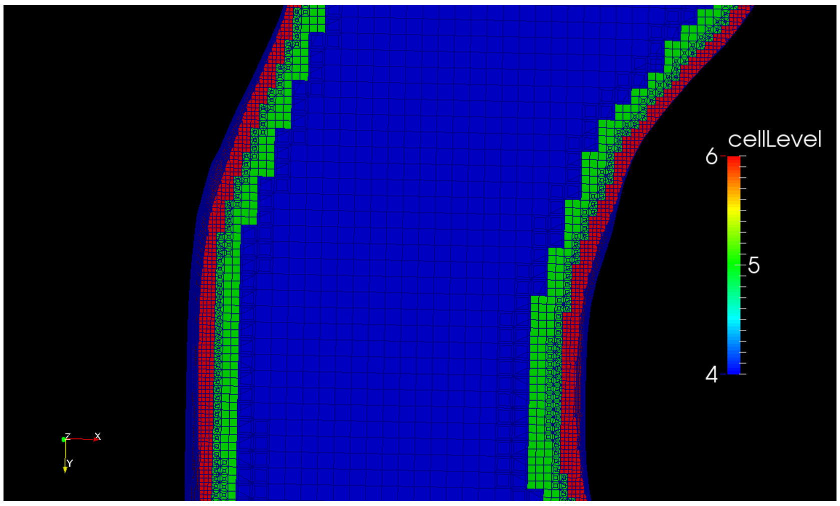

Figure 3.12: Detail of the cell level at the initial mesh of the aorta

Main difficulties:

– The dictionary for using snappyHexMesh is complex and therefore it is difficult to have a thorough command of it

– The time needed to carry out the meshing process is high. Moreover, the higher the cell refinement, the slower the iterations

– Due to the previous point, it is laborious to make tests with different mesh configurations to figure out which mesh is more suitable for the case

- Compared to other dictionaries, in snappyHexMesh it is more complicated to find out programming errors
- Although the process runs as expected and the mesh quality is acceptable, the surface of the mesh may present some irregularities

3.1.5 Refining the mesh to compute an accurate wall shear stress

Aim of the task: since it was one of the main objectives of the work and in order to contrast the results of the 4D method, a very accurate distribution of the wall shear stress was computed. To achieve this purpose, the distance between the walls of the aorta and the first node of the mesh has to be as low as possible. This is the reason why different mesh refining tools were investigated and tested to obtain very reliable results.

Work methodology: once the aorta geometry had been meshed, two different methods were used to refine the mesh at the walls of the aorta:

1. **addLayers:** it is the third and last meshing process of snappyHexMesh, and thus it uses the same dictionary shown in Appendix A.4. This utility does not change the geometry, but adds layers of cells at the walls of the domain. In addition to highly reducing the distance between the first nodes, this meshing process also corrects surface imperfections.

   In Figures 3.13 and Figure 3.14 it is possible to observe the results after adding the layers of cells. In particular, for the AortaFoam case, two layers of cells have been added, being the first 0.4 times thicker than the 6-level cells, and the second 0.5 times thicker than the previous cell layer:

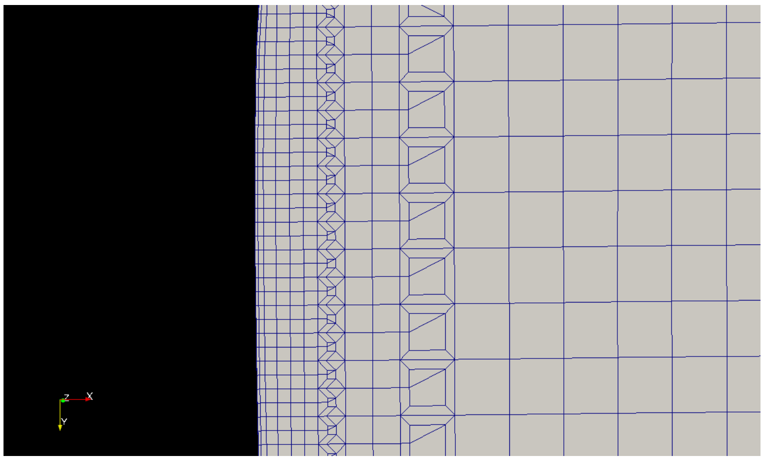

Figure 3.13: Detail of the cell refinement at the walls of the aorta

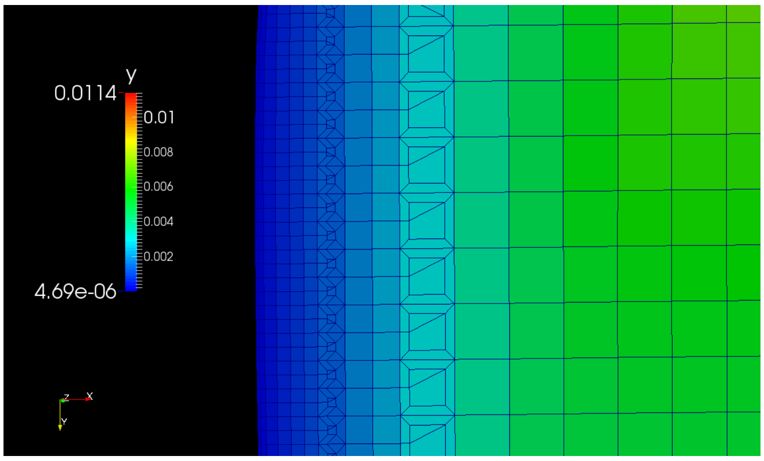

Figure 3.14: Detail of the cell refinement at the walls of the aorta with the magnitude of the distance between the wall and the nodes

As can be seen, the distance between the wall and the first node is of the order of micrometers (10^{-6} m). It is a very high cell refinement.

In Appendix A.5 the main quality parameters of the final mesh are shown once addLayers had been run. As can be seen, the mesh quality criteria have been maintained within an adequate range.

addLayers has been discovered as a fantastic tool to prepare the case for a thorough computation of the wall shear stress.

2. **refineWallLayer:** it is not a meshing process itself, but a utility which refines cells next to patches as much as specified. This method could not be finally used to pre-process the case: the quality of the mesh once it was applied was bad and inadequate for the simulation. As these

irregularities were not punctual but highly distributed along the whole mesh, no solution could be found to correct them and the refineWallLayer utility was finally discarded.

Main difficulties:

- The addLayers meshing process is even more slow than castellatedMesh and snap
- The second method might have given good results, but as the geometry was very irregular it could not be finally used. A lot of time was spent in trying to improve the quality of its mesh
- Only once the case has been simulated it is possible to observe the accuracy of the results of the wall shear stress as its computation is included in the post-processing

3.1.6 Defining patches for the simulation

Aim of the task: the aim of the methodology shown in this section is to define the required patches on the surface to apply the boundary conditions. So, as initially the whole surface was a generic patch, it was necessary to make a distinction between five different patches. Figure 3.15 shows the aorta geometry with the name of these required patches and their location:

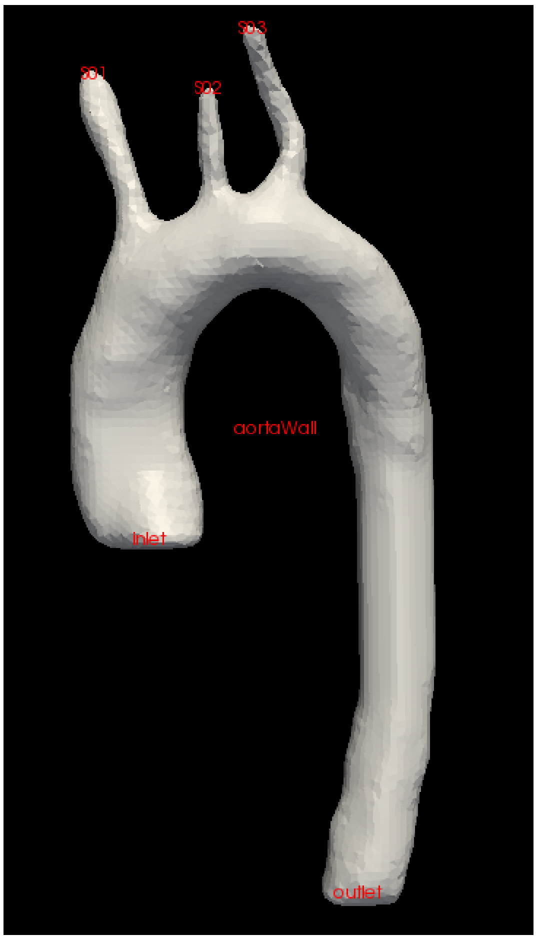

Figure 3.15: Geometry of the aorta with the name of the patches

Main characteristics of each patch:

AortaFoam patches

inlet:	patch including the faces at the inlet of the ascending aorta. Through this patch, the blood pumped in the heart penetrates into the ascending aorta
outlet:	patch including the faces at the outlet of the descending aorta
S01:	patch including the faces at the outlet of the brachiocephalic trunk
S02:	patch including the faces at the outlet of the left common carotid artery
S03:	patch including the faces at the outlet of the left subclavian artery
aortaWall:	patch including all the remaining faces, and where the wall shear stress is computed

Work methodology: in the majority of OpenFOAM simulations, this step would not have had any special relevance. However, as the aorta geometry has not been created with a 3D CAD software and the surface is irregular, a special treatment had to be used. OpenFOAM does not have a graphic interface for pre-processing, and thus the process of selecting a specific group of faces and redefine them as a new and different patch must be done by programming OpenFOAM files.

To face with this issue, two OpenFOAM utilities were used: topoSet and createPatch. The first one operates with cellSets/faceSets/pointSets through a dictionary. The second is a utility to create patches out of selected boundary faces. During the pre-processing, these two utilities were combined to define the required patches.

The main idea is that topoSet includes a group of selected faces (conforming the inlet, S01, etc.) into a set. Afterwards, createPatch defines this group of faces as a new patch where the appropriate boundary conditions will be applied. However, how can topoSet understand which specific group of faces must be included within this set?

The main steps have been the following:

1. First, it is necessary to edit the topoSetDict (Appendix A.6), which is the dictionary to control the topoSet utility, being located within *system*. In this file, it is specified (for each group) the name given to the set, what it is going to contain (cells, faces or points) and which geometric entity is going to be used. The key of the issue is that all the faces (or cells or points) of the initial geometry contained within the geometric entity will be assigned to the set.

   For the aorta simulation, 5 rectangular prisms (defined as box in *topoSetDict*) were used, plus another instruction to select all the external faces. Two of the six parts conforming *topoSetDict* are next shown:

```
    {
        name     allPatchSet;
        type     faceSet;
        action   new;
        source   boundaryToFace;
        sourceInfo
        {
        }
     }

    {
        name     c1;
        type     faceSet;
        action   new;
        source   boxToFace;
        sourceInfo
        {
        box (0.0425 0.0558 0.153) (0.0675 0.0708 0.177);
        }
     }
```

2. The second step consists of editing the *createPatchDict* file (Appendix A.7), the dictionary of the createPatch utility. There, for each patch it

is specified the name which will be given to them (inlet, S01, etc.), what type of new patch it is going to be and how it is going to be constructed (either from patches or sets). Again, two of the six parts of the dictionary are shown shown:

```
    {
        name inlet;

        patchInfo
        {
            type patch;
        }

        constructFrom set;

        patches (aortaWall);

        set definitiveInletSet;
    }

  {
        name outlet;

        patchInfo
        {
            type patch;
        }

        constructFrom set;

        patches (aortaWall);

        set definitiveOutletSet;
    }
```

3. Once both dictionaries have been successfully set, the standard procedure would be to activate both utilities typing:

   ```
   topoSet
   ```

   and afterwards:

   ```
   createPatch
   ```

   However, it does not work because createPatch can only use external faces to define the patches, whilst a great number of the faces contained within the sets created by topoSet are internal. To solve this problem, a script using *bash* programming was developed (completely unrelated to OpenFOAM dictionaries).

4. As it has previously been said, although there are 5 inlets and outlets in the geometry, a sixth instruction was defined, whose function is to select all the external faces of the geometry. Consequently, as each of the faces contained in the sets is represented by a number, the main idea consists of comparing the numbers of the set of external faces with the numbers of a set containing the faces selected by the boxes (where some are internal and some are external). According to this, two sets of numbers are compared (for instance, allPatchSet with boxOutletSet), and those faces in common are written to a third set. Finally, createPatch works directly to these third sets, and therefore only external faces are defined as new patches.

   The script (shown in Appendix A.8) to execute it must be used after topoSet and before createPatch. Next one of the five parts of the code is shown (the one used to define the inlet):

```
#!/bin/bash

cp AortaFoam/3/polyMesh/sets/c1 createPatchScript/c1Intermediate #Copy
    data from topoSet

sed -i 1,+19d createPatchScript/c1Intermediate #Erase header

sed -i '$d' createPatchScript/c1Intermediate

sed -i '$d' createPatchScript/c1Intermediate

sed -i '$d' createPatchScript/c1Intermediate


cp AortaFoam/3/polyMesh/sets/allPatchSet
    createPatchScript/allPatchSetIntermediate #Copy data from topoSet

sed -i 1,+19d createPatchScript/allPatchSetIntermediate #Erase header

sed -i '$d' createPatchScript/allPatchSetIntermediate

sed -i '$d' createPatchScript/allPatchSetIntermediate

sed -i '$d' createPatchScript/allPatchSetIntermediate

sort createPatchScript/c1Intermediate >
    createPatchScript/c1Intermediate.sort #Sort (necessary for the comm
    instruction)
sort createPatchScript/allPatchSetIntermediate >
    createPatchScript/allPatchSetIntermediate.sort

comm -12 createPatchScript/c1Intermediate.sort
    createPatchScript/allPatchSetIntermediate.sort >
    createPatchScript/definitiveInletSetIntermediate #Compare to find
    common faces shearing the condition of external face and being
        inside the box

wc -w < createPatchScript/definitiveInletSetIntermediate >
        createPatchScript/WordCounter #Count the number of faces of the
        resulting file

ed -s createPatchScript/definitiveInletSet <<< $'20r
        createPatchScript/definitiveInletSetIntermediate\nw'

ed -s createPatchScript/definitiveInletSet <<< $'18r
        createPatchScript/WordCounter\nw'

> createPatchScript/c1Intermediate #Reinitialize to 0 all the files
        which were used
> createPatchScript/allPatchSetIntermediate
> createPatchScript/WordCounter
> createPatchScript/c1Intermediate.sort
> createPatchScript/allPatchSetIntermediate.sort
> createPatchScript/definitiveInletSetIntermediate

cp createPatchScript/definitiveInletSet
        AortaFoam/3/polyMesh/sets/definitiveInletSet
cp createPatchTemplates/definitiveInletSetTemplate
        createPatchScript/definitiveInletSet
```

At the end of the process, the 6 different patches have been separated and independently defined in *polyMesh/boundary*. The results are shown in the following figures, where it is possible to observe which part was defined as aorta wall and which parts were defined as inlets or outlets:

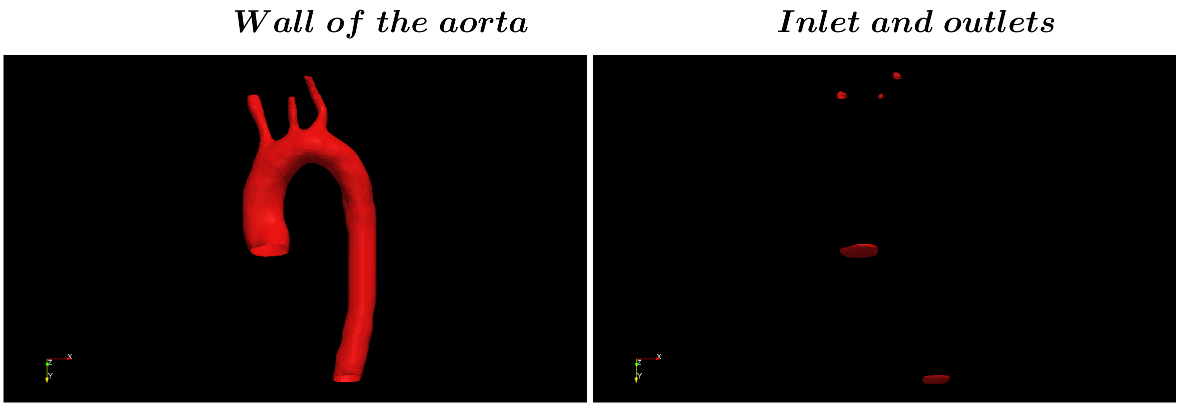

Comparison between the wall of the aorta and the faces were boundary conditions are applied once the patch definition process was carried out

Main difficulties:

– As it has been explained, no OpenFOAM utility could be found to solve the problem regarding createPatch and the external faces. This is the reason why many different methods were tested before concluding that this problem would require solutions external to OpenFOAM. After finding no alternative, the ad hoc solution using bash programming was developed

- The solution described in the previous point took a process of familiarization with bash programming
- As the method used in the script does not work directly to OpenFOAM dictionaries, there were at first adjustment problems between the script code and OpenFOAM
- The coordinates of the boxes used in *topoSetDict* had to be exhaustively calculated to accurately define the patches. Otherwise problems with the direction and magnitude of the boundary conditions might have appeared

3.2 Boundary conditions

Aim of the task: along with the mesh and the cell refinement, the boundary conditions are one of the main points of the pre-processing. The geometry of the aorta has been obtained from the images of a real body; however, to execute a realistic simulation of the mechanics of blood in the thoracic aorta, appropriate boundary conditions had to be applied.

For the application of the boundary conditions, the hypotheses shown in Section 2.8 were used. As peak systolic conditions are simulated (when the most critical conditions are achieved, and therefore higher values of wall shear stress are obtained), the boundary conditions are constant over time.

Initial approach: when simulating flow through pipes, the most common boundary conditions are to impose an inlet velocity and an outlet pressure (or viceversa). This is what was done in Model 1: a uniform inlet velocity (whose module and direction were obtained from the 4D viewing method, and therefore these values are not estimated but real) and a uniform outlet pressure. This pressure was set to 0 Pa, becoming the reference value.

However, when Models 2 and 3 were simulated, these boundary conditions had to be adapted due to the outgoing flow of the supra-aortic vessels.

Work methodology:

As explained in Section 2.4, the internal pressure in the supra-aortic vessels (patches S01, S02 and S03) is different than the pressure at the outlet of the thoracic aorta. As a consequence, if the same pressure boundary conditions would be applied to all of them, the results would not be physically realistic. In principle, neither the mass flow rate distribution nor the flow structure would match reality.

According to literature, and to solve this problem, it would have been necessary to introduce an electrical analogy to compute the pressure drop in each region. Nevertheless, two alternatives were tested thanks to the information provided by the 4D viewing method:

– Impose uniform outlet velocity at the supra-aortic vessels
– Impose uniform volumetric flow rate at the supra-aortic vessels

Both kinds of boundary conditions were pretended to be equivalent to imposing uniform values of pressure in each one of the supra-aortic vessels. However, as it is very difficult to obtain experimental pressure data in those regions, boundary conditions related to the velocity field were tested.

This is the reason why 3 different cases regarding boundary conditions were tested. Common features in all of them are a uniform aorta inlet velocity and a uniform aorta outlet pressure, but each case presents different boundary conditions at the supra-aortic vessels:

1. **First Case: uniform supra-aortic vessels outlet velocity**

   Scheme of the boundary conditions:

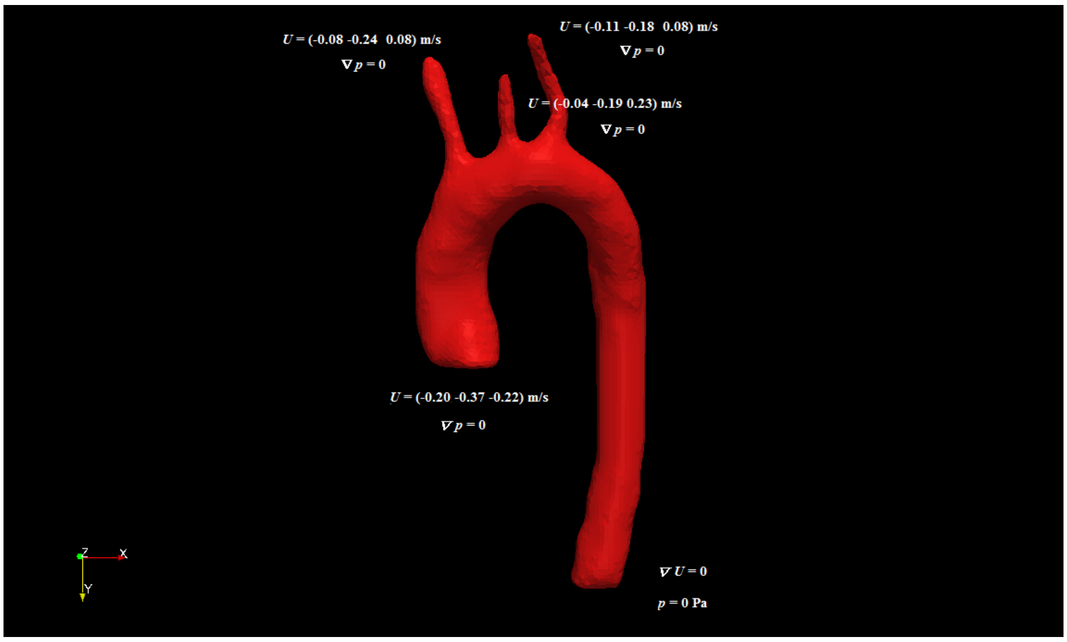

$U = (-0.08\ -0.24\ \ 0.08)$ m/s
$\nabla p = 0$
$U = (-0.11\ -0.18\ \ 0.08)$ m/s
$\nabla p = 0$
$U = (-0.04\ -0.19\ 0.23)$ m/s
$\nabla p = 0$
$U = (-0.20\ -0.37\ -0.22)$ m/s
$\nabla p = 0$
Z
X
Y
$\nabla U = 0$
$p = 0$ Pa

Figure 3.16: Boundary conditions applied to the First Case

Results:

Although the case converged, the solution did not present a physically realistic behaviour of the flow. Singular points appeared with large flow accelerations, mainly in the supra-aortic vessels.

2. **Second Case: uniform supra-aortic vessels volumetric flow rate**

   Scheme of the boundary conditions:

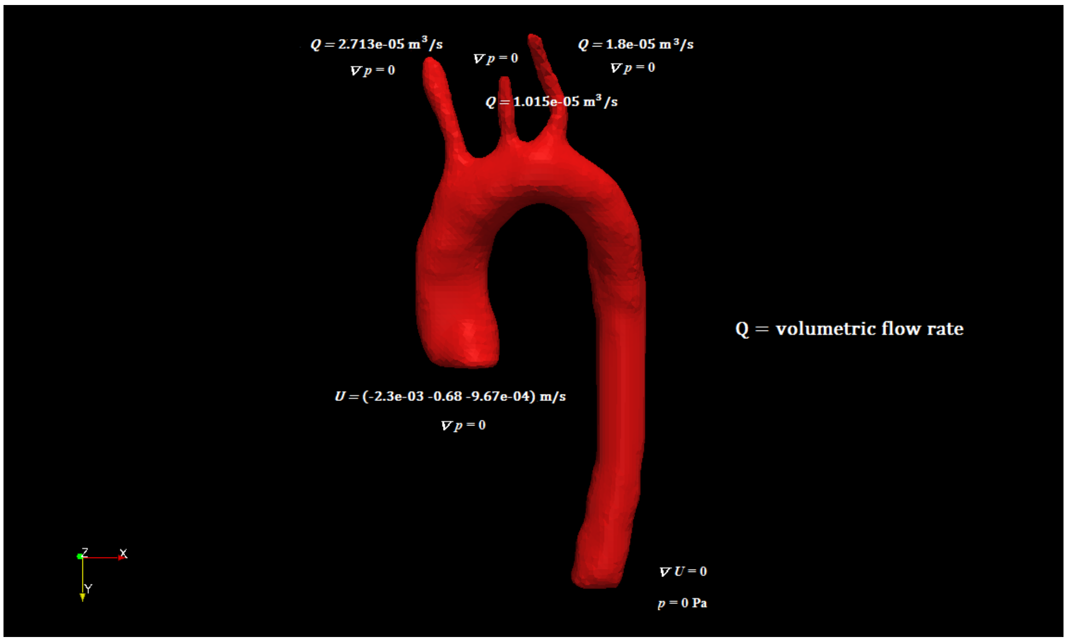
$Q = 2.713e\text{-}05\ m^3/s$
$\nabla p = 0$
$\nabla p = 0$
$Q = 1.8e\text{-}05\ m^3/s$
$\nabla p = 0$
$Q = 1.015e\text{-}05\ m^3/s$
Q = volumetric flow rate
$U = (-2.3e\text{-}03\ -0.68\ -9.67e\text{-}04)\ m/s$
$\nabla p = 0$
$\nabla U = 0$
$p = 0$ Pa
Z X
Y

Figure 3.17: Boundary conditions applied to the Second Case

Results:

As the First Case, it converged. At a first glance, the results seemed to adapt to reality. Before comparing them with the 4D method, it could be seen that they were realistic by observing specific flow structures as the flow detachment at the aortic arch, the behaviour of the streamlines and the velocity range, which was maintained within expected values.

Taking all this into account, the boundary conditons used in the Second Case were adopted as the good ones for simulating the main case.

3. **Third Case: uniform supra-aortic vessels pressure (equal to the value at the aorta outlet)**

   Scheme of the boundary conditions:

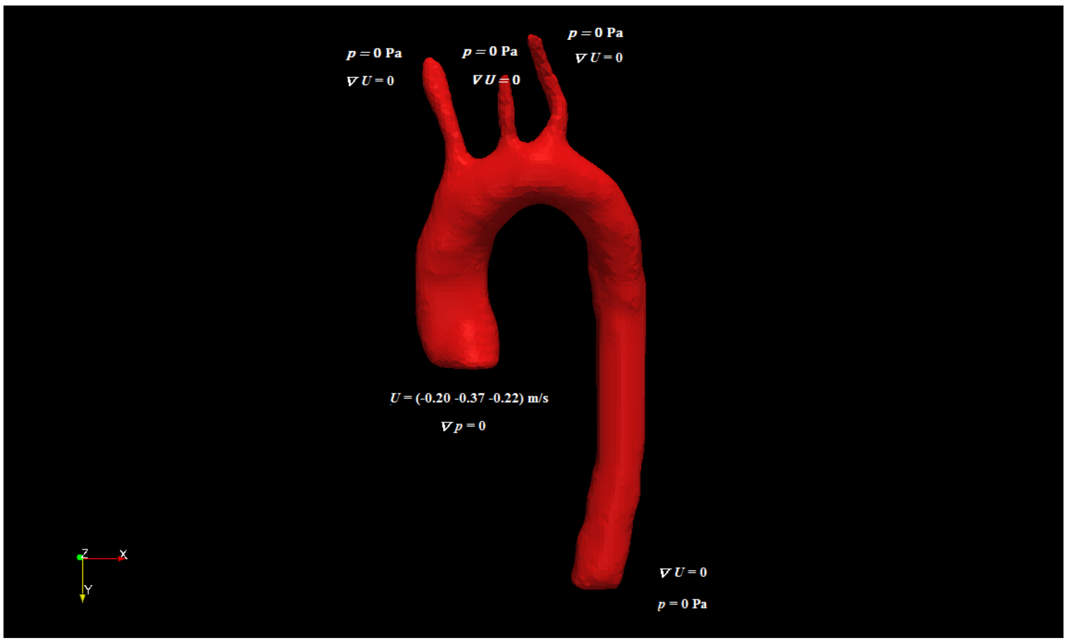

Figure 3.18: Boundary conditions applied to the Third Case

Results:

This kind of boundary conditions were known to be erroneous (as it has previously been explained). However, the Third Case had been simulated in order to observe which differences exist with respect to the Second Case. Furthermore, it would be possible to estimate how big is the error by assuming that all the outlets are at the same external pressure.

In the following table, it is possible to observe the distribution of flow rate depending on whether the boundary conditions of the Second Case or the Third Case are used:

Table 3.1: Percentage of flow rate in each vessel with respect to the inlet flow rate

Patch	**Second Case**	**Third Case**
S01	10.47 %	13.73%
S02	3.92 %	4.20%
S03	6.95 %	6.56%

The differences between the flow behaviour in each case can be observed in Figures 3.19 and 3.20:

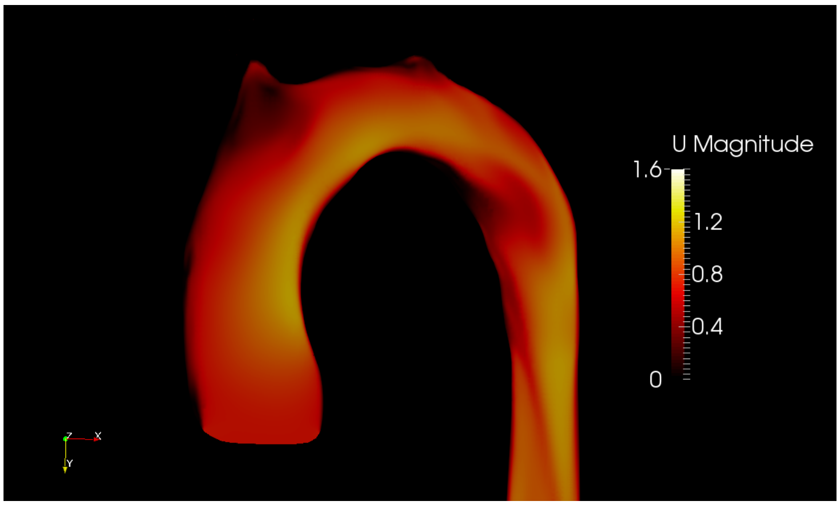

Figure 3.19: $|\mathbf{U}|$ in a section of the Second Case

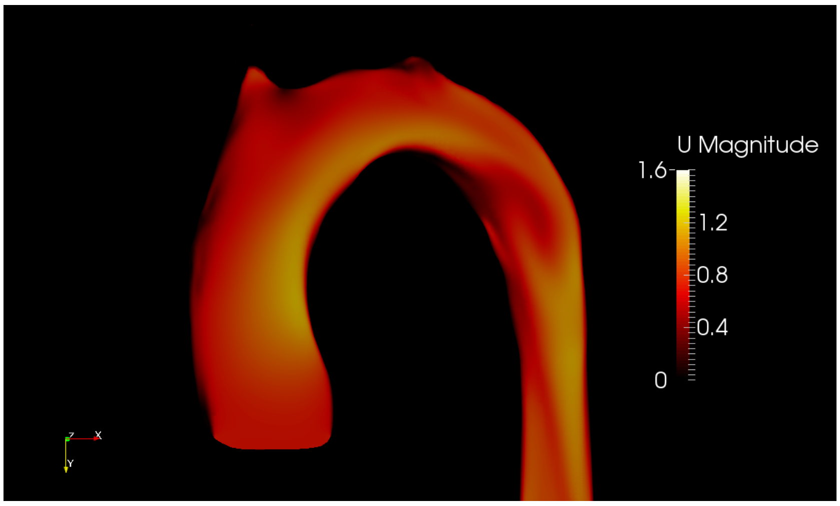

Figure 3.20: $|\mathbf{U}|$ in a section of the Third Case

As can be seen, although in the Third Case the boundary conditions are not appropriate, both the flow rate distribution and the flow behaviour are not very far from the results obtained in the Second Case. Perhaps the main difference comes from the fact that in the first supra-aortic vessel (patch `S01`) the fluid is being more strongly suctioned and therefore the flow rate increases with respect to the expected one. This higher suction can be explained by considering that in the Third Case the pressure at the outlets is lower than what is required and thus the suction force increases. However, as the values shown in Table 3.1 are not significantly different, and glancing at Figures 3.19 and 3.20 it can be appreciated that the main flow structure is similar, it might be hypothesized that the pressure drop between the supra-aortic vessels and the outlet of the thoracic aorta is not as different as it would be initially thought.

Computation of the boundary conditions in the Second Case:

As explained in Chapter 2, the inlet velocity is not uniform. As the flow is being pumped from the heart by a valve with a specific geometry, the inlet velocity profile presents a similarity with this geometry, as shown in Figure 3.21:

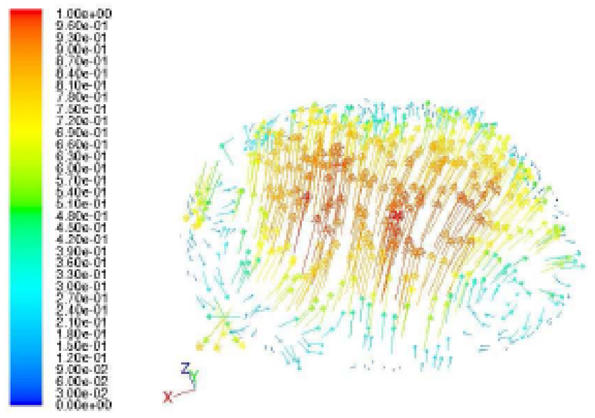

Figure 3.21: Real inlet velocity profile at the aorta inlet (m/s), extracted from [22]

This characteristic velocity profile is produced by the effect of the valve opening in the middle. However, once the fluid enters the aorta it rapidly acquires a parabolic velocity profile, so imposing a uniform velocity at the inlet does not significantly affect the results of the simulation.

For the computation of the inlet velocity vector, the following steps were followed:

(a) As the Second Case is based on imposing outlet flow rates in the supra-aortic vessels, the inlet flow rate needs to be set accordingly. By considering the real measures obtained from the 4D method, the inlet volumetric flow rate for that aorta geometry is 259.14 ml/s

(b) As the velocity boundary condition needs to be a vector and a standard model was considered, its direction was set parallel to the normal vector of the inlet patch

(c) The area vector of patch inlet was computed by using OpenFOAM utilites and is equal to $\vec{A} = (-1.2916\times10^{-6}\ 3.7814\times10^{-4}\ -5.33789\times 10^{-7})\ m^2$. Its module is $\|\vec{A}\| = 4.31163 \times 10^{-4}\ m^2$

(d) The module of the main inlet velocity was computed considering the inlet area and the volumetric flow rate:

$$U_{mean} = k_c \frac{Q_{inlet}}{\|\vec{A}\|} \tag{3.1}$$

where k_c is a constant that needs to be included because the inlet patch is not completely bidimensional:

$$k_c = \frac{flux\ required}{flux\ of\ a\ 3D\ inlet} = 0.42$$

This constant was necessary because when the simulation was carried out with an inlet velocity according to Equation 3.1 without k_c, the inlet flow rate computed after the simulation was higher than expected. It was concluded that this was due to the fact that the inlet patch was not completely two-dimensional. k_c then expresses the relation between the flow rate that was erroneously obtained and the required volumetric flow rate (259.14 ml/s).

(e) The area vector of patch inlet was normalized so that $\vec{n} = \frac{1}{\|\vec{A}\|} \vec{A} = (-2.9956 \times 10^{-3}\ 0.877\ -1.238 \times 10^{-3})$

(f) Finally, the velocity vector which was used as boundary condition was expressed according to:

$$\overrightarrow{U_{mean}} = U_{mean} \cdot \vec{n} = (-2.34 \times 10^{-3}\ -0.68\ -9.67 \times 10^{-4})\ m/s$$

In the following figure it is possible to observe the uniform inlet velocity profile used as inlet boundary condition, being applied parallel to the inlet's patch normal vector for a realistic simulation:

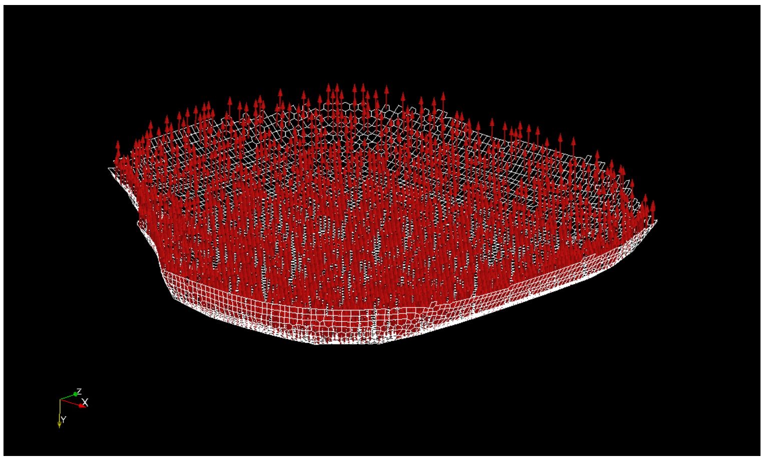

Figure 3.22: Aorta inlet velocity profile. Vectors perpendicular to the patch

Appendices A.9 and A.10 show dictionaries of the pressure (p) and velocity ($\mathbf{U}$). By way of example, the instructions of the pressure boundary conditions at the inlet and the outlet are next shown:

```
    inlet
    {
        type                zeroGradient;
    }

    outlet
    {
        type                fixedValue;
        value               uniform 0;
    }
```

and the velocity boundary conditions at the inlet and the S01:

```
    inlet
    {
        type                     fixedValue;
        value                    uniform (-2.3407e-03 -0.6853 -9.674e-04);
    }
    S01
    {
        type                     flowRateInletVelocity;
        volumetricFlowRate       -2.713e-05;
        value uniform            (0 0 0);
    }
```

Main difficulties:

- Initially, the First Case and the Third Case were used, as they represent standard types of boundary conditions (imposing either a velocity or a pressure). Once it could be seen that none of them offered suitable results, it took a long time to test new models and boundary conditions. Finally, the volumetric flow rate condition was implemented, and its results became the most valid
- Due to the fact that a volumetric flow rate is not commonly used as a boundary condition, its validity had to be studied and proved
- Initially, the flow rate distribution did not match reality because the velocity measures obtained from the 4D method had to be adapted to the OpenFOAM aorta patches (as they are differently defined). Accuracy with the proportion of flow rates in each patch was crucial in order to obtain suitable results and to simulate the aorta as realistically as possible
- The first method used to compute the flow rate in each vessel suggested that the flow is parabolic within the aorta when it is fully developed. Then, for parabolic velocity profiles, $U_{mean} = \frac{U_{max}}{2}$, and by using each patch area, the volumetric flow rate was computed. However, by using this method, the flow rate distribution did not offer realistic results and the process of computing the boundary conditions had to be changed

3.3 Physical properties

Aim of the task: the codes shown in this section complete the physical information of the simulations (together with the boundary conditions). Mainly, it is necessary to specify the kinematic viscosity and the nature of the case (laminar or turbulent).

Work methodology: as has been explained in Section 2.4, in this work blood is considered a Newtonian fluid (and therefore with constant viscosity). This information, as well as the value of the kinematic viscosity is included in the *transportProperties* file, in *constant*. It is shown in Appendix A.11.

On the other hand, as the case is laminar, no turbulence models had to be implemented. This information is included in the *RASProperties* file (Appendix A.12), also located within *constant*.

3.4 Control, discretization and linear-solver setting

Aim of the task: the codes shown in this section contain information related to the time control, the discretization and the linear-solver settings. They are mainly related to the mathematical treatment of the simulation and play a relevant role on its convergence.

Work methodology: to define these parameters, 3 different dictionaries were used:

1. **controlDict:** it specifies the solver of the case and how many time steps are used. Again, as peak systolic conditions are modeled (steady flow), simpleFoam has been used. simpleFoam is a steady-state solver for incompressible, turbulent flow. The *controlDict* dictionary is shown in Appendix A.13.
2. **fvSchemes:** it specifies the choice of finite volume discretization schemes (Appendix A.14).
3. **fvSolution:** it specifies the linear equation solvers, tolerances and other algorithm controls (Appendix A.15).

3.5 Justification of the mesh refinement

Aim of the task: as explained in Section 3.1.5, a very accurate cell refinement was obtained at the walls of the aorta (of the order of micrometers). However, as good as it may seem, it was necessary to estimate the error made when computing the wall shear stress. Only if the error stays bounded to low values, this refinement could be considered suitable.

Work methodology: as the real values of wall shear stress at the walls of the aorta are unknown (in fact, this is the aim of the work), there is no way of contrasting the results of the simulation. Therefore and with all due caution, an analogue of the aorta such as a circular pipe was modeled and simulated.

Although the geometries of a healthy aorta and a straight, large, circular pipe are different, by imposing the same cell refinement, boundary conditions, Reynolds number and volumetric flow rate, the comparison could provide acceptable conclusions regarding the error made by using this mesh refinement.

It could be done because in a large straight circular pipe the exact value of the wall shear stress can be analytically computed.

In Figure 3.23, a wedge of the pipe is shown with its values of refinement. y is the distance between the pipe wall and each node:

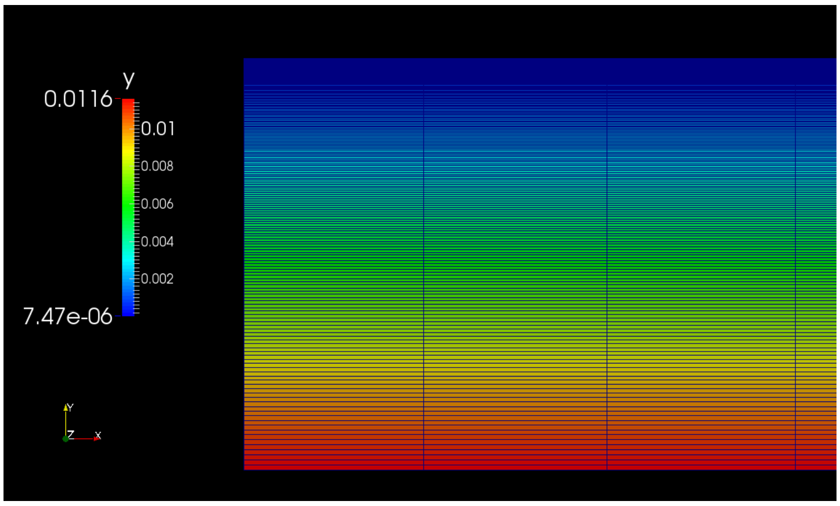

Figure 3.23: Wedge of the circular pipe used for testing the mesh refinement

Mathematically, the wall shear stress in a large, circular pipe is (in cylindrical coordinates):

$$\tau_w = \mu \frac{\partial U}{\partial r} = -\frac{dp}{dz}\frac{r}{2} \tag{3.2}$$

where r is the radius of the pipe. According to the boundary conditions, the analytical wall shear stress is:

$$\tau_w = 235.2355 \cdot 5.855 \times 10^{-3} = 1.37730 \; Pa$$

On the other hand, the wall shear stress computed by OpenFOAM with a mesh refinement at the walls similar to the one used for the aorta simulation is:

$$\tau_w = 1.37599 \; Pa$$

By comparing both values, a relative error of $e_r = 0.095\%$ is obtained.

Conclusion: the relative error obtained is very low. Consequently, although the geometry of a real aorta is different and the behaviour of the flow is more complex (there are detachments and vortices), the mesh refinement can be considered adequate. It can be concluded that although in the real simulation the average error may increase, since the relative error in the pipe simulation is extremely low, the real wall shear stress value will stay bounded into a suitable range.

4. Results of the aorta simulation

In the current chapter, the results of the simulation are presented, carried out according to the pre-processing instructions, processes and dictionaries included in Chapter 3.

4.1 Module of the velocity field

First of all, plots of the velocity field are displayed. In the following figures, the module of the velocity ($|\mathbf{U}|$) in each point is shown:

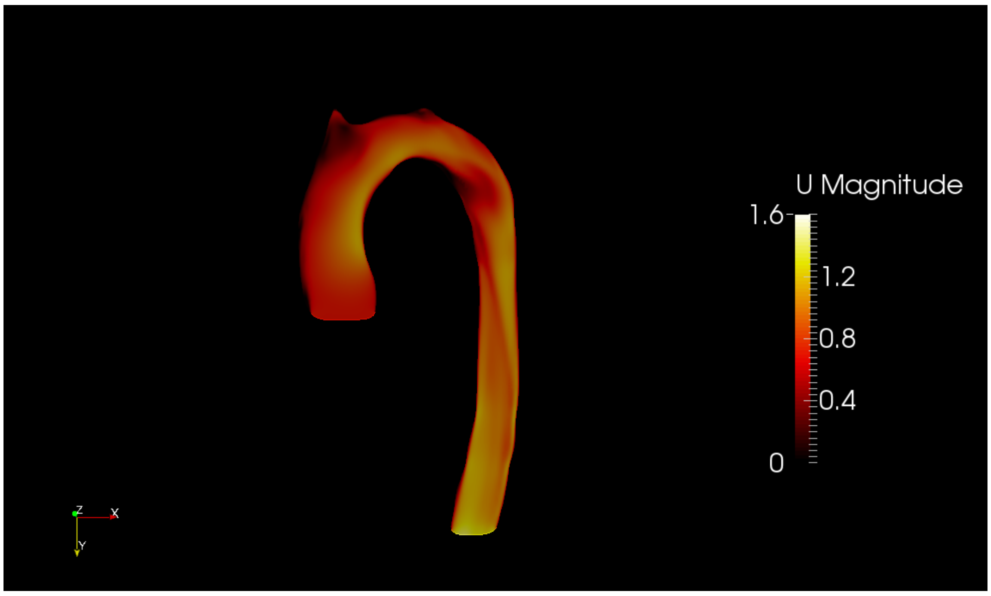

Figure 4.1: $|\mathbf{U}|$ in a general longitudinal slice of the aorta (m/s)

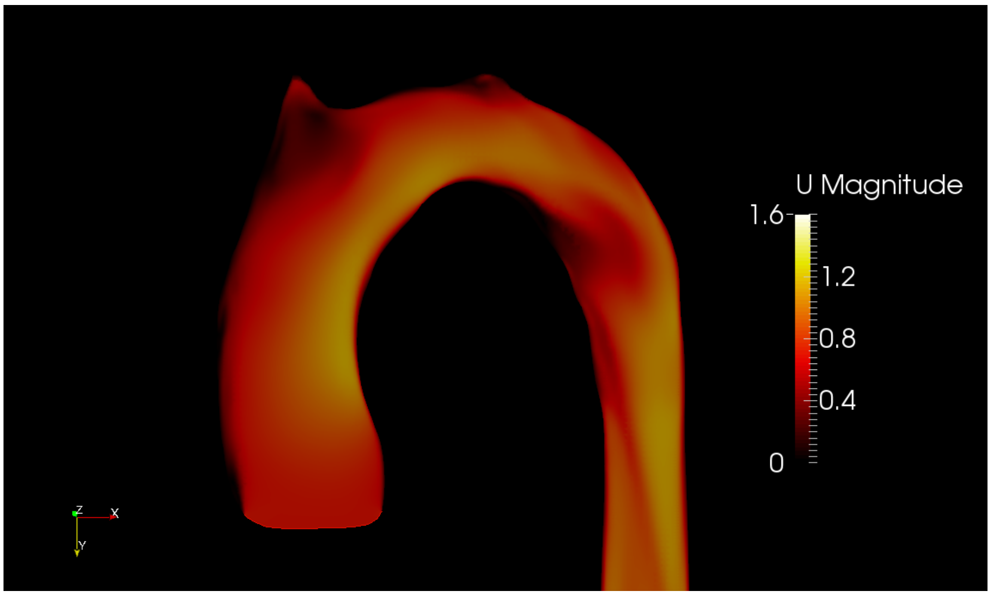

Figure 4.2: $|\mathbf{U}|$ in a longitudinal slice of the aortic arch (m/s)

Figures 4.3 and 4.4 show a longitudinal slice of the aorta with different transverse sections to adequately observe the behaviour of the flow in the whole geometry:

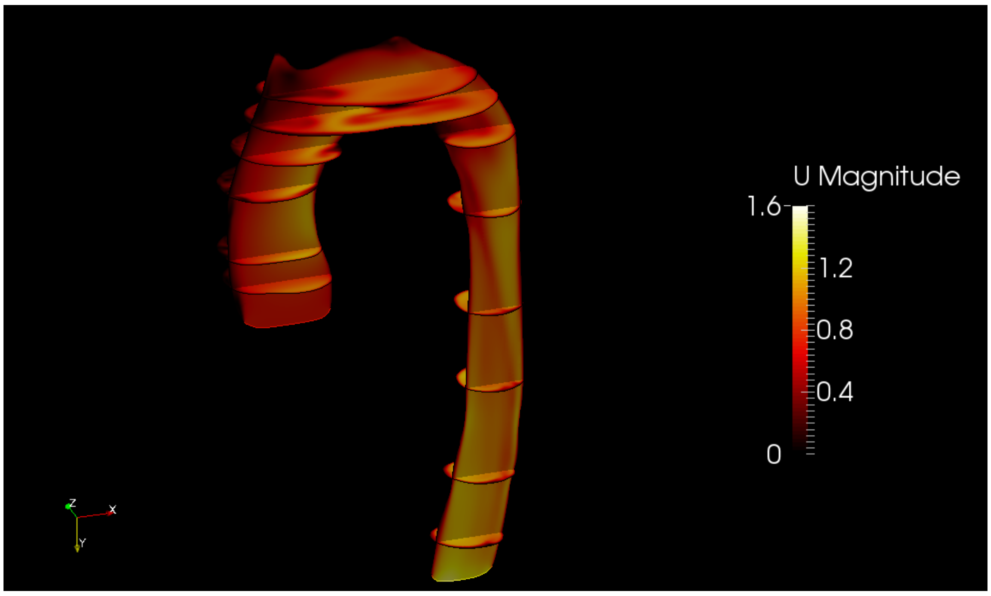

Figure 4.3: $|\mathbf{U}|$ in a longitudinal slice of the aorta from the front part (m/s)

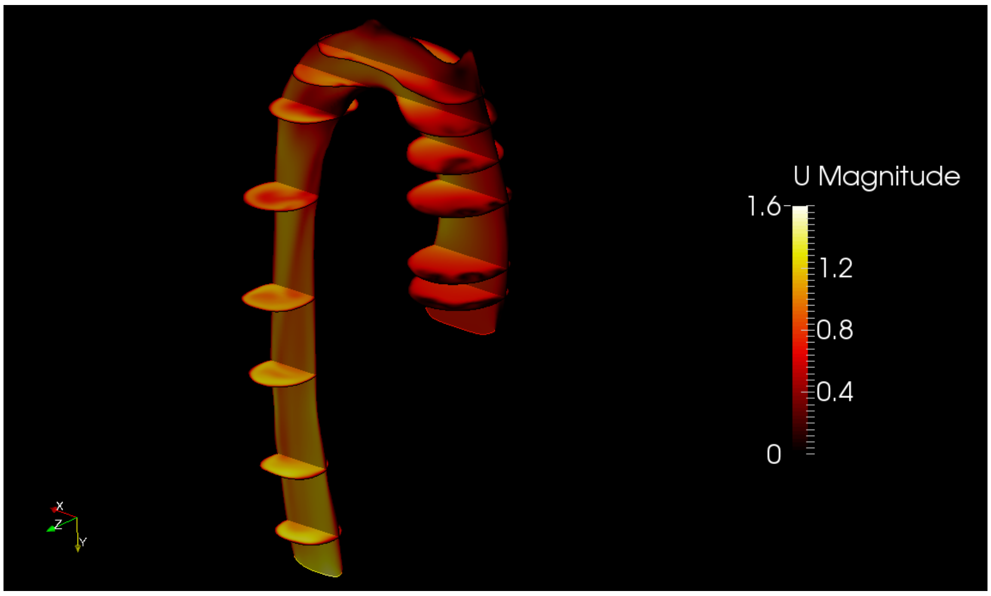

Figure 4.4: $|\mathbf{U}|$ in a longitudinal slice of the aorta from the back part (m/s)

Each one of the transverse slices previously shown is exposed in more detail (they are presented in an order such that they start at the inlet and end at the outlet):

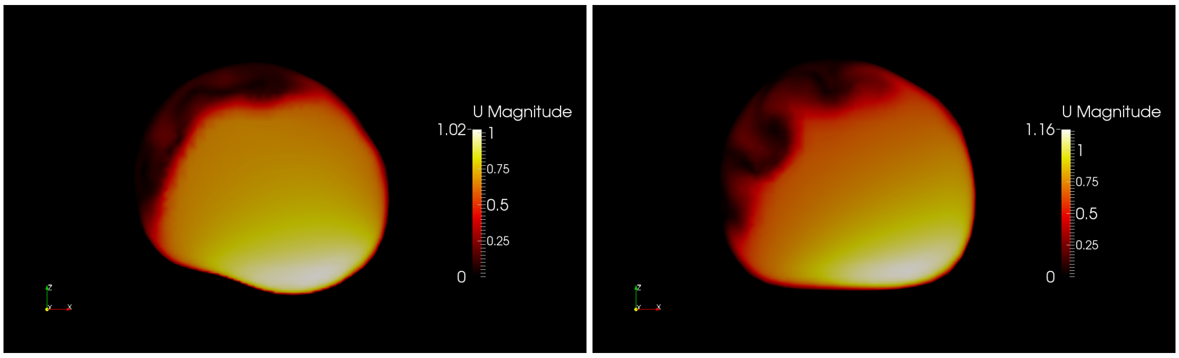

Velocity module in slices of the aorta simulated with OpenFOAM. Slices at $y = 0.005$ and $y = 0.039$

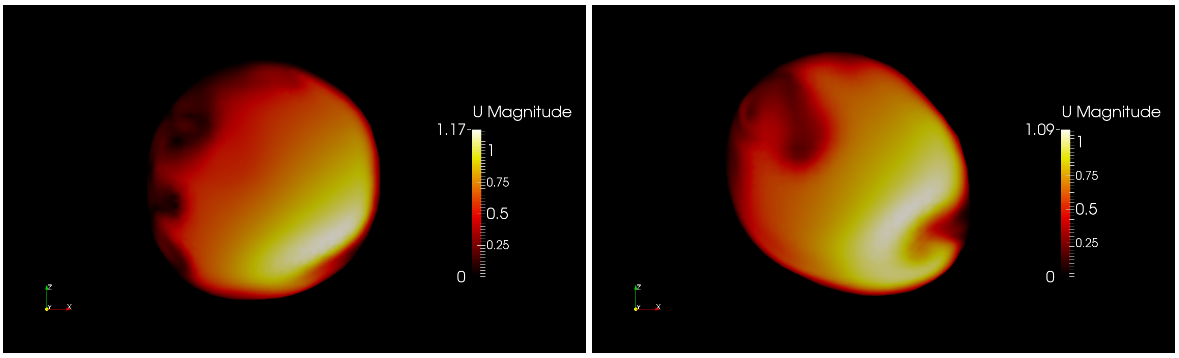

Velocity module in slices of the aorta simulated with OpenFOAM. Slices at $y = 0.022$ and $y = 0.013$

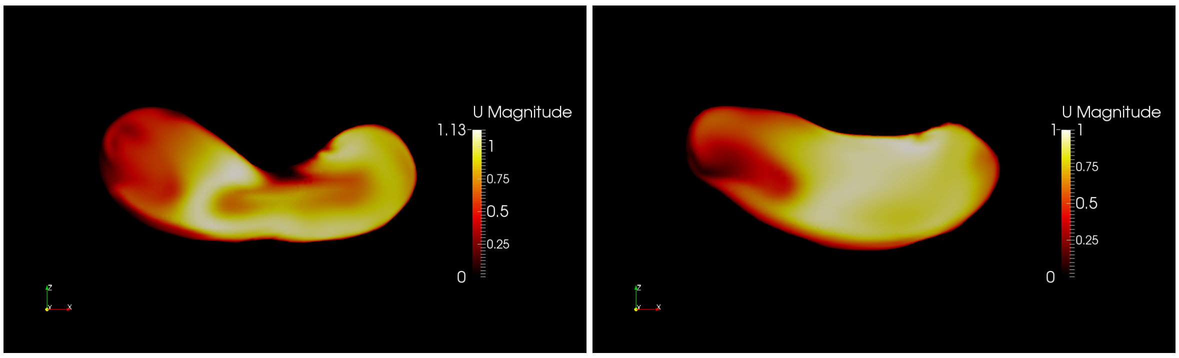

Velocity module in slices of the aorta simulated with OpenFOAM. Slices at $y = 0.005$ and $y = -0.002$

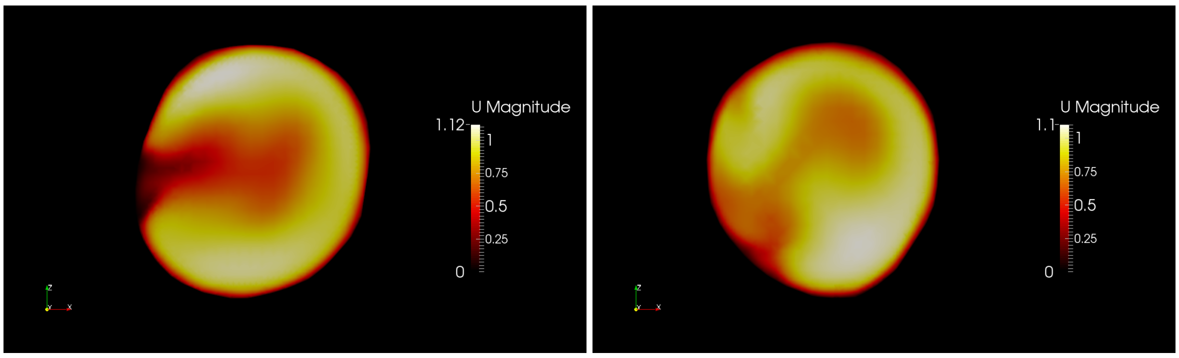

Velocity module in slices of the aorta simulated with OpenFOAM. Slices at $y = 0.014$ and $y = 0.036$

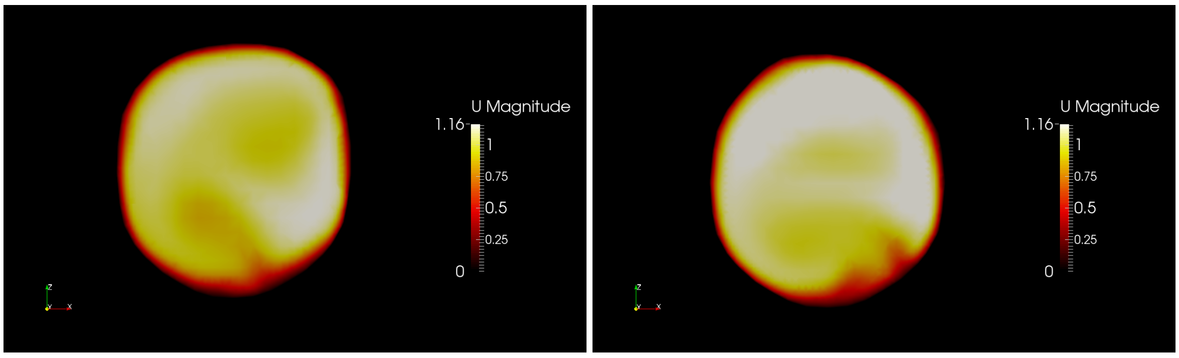

Velocity module in slices of the aorta simulated with OpenFOAM. Slices at $y = 0.062$ and $y = 0.082$

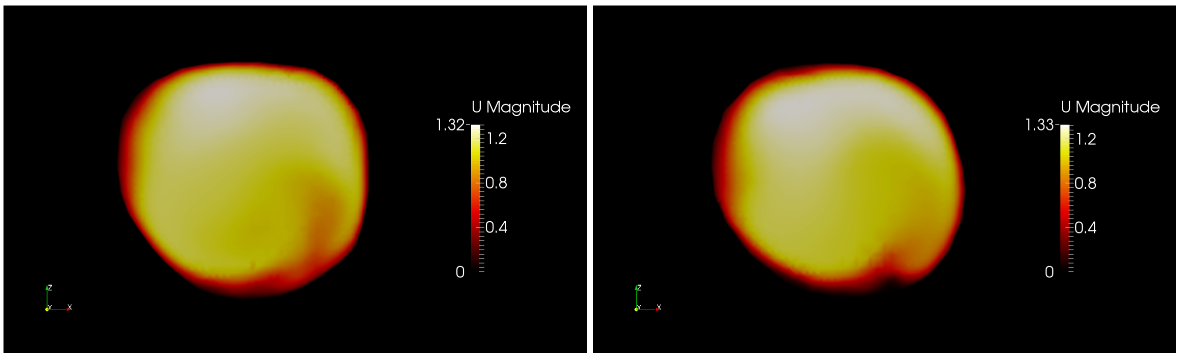

Velocity module in slices of the aorta simulated with OpenFOAM. Slices at $y = 0.105$ and $y = 0.121$

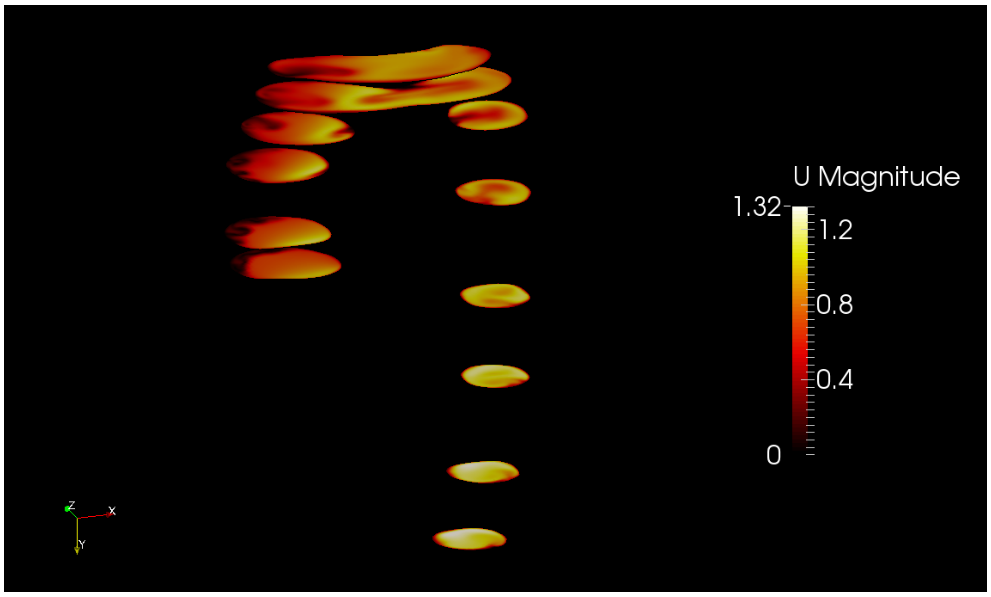

Figure 4.5: $|\mathbf{U}|$ in transverse slices seen from the front part (m/s)

4.2 Streamlines

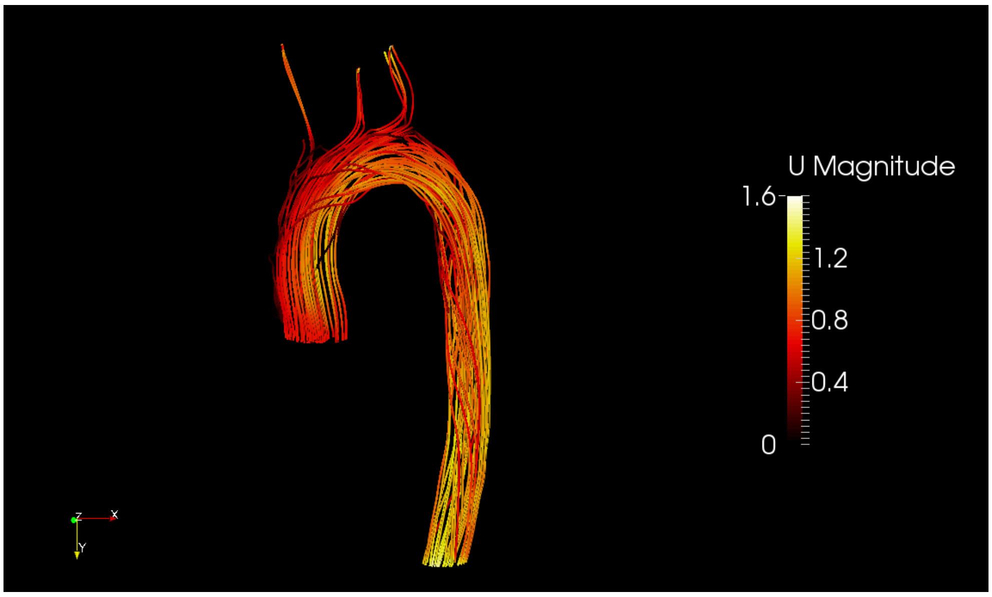

Figure 4.6: Streamlines of the flow seen from the front part (m/s)

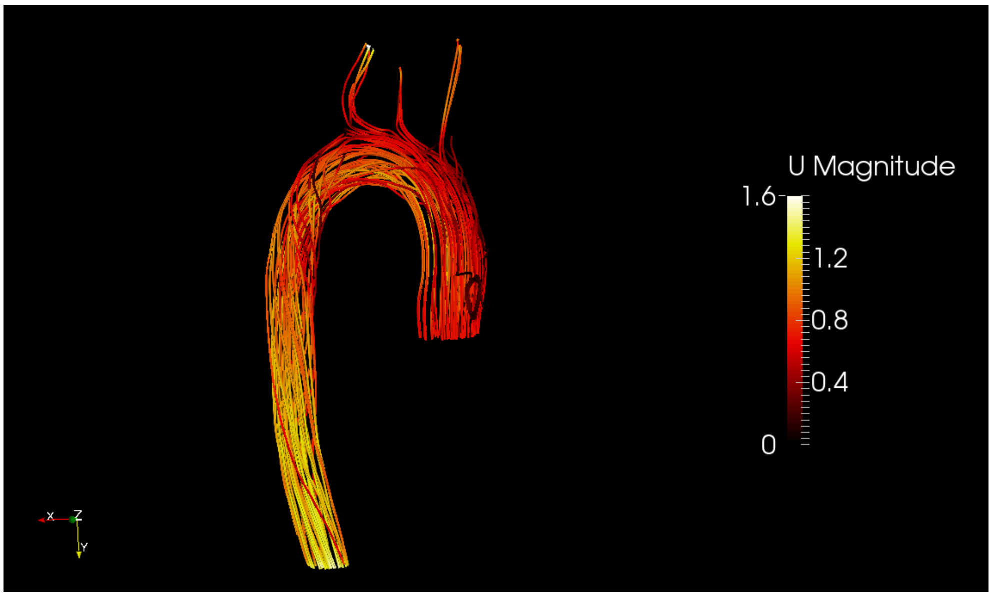

Figure 4.7: Streamlines of the flow seen from the back part (m/s)

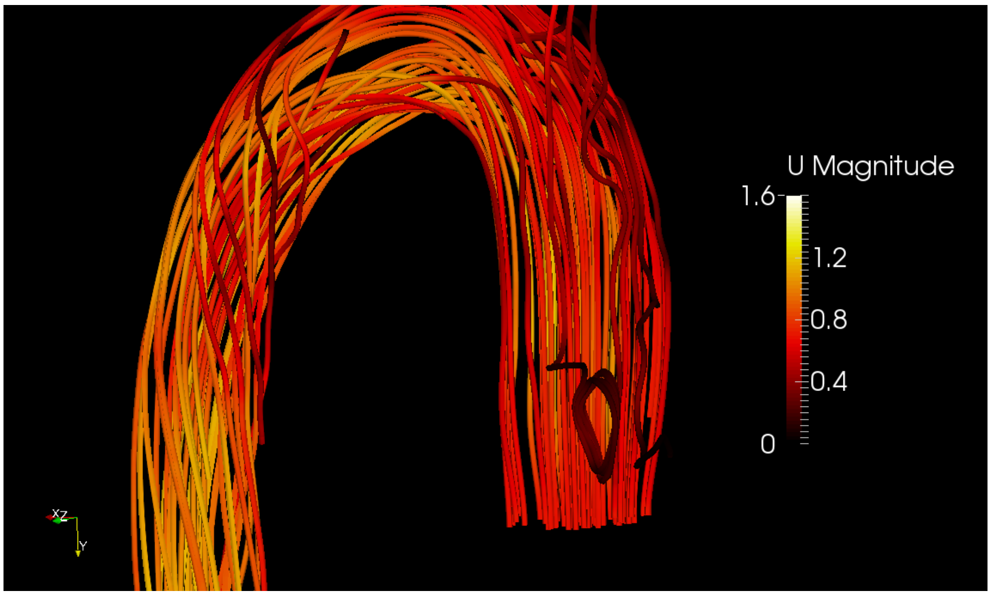

Figure 4.8: Detail of the streamlines of the flow at the inlet and the aortic arch (m/s)

Two interesting characteristics to observe are the vortices generated at the inlet and the torque component of the velocity after the aortic arch.

4.3 Vector field

The module of the vectors shown in the following figures does not correspond to the magnitude of their velocity, which is represented by their color. This has been done for a better understanding. The inlet vortices can be observed again in Figure 4.10:

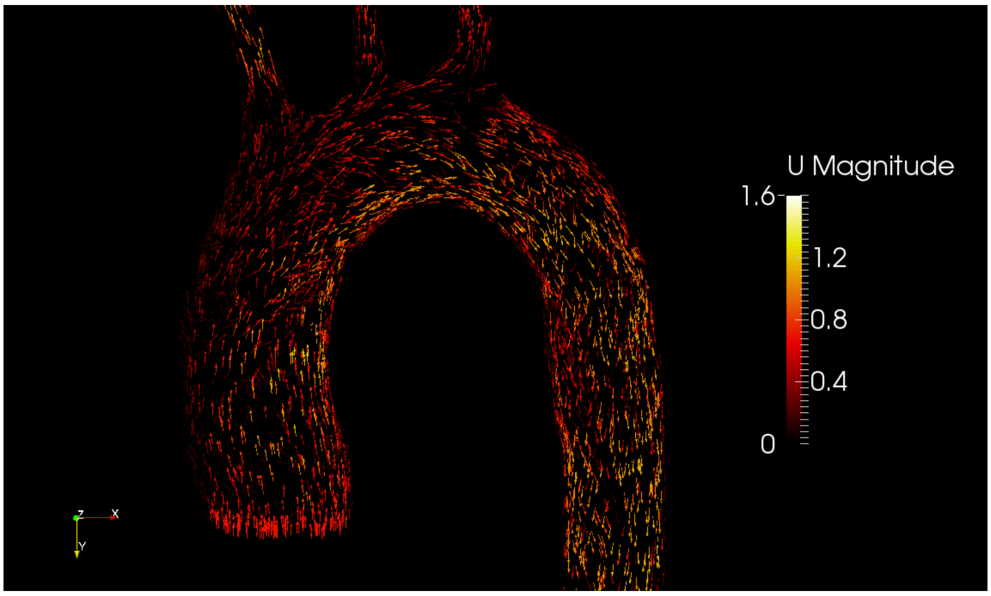

Figure 4.9: Velocity vectors at the aortic arch (m/s)

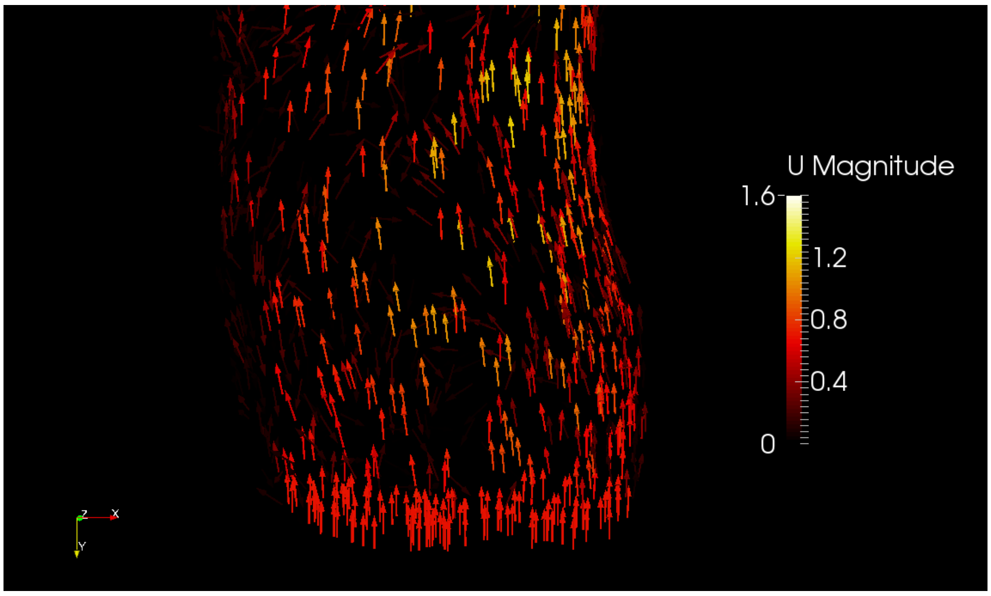

Figure 4.10: Velocity vectors at the aorta inlet (m/s)

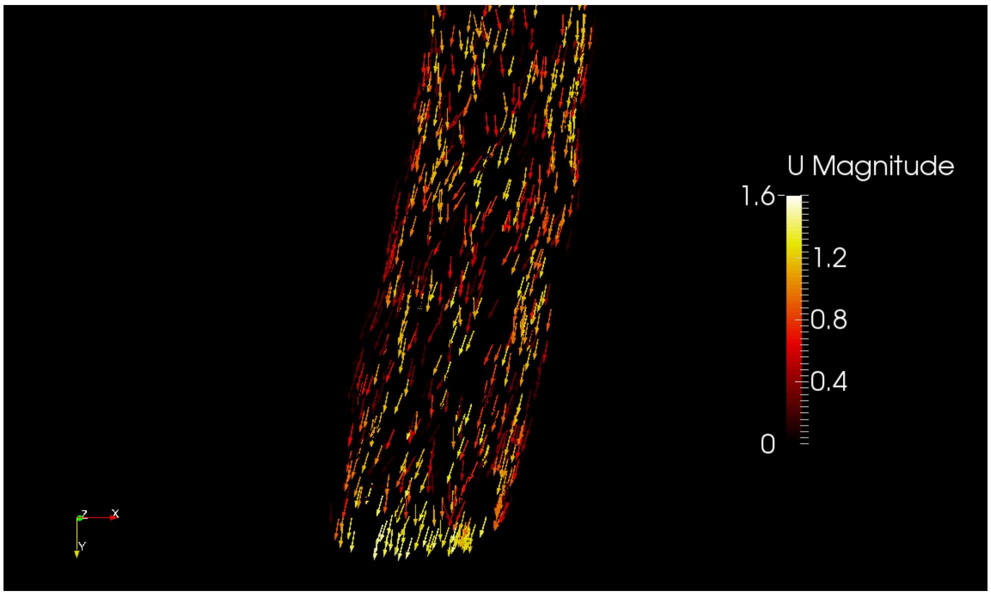

Figure 4.11: Velocity vectors at the aorta outlet (m/s)

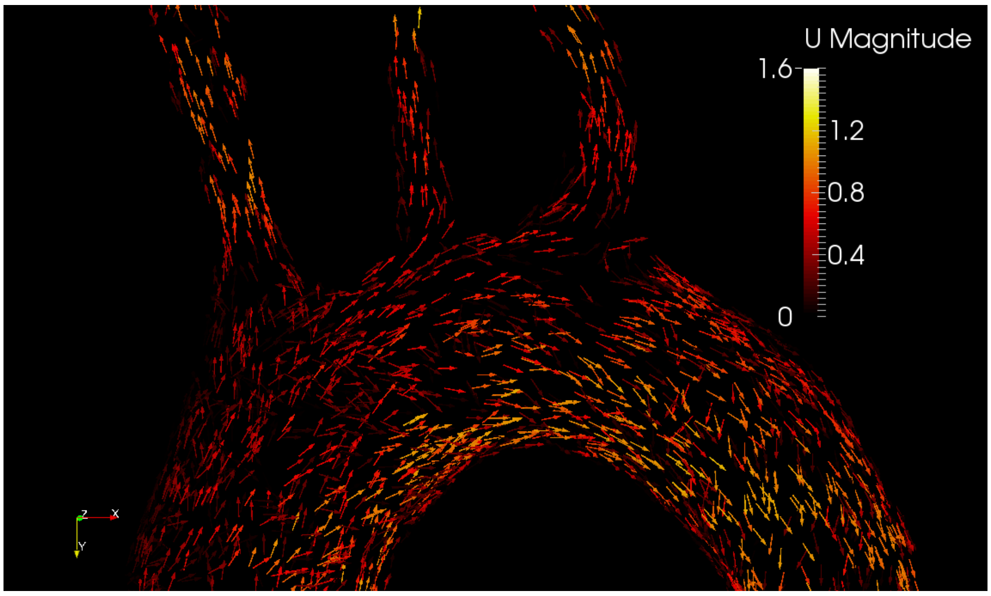

Figure 4.12: Velocity vectors at the inlet of the supra-aortic vessels (m/s)

4.4 Wall shear stress

It is first necessary to remember that the values of wall shear stress that OpenFOAM provides are divided by the value of the density ($\rho = 1040\ kg/m^3$ for blood) of the fluid:

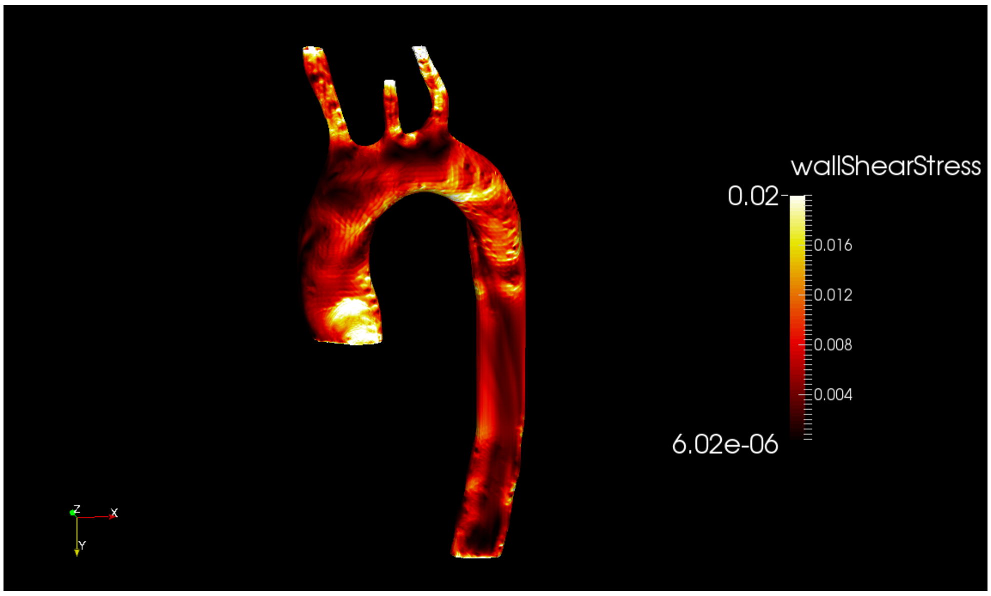

Figure 4.13: Wall shear stress at the front part of the aorta (m^2/s^2)

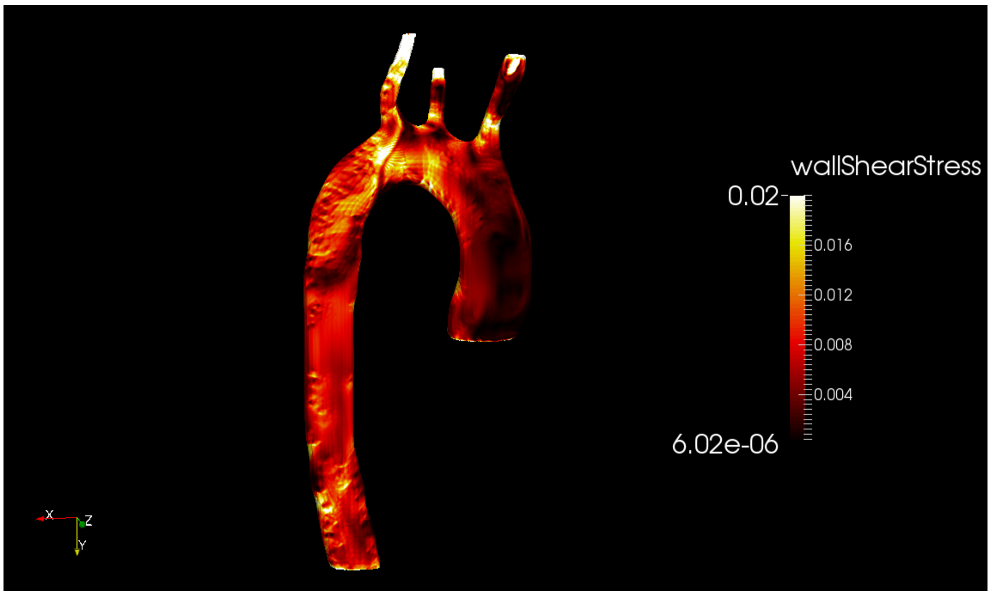

Figure 4.14: Wall shear stress at the back part of the aorta (m^2/s^2)

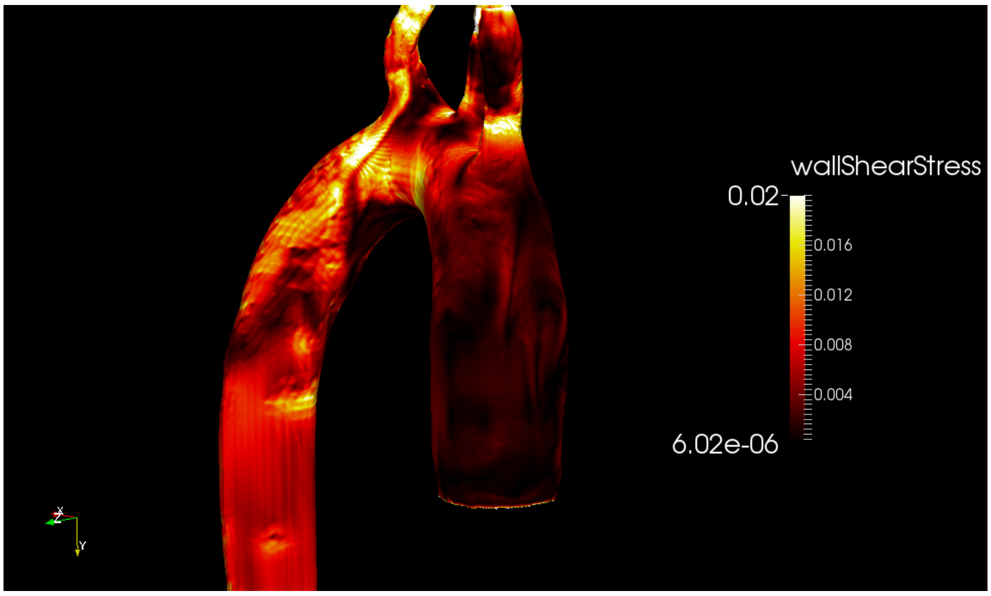

Figure 4.15: Detail of the wall shear stress at the aorta inlet and at the aortic arch (m^2/s^2)

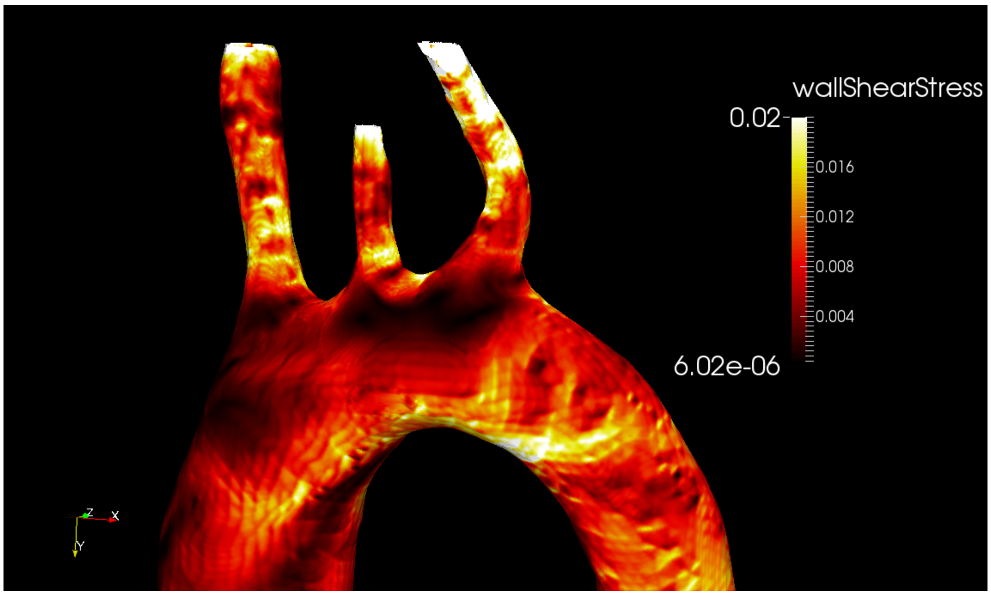

Figure 4.16: Detail of the wall shear stress at the inlet of the supra-aortic vessels (m^2/s^2)

5. Analysis of the results

5.1 Analysis of the OpenFOAM simulation

5.1.1 Validation of results

As explained in 3.5, real distributions of wall shear stress and flow patterns in healthy thoracic aortas are unknown, thus the results need to be analyzed and compared. The first step is to ensure that the main characteristics of blood through real aortas are met. There are particular aspects in literature (coming either from medical research or other CFD simulations) which are accepted as common flow patterns for standard thoracic aorta geometries and boundary conditions. Thereby, at a first glance, the simulation must resolve adequately the following aspects:

1. Flow detaching on the aortic arch due to an adverse pressure gradient
2. Flow rate through the supra-aortic vessels between 20% and 30% of the inlet flow rate (it was imposed, so it indeed adapts to reality)
3. Wall shear stress distribution compressed between 20 Pa and 0 Pa, with predominance of values around 8 Pa

All the above characteristics have been met with the OpenFOAM simulation, and are fundamental to initially guarantee that it ran properly. Furthermore, the streamlines and the vector field also show a coherent behaviour, and the velocity values stay bounded within a suitable range.

The second step is to compare the results of the OpenFOAM study with another CFD simulation. Accordingly, there is next a comparative between the wall shear stress distribution obtained with OpenFOAM and with Ansys Fluent. The study used for the comparison has been extracted from [22], the one found in the literature which resembles more the present OpenFOAM simulation.

The variable to be compared is the wall shear stress, as its computation represents the main objective of the current aorta study. Furthermore, as the wall shear stress is computed in the post-processing, if its distribution and values seem to adapt to other cases, the velocity field is then likely to also fit correctly. For the comparative, it has been intended to use an external simulation as close to the one carried out in this project as possible. It implies similar geometries (otherwise the wall shear stress distribution might differ although both had been correctly simulated), flat inlet velocity profile, outlet velocity profiles as boundary conditions, laminar Newtonian flow, peak systolic conditions and rigid and static aorta walls. The results are:

OpenFOAM ***Ansys Fluent***

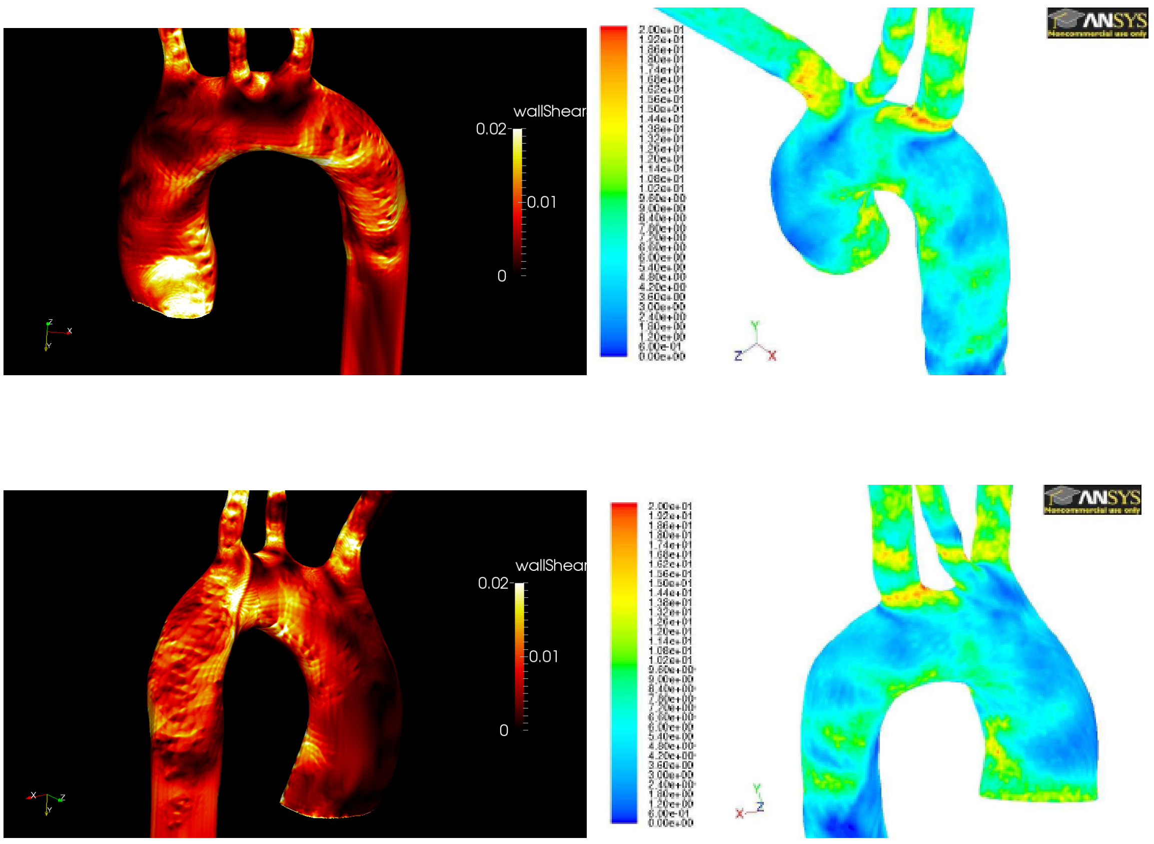

Comparison between simulations carried out with OpenFOAM or Ansys Fluent

The units of the wall shear stress in the Ansys Fluent simulation are *Pascals*, while in OpenFOAM are m^2/s^2.

Comments:

A first factor indicating that the results seem reliable is that both simulations present the range of the wall shear stress compressed between the same values, 0-20 Pa. It implies that the numerical results of both simulations are kept bounded within the same interval

Regarding the wall shear stress distribution, both simulations present similar patterns: in the ascending aorta, low values appear on its outer part and high values on its inner part. At the inlet of the supra-aortic vessels there are high flow accelerations, and therefore high values of wall shear stress. At the same time, near these areas and in the aortic arch there are zones presenting low concentrations of wall shear stress. Finally, just at the beginning of the descending aorta there are intermitent areas with high stress values, followed by a dark stain (low values), perhaps due to the flow detachment which occurs in this region

Both cases, using different MRI data, present the same uniform inlet velocity (approximately 0.69 m/s). It corroborates the method used in this project to compute this value (Section 3.2), guarantees that the inlet flow rate matches reality and that the MRI values used in this project are correct

Despite the above, there are some differences between both simulations, such as the fact that the stress at the inlet is higher for the OpenFOAM simulation. It probably happens due to the segmentation of the geometry used in each case. Since for the OpenFOAM simulation the inlet has been defined nearer to the heart, its topology is more adapted to the geometry of the aortic valve. Consequently, the wall shear stress values are higher and less focused

A key factor for the comparison is that the most extended value of wall shear stress is very similar in both cases (the one either in areas without high accelerations or flow detachment, which has been used as a representative value). For the Ansys Fluent simulation, it is represented by turquoise, whose numerical value corresponds at around 6 Pa and 8 Pa. For the case of the OpenFOAM simulation, this representative value may be the soft red, whose numerical value is compressed between $0.007 \cdot 1040 = 7.28$ Pa and $0.008 \cdot 1040 = 8.32$ Pa.

5.1.2 Discussion of results

In the previous Section, the main results were validated and contrasted. However there are other aspects of the simulation which are worth being discussed:

1. **Inlet vortices:** as it can be appreciated in Figures 4.7 and 4.8, there is a formation of vortices near the inlet of the aorta. They can also be observed in Figure 4.5, being represented by dark stains at the outer part of the ascending aorta. The vortices are formed due to the widening of the section just after the inlet, being a part of a natural mechanism of the circulatory system.

One of the hypothesis of the simulation is that right and left coronary arteries are not included. However, these little vessels can be found in real human bodies and are located just at the inlet of the aorta. The vortices that appear in the simulation are in reality generated during systole, providing rotational kinetic energy to the fluid particles to flow through the coronary arteries during diastole. As the geometry used for the simulation does not include them, vortices extend to the aortic arch.

2. **Flow detachment:** flow detaches at the aortic arch, which among other issues affects the velocity profile at the descending aorta. As it can be observed in Figure 4.5, the velocity distribution is parabolic, but with a distinct region presenting low flow speeds due to the detachment. This becomes smooth as the stream descends through the aorta.

3. **Spin flow:** due to the fact that the ascending and descending aorta are not contained within the same plane, a spin component in flow can be observed in the descending aorta. The streamlines of Figure 4.8 offer a clear-cut representation of this pattern.

5.2 Comparison between the CFD OpenFOAM simulations and the 4D medical images

Once the results of the OpenFOAM simulation have been analyzed, the results of the 4D method are introduced.

First of all, a longitudinal slice is presented (speed values of the 4D images are expressed in cm/s):

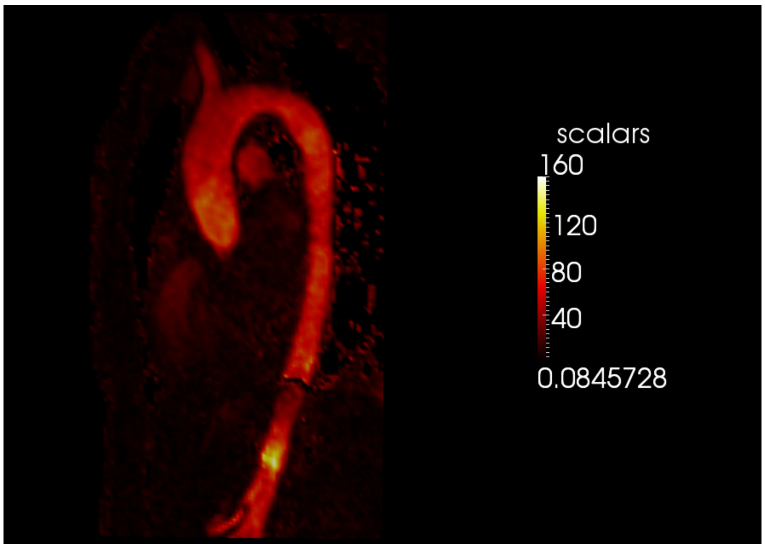

Figure 5.1: |**U**| in a longitudinal slice of the aorta obtained from the 4D method (cm/s)

Next, the same transverse slices presented in Section 4.1 are shown:

4D Images ***OpenFOAM***

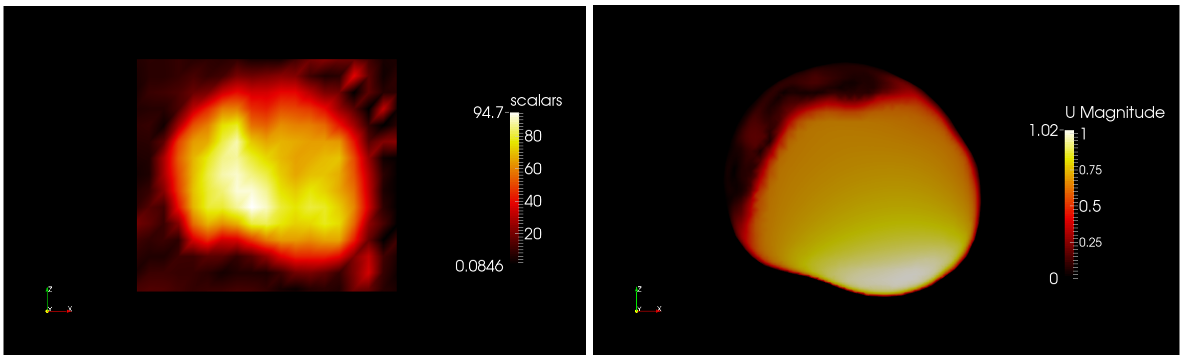

Comparison between the velocity module in slices of the aorta using the 4D method or simulating with OpenFOAM. Slices at $y = 0.046$

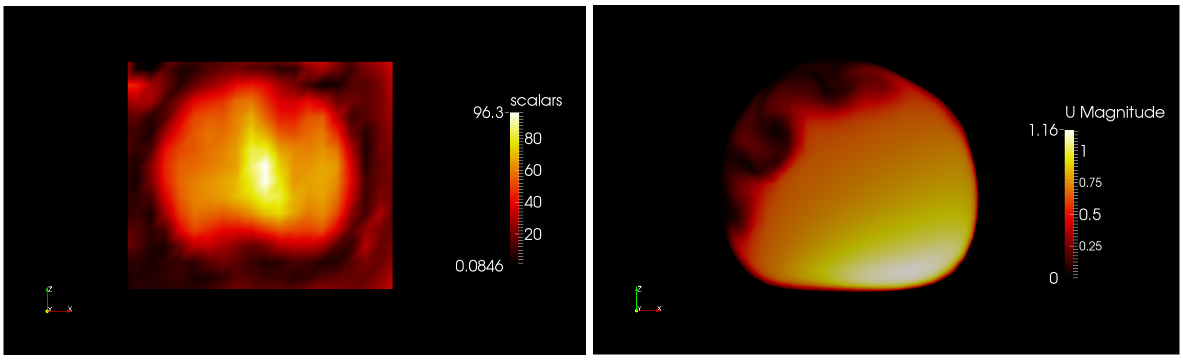

Comparison between the velocity module in slices of the aorta using the 4D method or simulating with OpenFOAM. Slices at $y = 0.039$

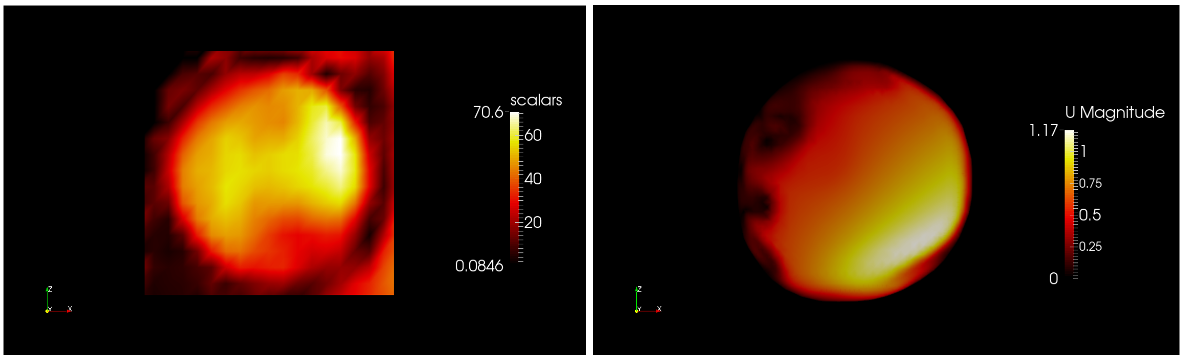

Comparison between the velocity module in slices of the aorta using the 4D method or simulating with OpenFOAM. Slices at $y = 0.022$

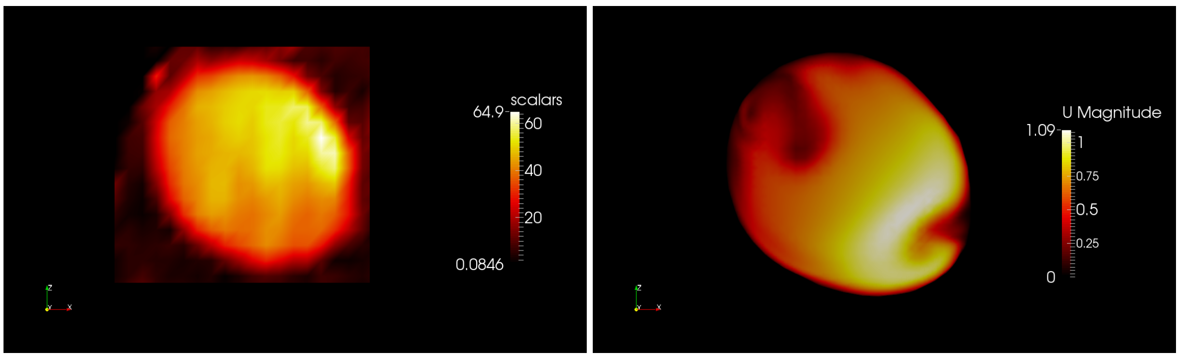

Comparison between the velocity module in slices of the aorta using the 4D method or simulating with OpenFOAM. Slices at $y = 0.013$

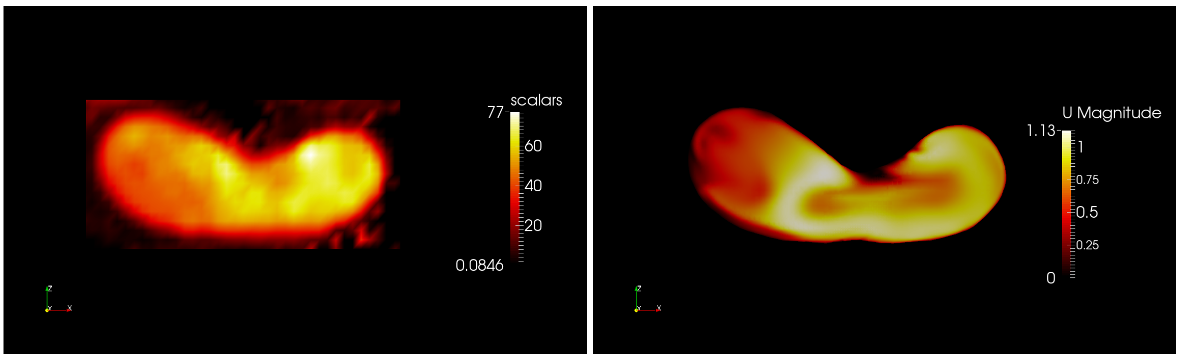

Comparison between the velocity module in slices of the aorta using the 4D method or simulating with OpenFOAM. Slices at $y = 0.005$

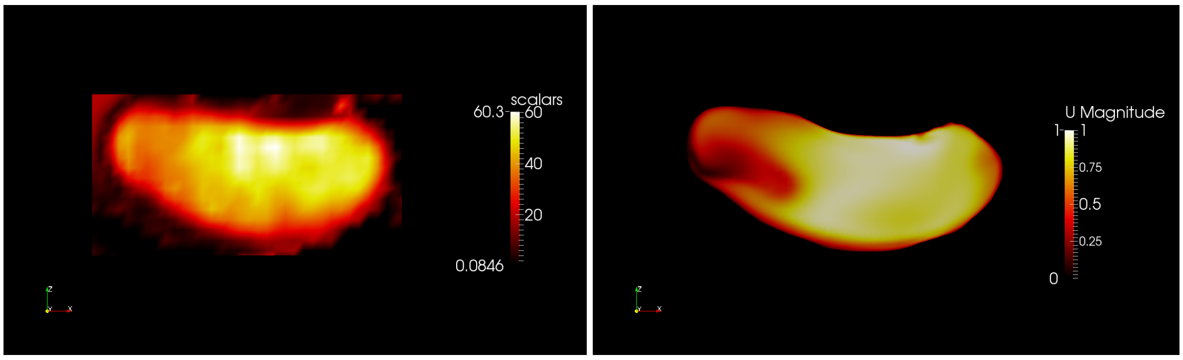

Comparison between the velocity module in slices of the aorta using the 4D method or simulating with OpenFOAM. Slices at $y = -0.002$

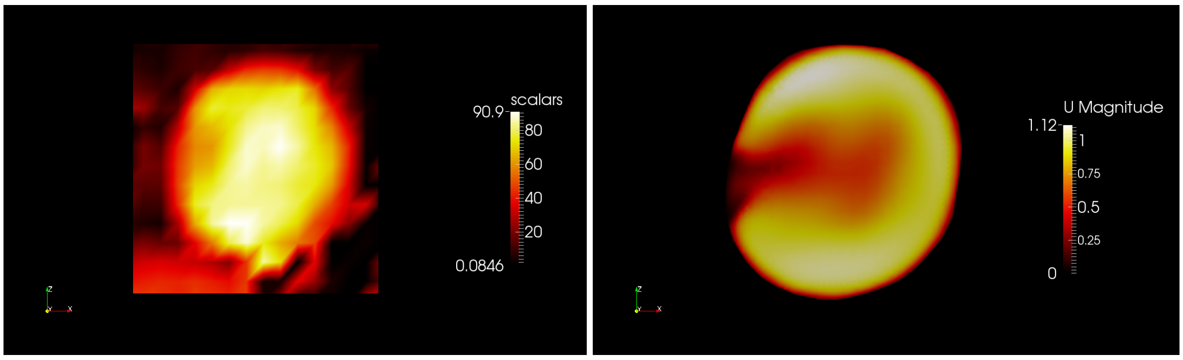

Comparison between the velocity module in slices of the aorta using the 4D method or simulating with OpenFOAM. Slices at $y = 0.001$

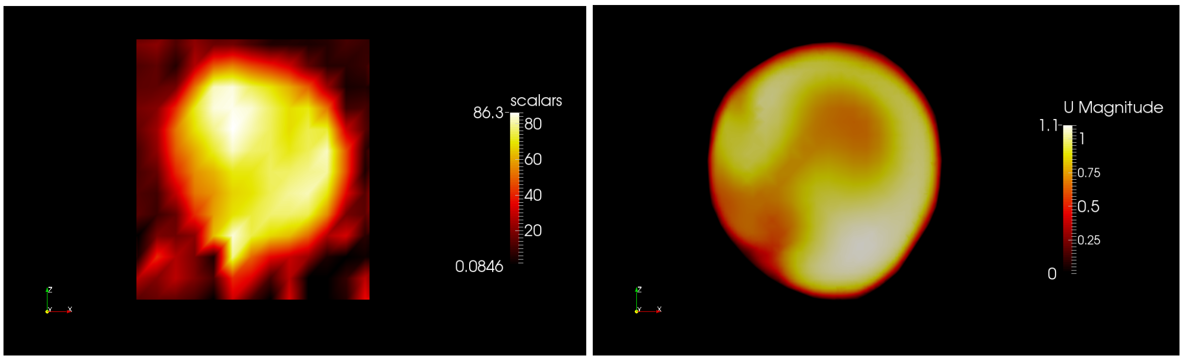

Comparison between the velocity module in slices of the aorta using the 4D method or simulating with OpenFOAM. Slices at $y = 0.004$

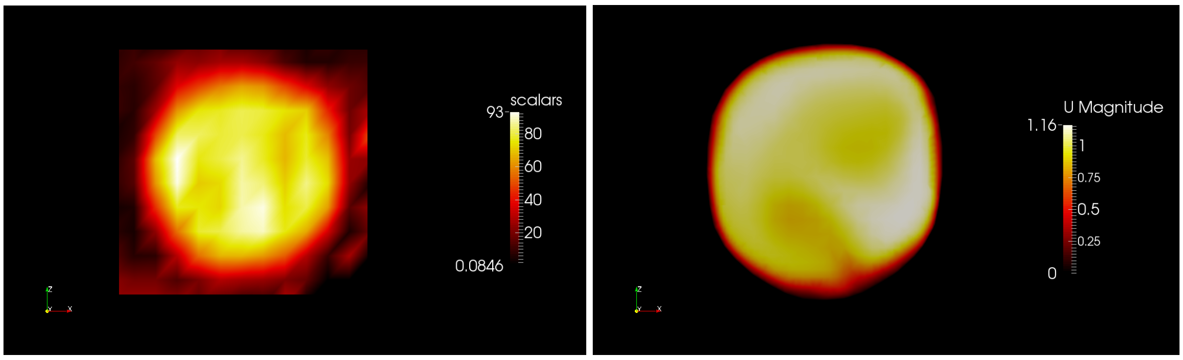

Comparison between the velocity module in slices of the aorta using the 4D method or simulating with OpenFOAM. Slices at $y = 0.062$

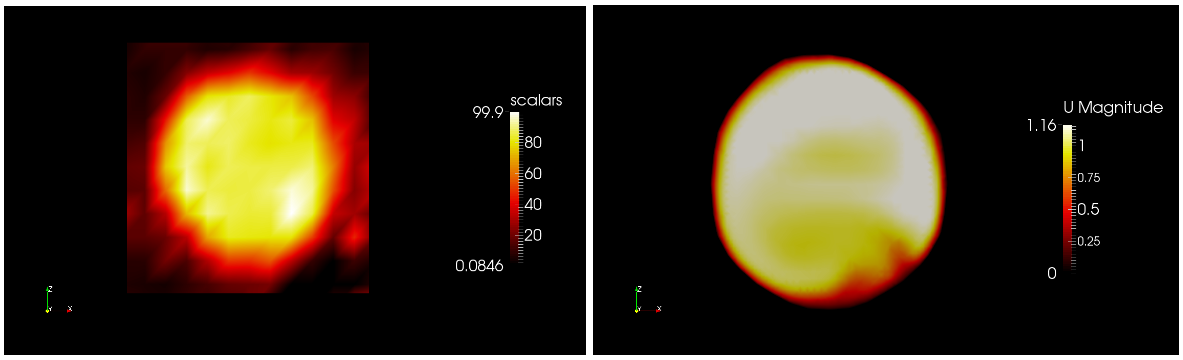

Comparison between the velocity module in slices of the aorta using the 4D method or simulating with OpenFOAM. Slices at $y = 0.082$

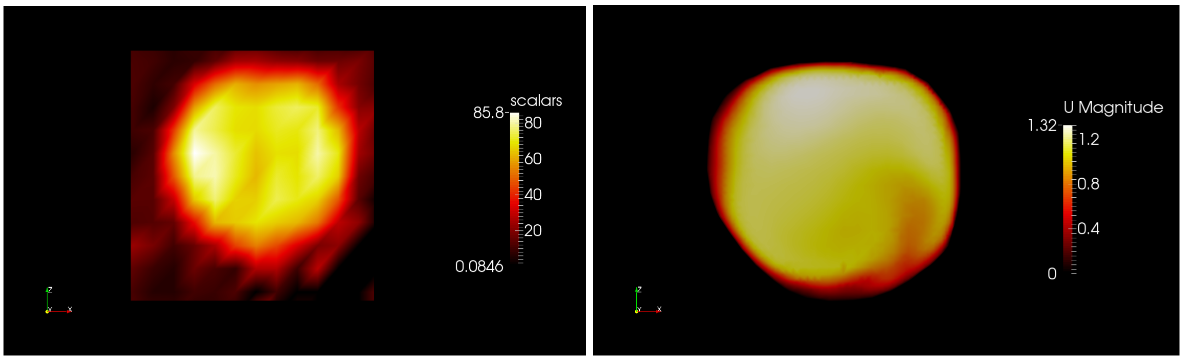

Comparison between the velocity module in slices of the aorta using the 4D method or simulating with OpenFOAM. Slices at $y = 0.105$

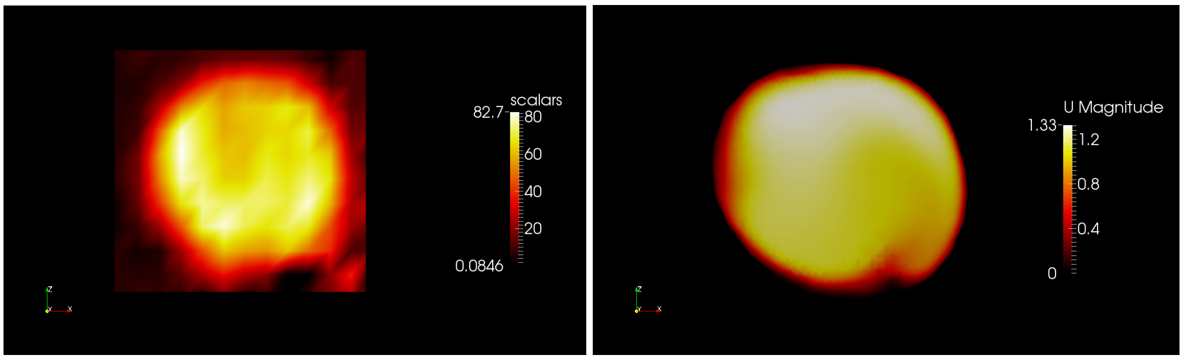

Comparison between the velocity module in slices of the aorta using the 4D method or simulating with OpenFOAM. Slices at $y = 0.121$

As the images to the left are obtained directly from the 4D method, it implies that some information comes from outside the aorta and it is difficult to discern between the velocity values only related to the aorta flow and external information. When considering the velocity distribution, Figure 5.1 may help in understanding which values have to be used for the comparison:

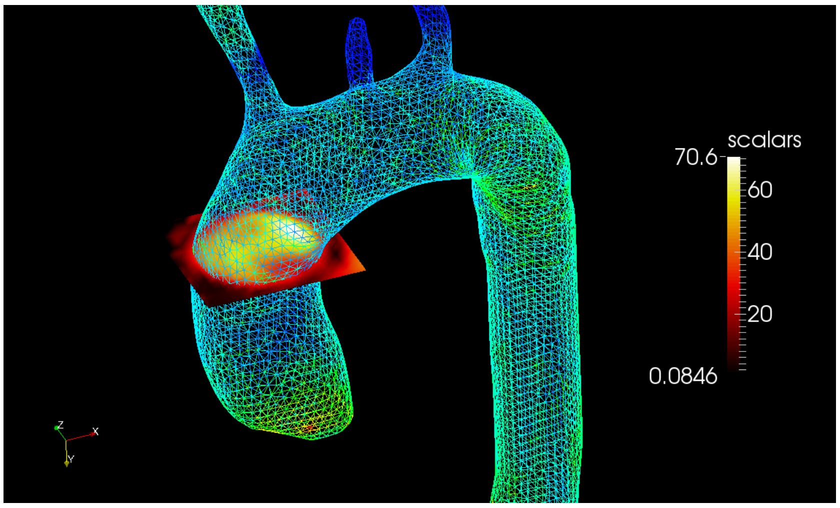

Figure 5.2: Relation between the slices shown in Section 5.2 and the aorta geometry

5.3 Analysis of the wall shear stress

5.3.1 Comparison of results according to OpenFOAM and the 4D method

The wall shear stress distribution obtained using both methods:

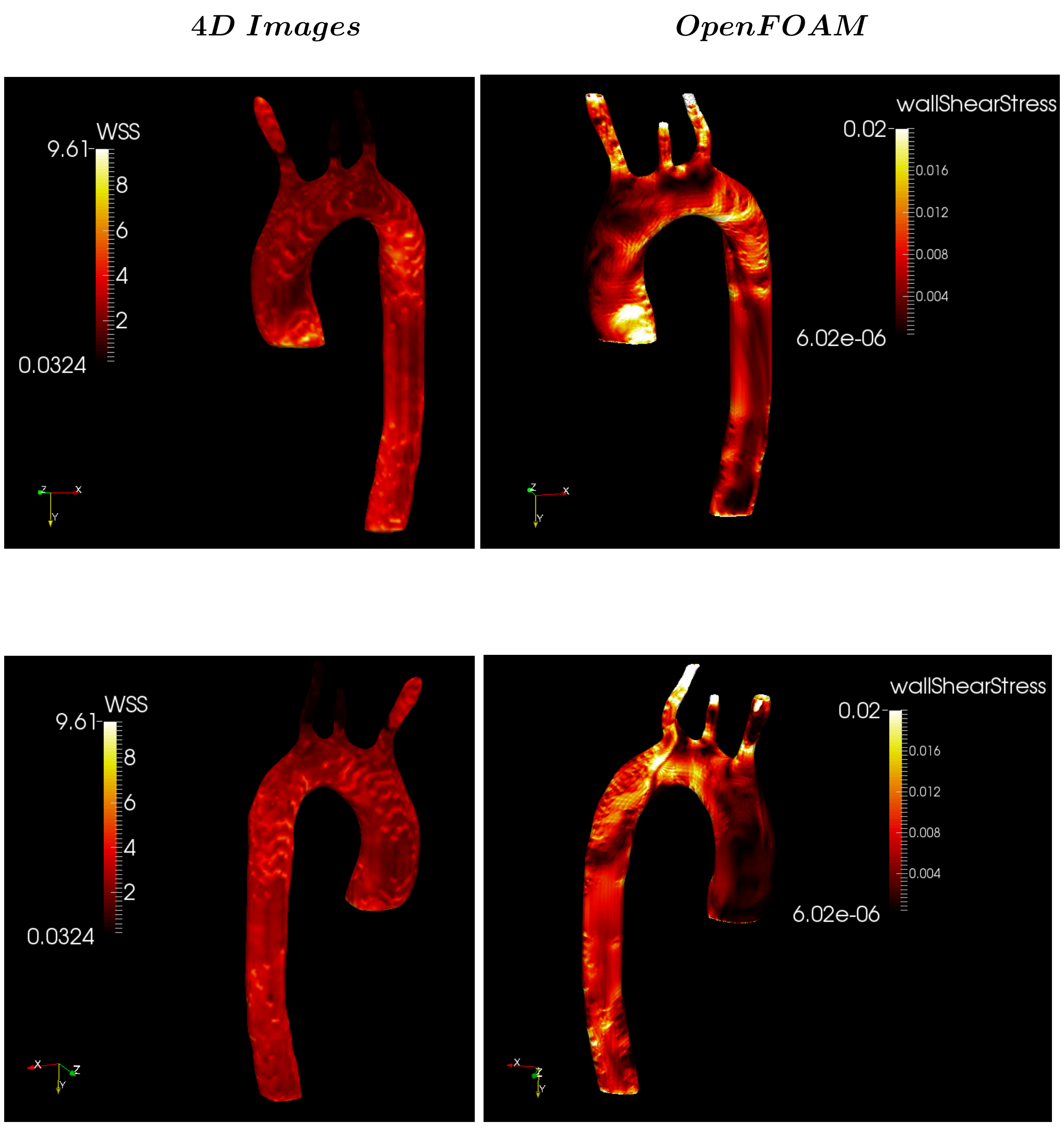

Comparison between wall shear stress distribution according to the results of the 4D method or the OpenFOAM simulation

For the comparison, two aspects must be considered:

- The units of the 4D images are expressed in *Pa*, whereas the OpenFOAM results are in m^2/s^2
- The range of the wall shear stress values in the 4D images goes from 0.0324 Pa to 9.61 Pa, whereas with the OpenFOAM simulation it goes from 6.1×10^{-3} Pa to 20.8 Pa. The ranges present different maximum values because the average

shear stress using the 4D method is lower and it would be then difficult to compare the results. Therefore, these images allow a comparison of the stress distribution more than its numerical values

As it can be seen, there are common patterns, especially reflected in those regions with higher and lower values of wall shear stress. On average, the stress is lower in the 4D method, whose values present a lower definition due to the fact that the spatial discretization is not as accurate as with the OpenFOAM mesh. As the wall shear stress is proportional to the derivative of the velocity profile at the walls of the aorta, a lower spatial discretization on the walls would imply less accuracy.

For a better analysis, the frequency distribution of wall shear stress in each case is presented. The frequency distribution shows how often are specific ranges of wall shear stress repeated with respect to the whole distribution. It allows the computation of an average value, the understanding of which values of wall shear stress are more abundant and to observe the dispersion of the results. Due to the fact that the OpenFOAM mesh contains more points (it presents a higher refinement), there are more values on the frequency distribution in Figure 5.4 than in Figure 5.5, as each value of shear stress has been calculated in a wall point of the mesh:

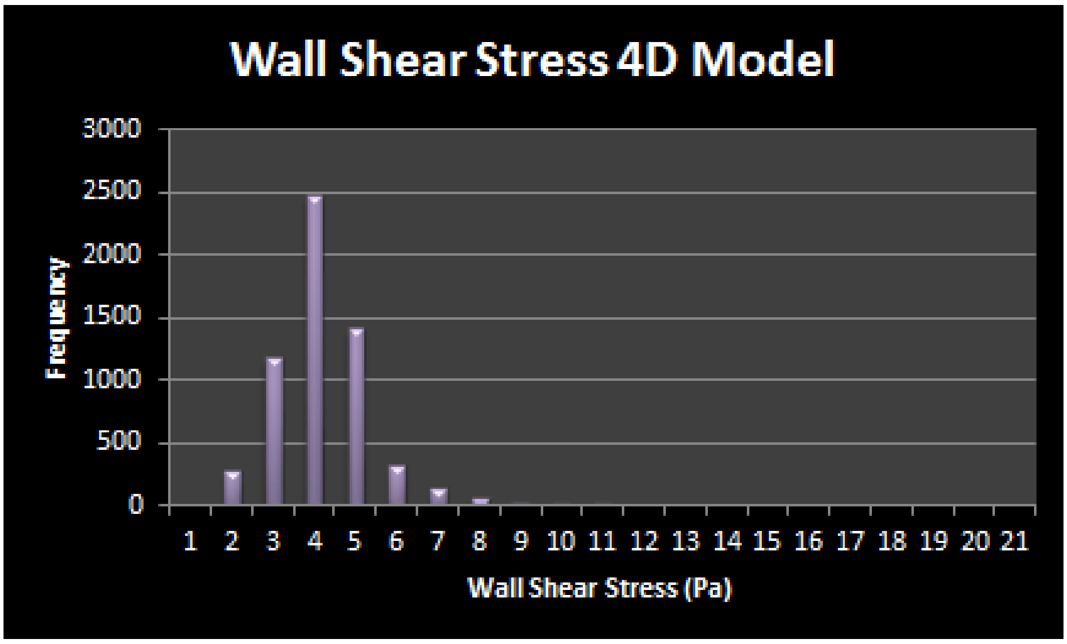

Figure 5.3: Frequency distribution of the wall shear stress obtained with the 4D method

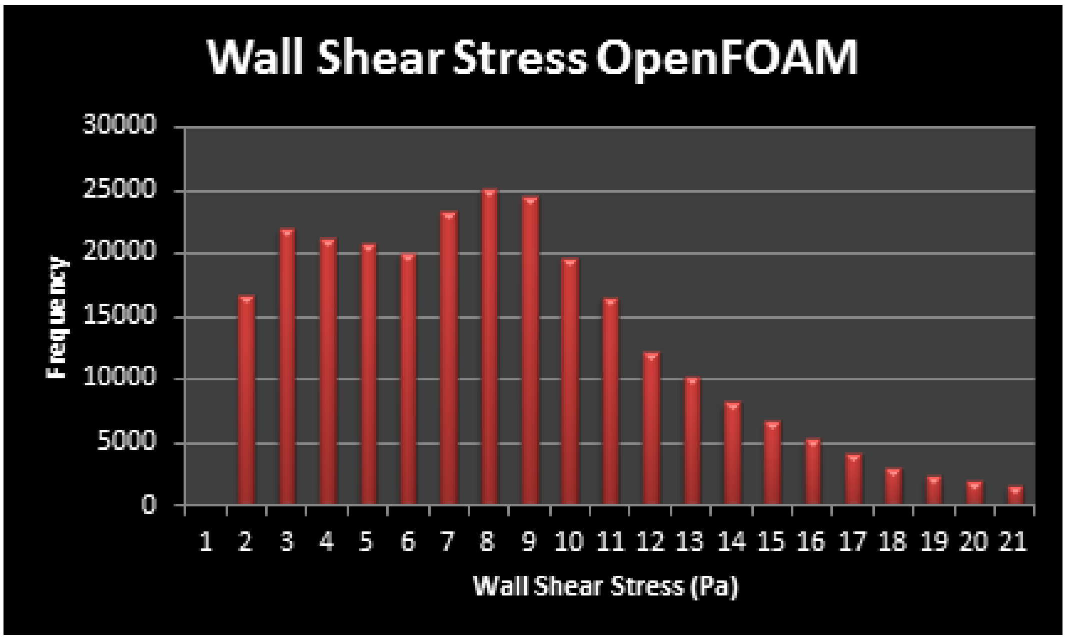

Figure 5.4: Frequency distribution of the wall shear stress obtained with OpenFOAM

Some relevant conclusions that can be extracted from the previous results are:

- The mean value and the standard deviation in both cases are:

Table 5.1: Means and standard deviations of the wall shear stress distributions

	4D Model	**OpenFOAM Model**
Mean	3.18	7.25
Standard deviation	1.135	4.294

- Both the mean and the standard deviation are significantly lower in Figure 5.5
- It may be hypothesized that the standard deviation is lower in Figure 5.5 due to the fact that the spatial discretization (especially at the walls of the aorta) is not as accurate as with Figure 5.4. Consequently, with the OpenFOAM simulation it is possible to differentiate more accurately between the great variety of stress values that are obtained
- The difference in the standard deviations reflects that the two methods present different resolutions. However, the difference between the mean values indi-

cates that either one method tends to underestimate or the other tends to overestimate the values of the wall shear stress

5.3.2 Analysis of wall shear stress results depending on the spatial discretization used for the simulation

Finally, the current section presents a comparison between the wall shear stress distribution depending on what kind of mesh is used for the OpenFOAM simulation, with the aim of:

- Justificate the mesh used for the OpenFOAM simulations, taking into consideration the convergence time, the number of cells of the mesh and the results obtained
- Simulate the case with OpenFOAM using a mesh similar to the one used in the 4D method. In this case, the spatial discretization is similar, but the calculation methods are different. It may help in extracting suitable conclusions
- Compare the wall shear stress frequency distributions using different kinds of spatial discretization

Accordingly, four different cases are shown:

4 models of study

4D Model:	case presenting a uniform spatial discretization, solved using the 4D method. Voxels with dimensions of 1.78 × 1.78 × 2 mm
Mesh Model 1:	same spatial discretization as 4D Model but solved with OpenFOAM
Mesh Model 2:	uniform spatial discretization but more refined than the previous models: uniform cell level equal to 4 with respect to the initial mesh. Solved with OpenFOAM
Mesh Model 3:	is the main case of this work, presented in Chapter 3. Mesh refined at the walls up to level 6 and with two layers of cells to obtain a high refinement. Solved with OpenFOAM

The different kinds of spatial discretization are depicted in the following figures:

4D Model

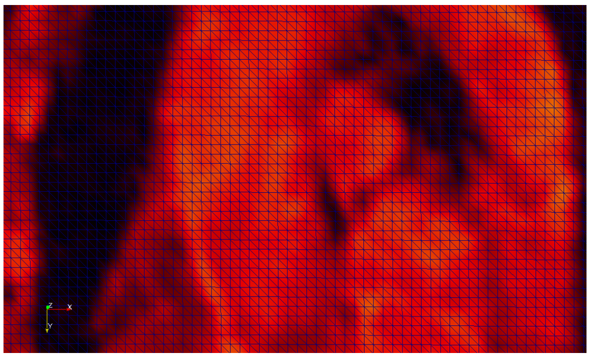

***Mesh Model* 1**

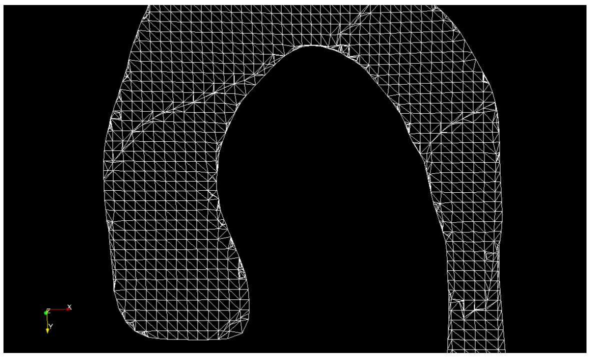

***Mesh Model* 2**

***Mesh Model* 3**

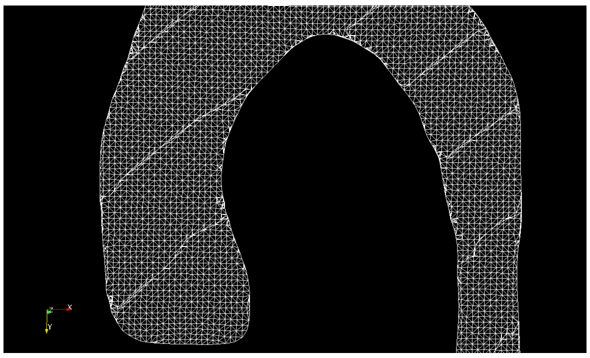

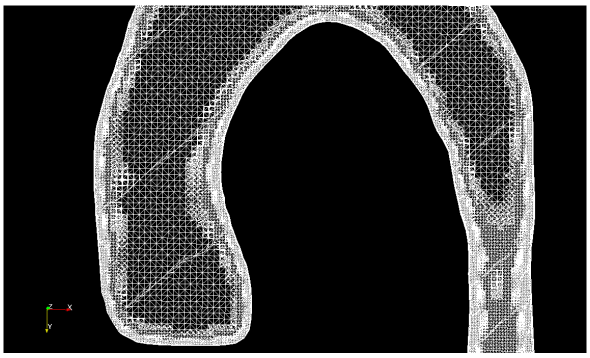

The wall shear stress distribution obtained with each case:

4D Model ***Mesh Model* 1**

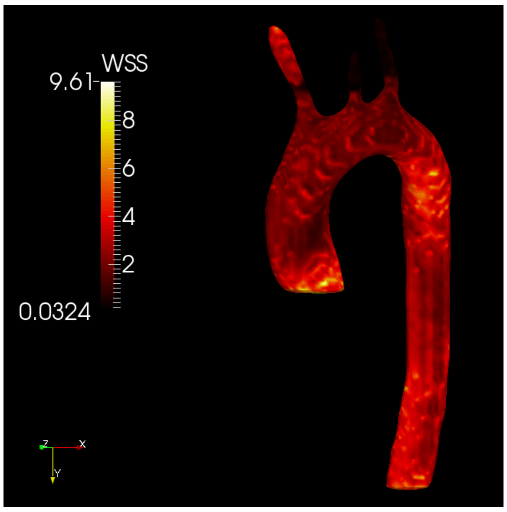

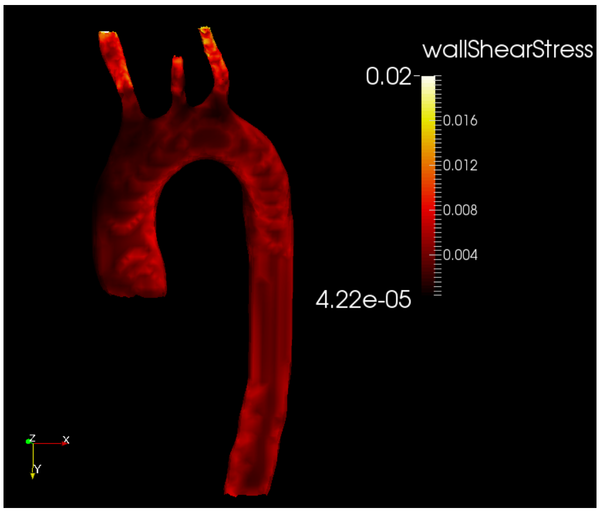

Mesh Model 2 ***Mesh Model 3***

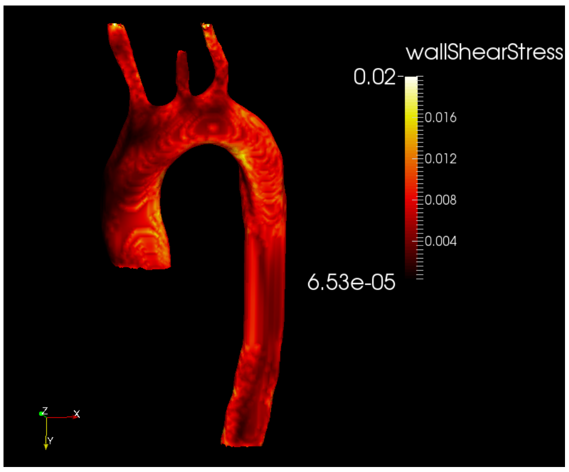

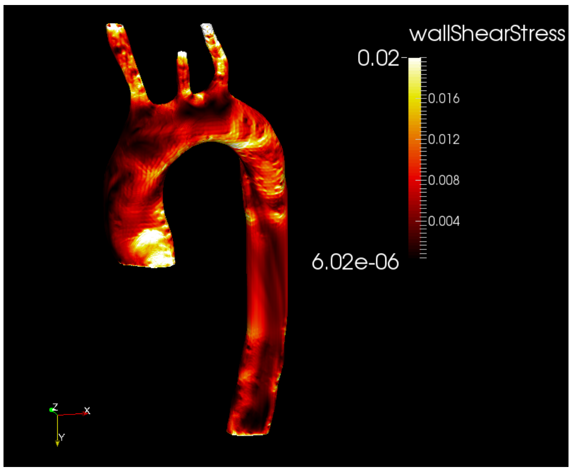

By using these simulations, the wall shear stress frequency distributions are:

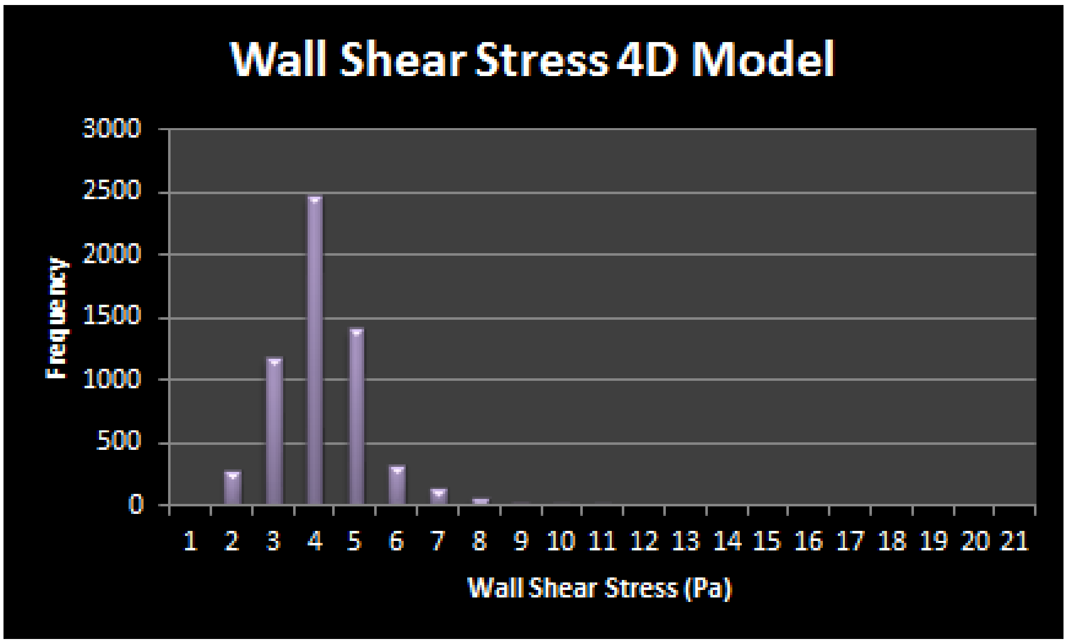

Figure 5.5: Frequency distribution of the wall shear stress obtained with 4D Model

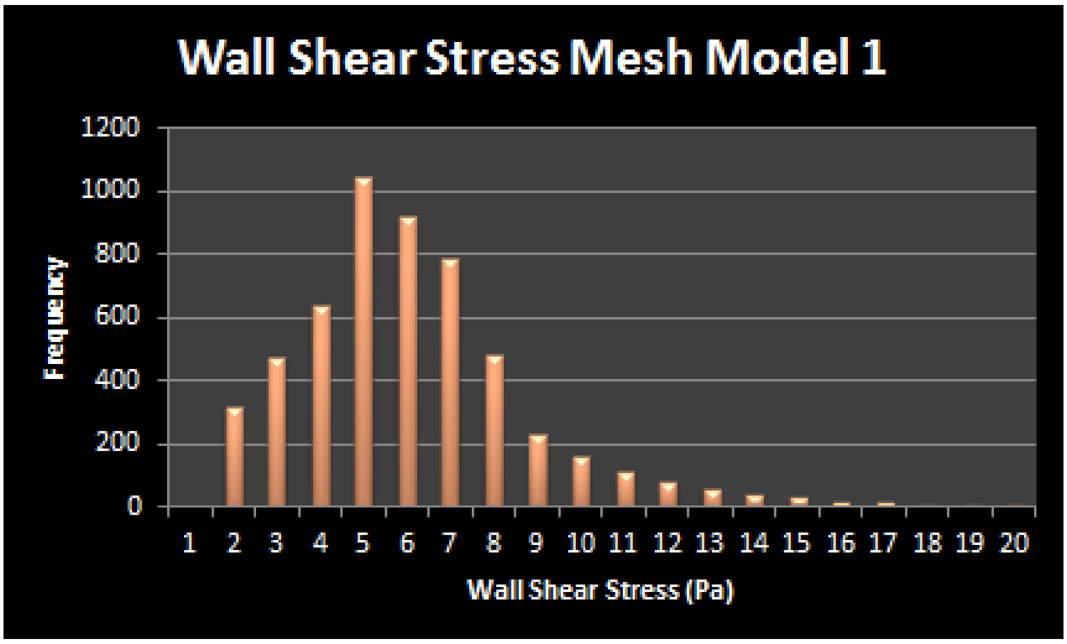

Figure 5.6: Frequency distribution of the wall shear stress obtained with Mesh Model 1

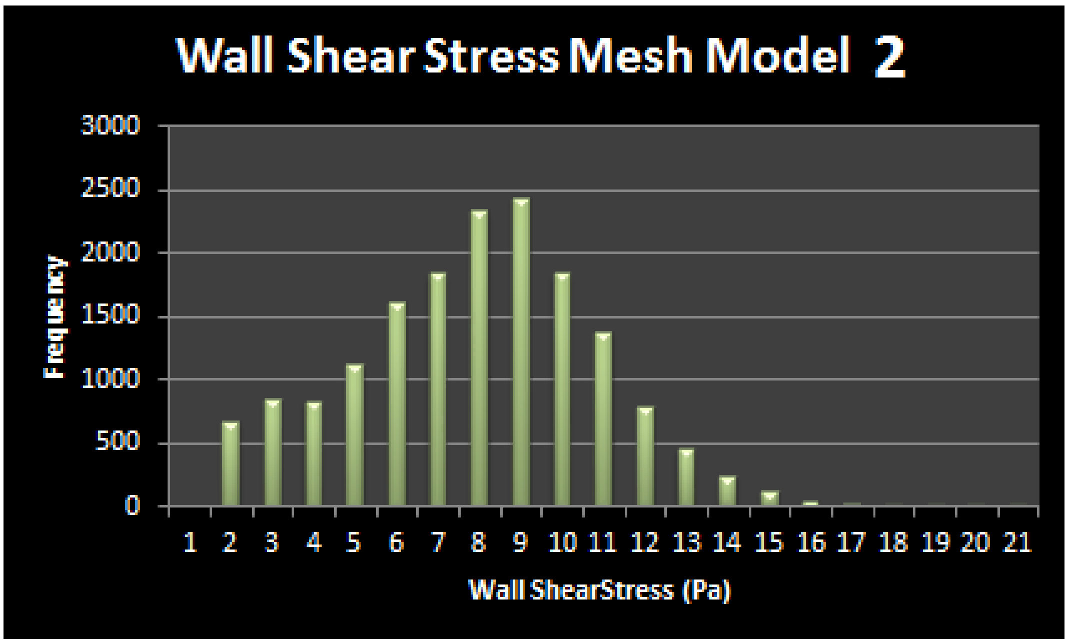

Figure 5.7: Frequency distribution of the wall shear stress obtained with Mesh Model 2

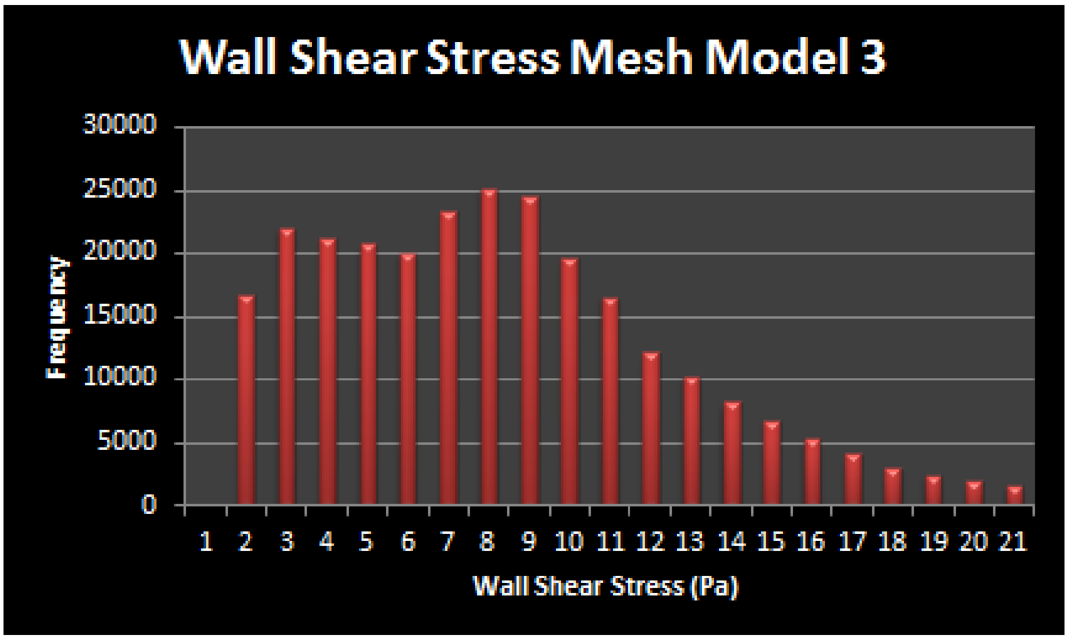

Figure 5.8: Frequency distribution of the wall shear stress obtained with Mesh Model 3

Again, the mean values and the standard deviations have been computed. Also the number of cells of each mesh, as well as the convergence time needed in the simulations are included:

Table 5.2: Means, standard deviations, number of cells and convergence time of each model

	4D Model	**Model 1**	**Model 2**	**Model 3**
Mean	3.18	5.13	6.94	7.25
Standard deviation	1.135	2.744	2.965	4.294
Number of cells	-	12870	81766	1517676
Convergence time	-	64 s	101 s	3534 s

From these figures and tables, and according to the results presented in the whole Chapter 5, it is possible to conclude that:

- The higher the mesh refinement (globally and especially at the aorta walls), the higher the mean values and the standard deviations

- High mesh refinements may contribute through two different ways. The first is related to the resolution of the internal flow. The internal mesh has to adequately solve the whole flow structure, which affects the main flow characteristics and therefore the velocity gradient at the walls. The second is the resolution of the boundary layer, directly involved in the computation of the wall shear stress. It is possible to observe this influence by comparing the results obtained with Mesh Model 3 and the other cases

- In the supra-aortic branches, there are high flow accelerations and thus high values of wall shear stress. These high values are influenced by the simulation itself, rather than having a relevant physical meaning. Hence, such values have been discarded from the distribution as they are not contained within the range of 0-20 Pa. As a consequence, erroneous flow resolutions at the supra-aortic vessels do not influence the histograms presented in this section

- Between 4D Model and Mesh Model 1, the shape of the shear stress frequency distribution is similar, although the mean values and the standard deviations differ

- Between Mesh Model 1 and Mesh Model 2, the main differences come from the fact that the mean value of the frequency distribution shifts to the left and the values are more scattered

- Between Mesh Model 2 and Mesh Model 3, the same pattern of the previous point is obtained again, with the peculiarity that left frequency values increased significantly. It has been found that this increase is due to the fact that with the mesh of Model 3 very low flow speeds can be computed, coming from the inlet vortices, the flow detachment, etc. The previous models do not adequately solve the flow in these areas and therefore low speed values could not be obtained

- There is more difference in mean values between Models 1 and 2 than between 2 and 3. However, the opposite happens with the standard deviations. This may be due to the fact that the main distinction between Models 1 and 2 is the internal cell density (difference in internal flow resolution), whereas the main differences between Models 2 and 3 are the mesh refinements at the walls (difference in the wall shear stress computation).

6. Conclusions

- According to the initial hypothesis, hemodynamics of blood through a thoracic aorta has been solved

- It has been possible to model important and relevant flow patterns, as for instance flow detachment at the aortic arch or generation of vortices at the widening after the inlet

- By smoothing the surface of the aorta using OpenFOAM utilities, it has been possible to smoothen surface imperfections and avoid unphysical stress concentrators

- Different kinds of boundary conditions at the supra-aortic vessels have been tested. When imposing outlet velocities, the simulations did not succeed and when imposing equal pressure values the simulations did not provide physically realistic results. The chosen solution was to impose outlet flow rates, according to experimental data obtained from MRI measures. With these boundary conditions and with a uniform inlet flow rate, the simulations converged and offered suitable results

- Without an OpenFOAM GUI, it became difficult to define new patches on the initial aorta geometry to apply the boundary conditions. In this case, the topoSet and createPatch utilities were used, plus a personal bash code developed to manage different Linux instructions

- High values of wall refinement have been obtained in the aorta mesh (the distance between the aorta wall and the first nodes are of the order of micrometers). This guarantees that the boundary layer is correctly solved and wall shear stress values are accurately computed

- The OpenFOAM simulation carried out in this work has been compared with similar cases studied with commercial CFD packages. In the majority of cases, the results agreed

- The wall shear stress values computed with the OpenFOAM simulation are maintained within an adequate range and their average value is close to the expected one

- In contrast with other CFD aorta resolutions, and due to the high mesh refinement which has been obtained, the distribution of wall shear stress computed with the current OpenFOAM simulation is more realistic: the different regions according to each phenomenon are clearly separated and therefore it is possible to analyze medical implications more accurately

- The numerical solution of those cases of the guide with a well-known analytical solution perfectly matched the results. Very low errors with no significantly large or heavy simulations were obtained. This is a demonstration of the enormous power of the CFD tools and their importance in the future of fluid mechanics

- By comparing the results of the OpenFOAM simulation with the images of the 4D method, it can be concluded that the main flow patterns are similar, although the average value of shear stress is lower when using the second method

- As the mesh used for the 4D method is coarser, its wall shear distribution is not as detailed as the one obtained with OpenFOAM. However, with the 4D method, real velocity values are used. There is a compromise between an OpenFOAM simulation with mathematically computed values but with an accurate mesh, and a 4D method, managing velocity values directly measured from real aortas but with low mesh resolution

- When comparing the wall shear stress frequency distributions, the standard deviations of the results of the 4D method were found similar to the ones obtained with an OpenFOAM simulation with the same spatial discretization. However, the mean values increased from 3.18 Pa to 5.13 Pa

- The higher the number of cells of the mesh of the OpenFOAM simulations, the higher the mean values of the wall shear stress distribution, as well as the standard deviations

- When comparing the results of the 4D method with the main OpenFOAM simulation of this work, the difference in standard deviation of the wall shear stress distributions may be indicative of the accuracy of the results. The more refined the mesh, the higher the variety of stress values that can be computed.

Therefore the dispersion of the results increases. The difference in mean values might come from three different aspects: the internal flow resolution, the definition and treatment of the aorta walls during its segmentation and the computation of the wall shear stress according to the values obtained with MRI

6.1 Further steps

At the end of this work, interesting points considered by the author to continue the analyses and simulations developed during its realization are discussed.

1. To contrast the numerical results collected in the guide with experimental work in a laboratory, including for instance wind tunnel experiments for the external flow cases
2. To thoroughly focus on turbulence. Only RAS turbulence models have been used, so it would be interesting to study and simulate new cases by using LES or DNS
3. To simulate with OpenFOAM unhealthy aorta geometries (mainly with an aneurysm or with an inlet flow with excentricity)
4. To introduce more accurate boundary conditions and physical properties such as an inlet flow adapted to the inlet valve or suitable turbulence models
5. To simulate a whole cardiac cycle
6. To determine the wall shear stress by using experimental techniques and compare it with the OpenFOAM simulations and the 4D method

A. Appendix

A.1 surfaceFeatureExtractDict

```
lastAortaSmooth10It.stl
{
    // How to obtain raw features (extractFromFile || extractFromSurface)
    extractionMethod    extractFromSurface;

    extractFromSurfaceCoeffs
    {
        // Mark edges whose adjacent surface normals are at an angle less
        // than includedAngle as features
        // - 0  : selects no edges
        // - 180: selects all edges
        includedAngle   150;
    }

    subsetFeatures
    {
        // Keep nonManifold edges (edges with >2 connected faces)
        nonManifoldEdges       no;

        // Keep open edges (edges with 1 connected face)
        openEdges       yes;
    }

    // Write options

        // Write features to obj format for postprocessing
        writeObj                yes;
}

// ************************************************************************* //
```

A.2 blockMeshDict

```
/*--------------------------------*- C++ -*----------------------------------*\
| =========                 |                                                 |
| \\      /  F ield         | OpenFOAM: The Open Source CFD Toolbox           |
|  \\    /   O peration     | Version:  2.2.1                                 |
|   \\  /    A nd           | Web:      www.OpenFOAM.org                      |
|    \\/     M anipulation  |                                                                        |
\*---------------------------------------------------------------------------*/
FoamFile
{
    version     2.0;
    format      ascii;
    class       dictionary;
    object      blockMeshDict;
}

// * * * * * * * * * * * * * * * * * * * * * * * * * * * * * * * * * * * * * //

convertToMeters 0.1;

vertices
(
    (-1 -1 -0.1)
    (2 -1 -0.1)
    (2  2 -0.1)
    (-1  2 -0.1)
    (-1 -1 3)
    (2 -1 3)
    (2  2 3)
    (-1  2 3)
);

blocks
(
    hex (0 1 2 3 4 5 6 7) (20 20 20) simpleGrading (1 1 1)
);

edges
(
);

boundary
(
    frontAndBack
    {
        type slip;
        faces
        (
            (3 7 6 2)
            (1 5 4 0)
        );
    }
    leftWall
    {
        type slip;
        faces
        (
            (0 4 7 3)
        );
    }
    rightWall
    {
        type slip;
        faces
        (
            (2 6 5 1)
        );
    }
    topWall
    {
        type slip;
        faces
        (
            (0 3 2 1)
        );
    }
    bottomWall
    {
        type slip;
        faces
        (
            (4 5 6 7)
        );
    }
);

// ************************************************************************* //
```

A.3 boundary

```
/*--------------------------------*- C++ -*----------------------------------*\
| =========                 |                                                 |
| \\      /  F ield         | OpenFOAM: The Open Source CFD Toolbox           |
|  \\    /   O peration     | Version:  2.3.0                                 |
|   \\  /    A nd           | Web:      www.OpenFOAM.org                      |
|    \\/     M anipulation  |                                                 |
\*---------------------------------------------------------------------------*/
FoamFile
{
    version     2.0;
    format      binary;
    class       polyBoundaryMesh;
    location    "constant/polyMesh";
    object      boundary;
}
// * * * * * * * * * * * * * * * * * * * * * * * * * * * * * * * * * * * * //

5
(
    frontAndBack
    {
        type            slip;
        inGroups        1(slip);
        nFaces          800;
        startFace       22800;
        inGroups        1 ( slip );
        faces           ( ( 3 7 6 2 ) ( 1 5 4 0 ) );
    }
    leftWall
    {
        type            slip;
        inGroups        1(slip);
        nFaces          400;
        startFace       23600;
        inGroups        1 ( slip );
        faces           ( ( 0 4 7 3 ) );
    }
    rightWall
    {
        type            slip;
        inGroups        1(slip);
        nFaces          400;
        startFace       24000;
        inGroups        1 ( slip );
        faces           ( ( 2 6 5 1 ) );
    }
    topWall
    {
        type            slip;
        inGroups        1(slip);
        nFaces          400;
        startFace       24400;
        inGroups        1 ( slip );
        faces           ( ( 0 3 2 1 ) );
    }
    bottomWall
    {
        type            slip;
        inGroups        1(slip);
        nFaces          400;
        startFace       24800;
        inGroups        1 ( slip );
        faces           ( ( 4 5 6 7 ) );
    }
)

// ************************************************************************* //
```

A.4 snappyHexMeshDict

```
/*--------------------------------*- C++ -*----------------------------------*\
| =========                 |                                                 |
| \\      /  F ield         | OpenFOAM: The Open Source CFD Toolbox           |
|  \\    /   O peration     | Version:  2.2.0                                 |
|   \\  /    A nd           | Web:      www.OpenFOAM.org                      |
|    \\/     M anipulation  |                                                 |
\*---------------------------------------------------------------------------*/
FoamFile
{
    version     2.0;
    format      ascii;
    class       dictionary;
    object      snappyHexMeshDict;
}
// * * * * * * * * * * * * * * * * * * * * * * * * * * * * * * * * * * * * * * //

// Which of the steps to run
castellatedMesh true;
snap            true;
addLayers       true;

// Geometry. Definition of all surfaces. All surfaces are of class
// searchableSurface.
// Surfaces are used
// - to specify refinement for any mesh cell intersecting it
// - to specify refinement for any mesh cell inside/outside/near
// - to 'snap' the mesh boundary to the surface
geometry
{

    lastAortaSmooth10It.stl //STL filename where all the regions are added
    {
        type triSurfaceMesh;

        regions
  {
    zone0            //Named region in the STL file
    {
      name aortaWall;   //User-defined patch name. If not provided will be
          <name>_<region>
    }
  }
    }

    refinementBox //Geometry to refine. Entities: Box, Cylinder, Sphere, Plane
    {
        type searchableBox;
        min (0.0375 -0.0495 0.145);
        max (0.102 -0.0045 0.185);
    }
};

// Settings for the castellatedMesh generation.
castellatedMeshControls
{

    // Refinement parameters
    // ~~~~~~~~~~~~~~~~~~~~

    // If local number of cells is >= maxLocalCells on any processor
    // switches from from refinement followed by balancing
    // (current method) to (weighted) balancing before refinement.
    maxLocalCells 15000000;

    // Overall cell limit (approximately). Refinement will stop immediately
    // upon reaching this number so a refinement level might not complete.
```

```
    // Note that this is the number of cells before removing the part which
    // is not 'visible' from the keepPoint. The final number of cells might
    // actually be a lot less.
    maxGlobalCells 20000000;

    // The surface refinement loop might spend lots of iterations refining just a
    // few cells. This setting will cause refinement to stop if <= minimumRefine
    // are selected for refinement. Note: it will at least do one iteration
    // (unless the number of cells to refine is 0)
    minRefinementCells 0;

    // Allow a certain level of imbalance during refining
    // (since balancing is quite expensive)
    // Expressed as fraction of perfect balance (= overall number of cells /
    // nProcs). 0=balance always.
    maxLoadUnbalance 0.1;

    // Number of buffer layers between different levels.
    // 1 means normal 2:1 refinement restriction, larger means slower
    // refinement.
    nCellsBetweenLevels 3;


    // Explicit feature edge refinement
    // ~~~~~~~~~~~~~~~~~~~~~~~~~~~~~~~~

    // Specifies a level for any cell intersected by explicitly provided
    // edges.
    // This is a featureEdgeMesh, read from constant/triSurface for now.
    // Specify 'levels' in the same way as the 'distance' mode in the
    // refinementRegions (see below). The old specification
    //      level   2;
    // is equivalent to
    //      levels  ((0 2));

    features
    (
        {
            file "lastAortaSmooth10It.eMesh";
            levels ((4 4));
        }
    );


    // Surface based refinement
    // ~~~~~~~~~~~~~~~~~~~~~~~~

    // Specifies two levels for every surface. The first is the minimum level,
    // every cell intersecting a surface gets refined up to the minimum level.
    // The second level is the maximum level. Cells that 'see' multiple
    // intersections where the intersections make an
    // angle > resolveFeatureAngle get refined up to the maximum level.

    refinementSurfaces
    {

      lastAortaSmooth10It.stl   //STL filename where all the regions are added
```

```
            {
        level (6 6);
        regions
        {
          /*zone0 //Named region in the STL file
          {
                      // Surface-wise min and max refinement level
            level (3 3);
                          // Optional specification of patch type (default is wall). No
                          // constraint types (cyclic, symmetry) etc. are allowed.
                      patchInfo
                      {
                          type patch;
                          inGroups (meshedPatches);
                          }
          }*/
        }
      }
        }

        // Feature angle:
        // - used if min and max refinement level of a surface differ
        // - used if feature snapping (see snapControls below) is used
        resolveFeatureAngle 30;


        // Region-wise refinement
        // ~~~~~~~~~~~~~~~~~~~~~~

        // Specifies refinement level for cells in relation to a surface. One of
        // three modes
        // - distance. 'levels' specifies per distance to the surface the
        //   wanted refinement level. The distances need to be specified in
        //   increasing order.
        // - inside. 'levels' is only one entry and only the level is used. All
        //   cells inside the surface get refined up to the level. The surface
        //   needs to be closed for this to be possible.
        // - outside. Same but cells outside.

        refinementRegions
        {
            refinementCylinder
            {
                mode inside;
                levels ((1E15 7));
            }
        }

        // Mesh selection
        // ~~~~~~~~~~~~~~

        // After refinement patches get added for all refinementSurfaces and
        // all cells intersecting the surfaces get put into these patches. The
        // section reachable from the locationInMesh is kept.
        // NOTE: This point should never be on a face, always inside a cell, even
        // after refinement.
        locationInMesh (0.05 0.03 0.175);
```

```

    // Whether any faceZones (as specified in the refinementSurfaces)
    // are only on the boundary of corresponding cellZones or also allow
    // free-standing zone faces. Not used if there are no faceZones.
    allowFreeStandingZoneFaces true;
}

// Settings for the snapping.
snapControls
{
    // Number of patch smoothing iterations before finding correspondence
    // to surface
    nSmoothPatch 3;

    // Maximum relative distance for points to be attracted by surface.
    // True distance is this factor times local maximum edge length.
    // Note: changed(corrected) w.r.t 17x! (17x used 2* tolerance)
    tolerance 1.0;

    // Number of mesh displacement relaxation iterations.
    nSolveIter 30;

    // Maximum number of snapping relaxation iterations. Should stop
    // before upon reaching a correct mesh.
    nRelaxIter 5;

    // Feature snapping

        // Number of feature edge snapping iterations.
        // Leave out altogether to disable.
        nFeatureSnapIter 10;

        // Detect (geometric only) features by sampling the surface
        // (default=false).
        implicitFeatureSnap false;

        // Use castellatedMeshControls::features (default = true)
        explicitFeatureSnap true;

        // Detect features between multiple surfaces
        // (only for explicitFeatureSnap, default = false)
        multiRegionFeatureSnap false;
}

// Settings for the layer addition.
addLayersControls
{
    // Are the thickness parameters below relative to the undistorted
    // size of the refined cell outside layer (true) or absolute sizes (false).
    relativeSizes true;

    // Layer thickness specification. This can be specified in one of four ways
    // - expansionRatio and finalLayerThickness (cell nearest internal mesh)
    // - expansionRatio and firstLayerThickness (cell on surface)
    // - overall thickness and firstLayerThickness
    // - overall thickness and finalLayerThickness

```

```
            // Expansion factor for layer mesh
            expansionRatio 2;

            // Wanted thickness of the layer furthest away from the wall.
            // If relativeSizes this is relative to undistorted size of cell
            // outside layer.
            finalLayerThickness 0.4;

            // Wanted thickness of the layer next to the wall.
            // If relativeSizes this is relative to undistorted size of cell
            // outside layer.
            //firstLayerThickness 0.3;

            // Wanted overall thickness of layers.
            // If relativeSizes this is relative to undistorted size of cell
            // outside layer.
            //thickness 0.5


        // Minimum overall thickness of total layers. If for any reason layer
        // cannot be above minThickness do not add layer.
        // If relativeSizes this is relative to undistorted size of cell
        // outside layer..
        minThickness 0.1;


        // Per final patch (so not geometry!) the layer information
        // Note: This behaviour changed after 21x. Any non-mentioned patches
        //       now slide unless:
        //           - nSurfaceLayers is explicitly mentioned to be 0.
        //           - angle to nearest surface < slipFeatureAngle (see below)
        layers
        {
            aortaWall
            {
                nSurfaceLayers 2;

            }
            maxY
            {
                nSurfaceLayers 2;
                // Per patch layer data
                expansionRatio      2;
                finalLayerThickness 0.4;
                minThickness        0.1;
            }

            // Disable any mesh shrinking and layer addition on any point of
            // a patch by setting nSurfaceLayers to 0
            frozenPatches
            {
                nSurfaceLayers 0;
            }
        }

        // If points get not extruded do nGrow layers of connected faces that are
        // also not grown. This helps convergence of the layer addition process
```

```
    // close to features.
    // Note: changed(corrected) w.r.t 17x! (didn't do anything in 17x)
    nGrow 0;

    // Advanced settings

    // When not to extrude surface. 0 is flat surface, 90 is when two faces
    // are perpendicular
    featureAngle 60;

    // At non-patched sides allow mesh to slip if extrusion direction makes
    // angle larger than slipFeatureAngle.
    slipFeatureAngle 30;

    // Maximum number of snapping relaxation iterations. Should stop
    // before upon reaching a correct mesh.
    nRelaxIter 5;

    // Number of smoothing iterations of surface normals
    nSmoothSurfaceNormals 1;

    // Number of smoothing iterations of interior mesh movement direction
    nSmoothNormals 3;

    // Smooth layer thickness over surface patches
    nSmoothThickness 10;

    // Stop layer growth on highly warped cells
    maxFaceThicknessRatio 0.5;

    // Reduce layer growth where ratio thickness to medial
    // distance is large
    maxThicknessToMedialRatio 0.3;

    // Angle used to pick up medial axis points
    // Note: changed(corrected) w.r.t 17x! 90 degrees corresponds to 130 in 17x.
    minMedianAxisAngle 90;

    // Create buffer region for new layer terminations
    nBufferCellsNoExtrude 0;

    // Overall max number of layer addition iterations. The mesher will exit
    // if it reaches this number of iterations; possibly with an illegal
    // mesh.
    nLayerIter 50;

    // Max number of iterations after which relaxed meshQuality controls
    // get used. Up to nRelaxIter it uses the settings in meshQualityControls,
    // after nRelaxIter it uses the values in meshQualityControls::relaxed.
    nRelaxedIter 20;

    // Additional reporting: if there are just a few faces where there
    // are mesh errors (after adding the layers) print their face centres.
    // This helps in tracking down problematic mesh areas.
    //additionalReporting true;
}

```

```
// Generic mesh quality settings. At any undoable phase these determine
// where to undo.
meshQualityControls
{
    // Maximum non-orthogonality allowed. Set to 180 to disable.
    maxNonOrtho 45;

    // Max skewness allowed. Set to <0 to disable.
    maxBoundarySkewness 20;
    maxInternalSkewness 4;

    // Max concaveness allowed. Is angle (in degrees) below which concavity
    // is allowed. 0 is straight face, <0 would be convex face.
    // Set to 180 to disable.
    maxConcave 80;

    // Minimum pyramid volume. Is absolute volume of cell pyramid.
    // Set to a sensible fraction of the smallest cell volume expected.
    // Set to very negative number (e.g. -1E30) to disable.
    minVol 1e-13;

    // Minimum quality of the tet formed by the face-centre
    // and variable base point minimum decomposition triangles and
    // the cell centre. This has to be a positive number for tracking
    // to work. Set to very negative number (e.g. -1E30) to
    // disable.
    //     <0 = inside out tet,
    //      0 = flat tet
    //      1 = regular tet
    minTetQuality 1e-9;

    // Minimum face area. Set to <0 to disable.
    minArea -1;

    // Minimum face twist. Set to <-1 to disable. dot product of face normal
    // and face centre triangles normal
    minTwist 0.05;

    // minimum normalised cell determinant
    // 1 = hex, <= 0 = folded or flattened illegal cell
    minDeterminant 0.001;

    // minFaceWeight (0 -> 0.5)
    minFaceWeight 0.05;

    // minVolRatio (0 -> 1)
    minVolRatio 0.01;

    // must be >0 for Fluent compatibility
    minTriangleTwist -1;

    //- if >0 : preserve single cells with all points on the surface if the
    //  resulting volume after snapping (by approximation) is larger than
    //  minVolCollapseRatio times old volume (i.e. not collapsed to flat cell).
    //  If <0 : delete always.
    //minVolCollapseRatio 0.5;

    // Advanced

    // Number of error distribution iterations
    nSmoothScale 4;
    // amount to scale back displacement at error points
    errorReduction 0.75;

    // Optional : some meshing phases allow usage of relaxed rules.
    // See e.g. addLayersControls::nRelaxedIter.
    relaxed
    {
        //- Maximum non-orthogonality allowed. Set to 180 to disable.
        maxNonOrtho 45;
    }
}

// Advanced

// Flags for optional output
// 0 : only write final meshes
// 1 : write intermediate meshes
// 2 : write volScalarField with cellLevel for postprocessing
// 4 : write current intersections as .obj files
debug 0;

// Merge tolerance. Is fraction of overall bounding box of initial mesh.
// Note: the write tolerance needs to be higher than this.
mergeTolerance 1e-6;

// ************************************************************************* //
```

A.5 checkMesh

```
/*---------------------------------------------------------------------------*\
| =========                 |                                                 |
| \\      /  F ield         | OpenFOAM: The Open Source CFD Toolbox           |
|  \\    /   O peration     | Version:  2.3.0                                 |
|   \\  /    A nd           | Web:      www.OpenFOAM.org                      |
|    \\/     M anipulation  |                                                 |
\*---------------------------------------------------------------------------*/
Build  : 2.3.0-f5222ca19ce6
Exec   : checkMesh
Date   : May 23 2014
Time   : 17:48:31
Host   : "H25109"
PID    : 7022
Case   : /home/jordi/Escriptori/AortaFoam
nProcs : 1
sigFpe : Enabling floating point exception trapping (FOAM_SIGFPE).
fileModificationChecking : Monitoring run-time modified files using timeStampMaster
allowSystemOperations : Disallowing user-supplied system call operations

// * * * * * * * * * * * * * * * * * * * * * * * * * * * * * * * * * * * * //
```

```
Create time

Create polyMesh for time = 1

Time = 1

Mesh stats
    points:           1493135
    faces:            3749654
    internal faces:   3348304
    cells:            1128520
    faces per cell:   6.28962
    boundary patches: 6
    point zones:      0
    face zones:       0
    cell zones:       0

Overall number of cells of each type:
    hexahedra:     1035405
    prisms:        0
    wedges:        0
    pyramids:      0
    tet wedges:    0
    tetrahedra:    0
    polyhedra:     93115
    Breakdown of polyhedra by number of faces:
        faces   number of cells
            6   28221
            9   32886
           12   20459
           15   11054
           18   495

Checking topology...
    Boundary definition OK.
    Cell to face addressing OK.
    Point usage OK.
    Upper triangular ordering OK.
    Face vertices OK.
    Number of regions: 1 (OK).

Checking patch topology for multiply connected surfaces...
                   Patch    Faces   Points                  Surface topology
            frontAndBack        0        0                        ok (empty)
                leftWall        0        0                        ok (empty)
               rightWall        0        0                        ok (empty)
                 topWall        0        0                        ok (empty)
              bottomWall        0        0                        ok (empty)
               aortaWall   401350   401352      ok (closed singly connected)

Checking geometry...
    Overall domain bounding box (0.0389844 -0.0442188 0.149359) (0.11375 0.131328
        0.183023)
    Mesh (non-empty, non-wedge) directions (1 1 1)
    Mesh (non-empty) directions (1 1 1)
    Boundary openness (4.90475e-16 -1.88181e-17 -2.36364e-16) OK.
    Max cell openness = 3.05442e-16 OK.
    Max aspect ratio = 1.03333 OK.
    Minimum face area = 5.49316e-08. Maximum face area = 9.08203e-07.  Face area
        magnitudes OK.
    Min volume = 1.33038e-11. Max volume = 8.5144e-10.  Total volume =
        6.96518e-05.  Cell volumes OK.
    Mesh non-orthogonality Max: 25.6096 average: 9.01125
    Non-orthogonality check OK.
    Face pyramids OK.
    Max skewness = 0.333367 OK.
    Coupled point location match (average 0) OK.

Mesh OK.

Time = 2

Mesh stats
    points:           1377941
    faces:            3596786
    internal faces:   3348304
    cells:            1128520
    faces per cell:   6.15416
    boundary patches: 6
    point zones:      0
    face zones:       0
    cell zones:       0

Overall number of cells of each type:
    hexahedra:     921527
    prisms:        52632
    wedges:        0
    pyramids:      0
    tet wedges:    463
    tetrahedra:    1
    polyhedra:     153897
    Breakdown of polyhedra by number of faces:
        faces   number of cells
            4   38526
            5   22256
            6   28221
            9   32886
           12   20459
           15   11054
           18   495

Checking topology...
    Boundary definition OK.
    Cell to face addressing OK.
    Point usage OK.
    Upper triangular ordering OK.
    Face vertices OK.
    Number of regions: 1 (OK).

Checking patch topology for multiply connected surfaces...
                   Patch    Faces   Points                  Surface topology
            frontAndBack        0        0                        ok (empty)
                leftWall        0        0                        ok (empty)
               rightWall        0        0                        ok (empty)
```

```
                 topWall         0         0                         ok (empty)
              bottomWall         0         0                         ok (empty)
               aortaWall    248482    286158      ok (closed singly connected)

Checking geometry...
    Overall domain bounding box (0.0389332 -0.0443906 0.149293) (0.113807 0.131309
        0.183016)
    Mesh (non-empty, non-wedge) directions (1 1 1)
    Mesh (non-empty) directions (1 1 1)
    Boundary openness (-1.43363e-16 1.58962e-17 2.76816e-16) OK.
    Max cell openness = 3.59876e-16 OK.
    Max aspect ratio = 5.54205 OK.
    Minimum face area = 3.08657e-09. Maximum face area = 9.68777e-07.  Face area
        magnitudes OK.
    Min volume = 1.5113e-12. Max volume = 9.13292e-10.  Total volume =
        6.96441e-05.  Cell volumes OK.
    Mesh non-orthogonality Max: 44.994 average: 10.5987
    Non-orthogonality check OK.
    Face pyramids OK.
    Max skewness = 2.92068 OK.
    Coupled point location match (average 0) OK.

Mesh OK.

--> FOAM Warning :
    From function polyMesh::readUpdateState polyMesh::readUpdate()
    in file meshes/polyMesh/polyMeshIO.C at line 207
    Number of patches has changed.  This may have unexpected consequences.
        Proceed with care.
Time = 3

Mesh stats
    points:           1882949
    faces:            4987227
    internal faces:   4739360
    cells:            1571329
    faces per cell:   6.19004
    boundary patches: 6
    point zones:      0
    face zones:       0
    cell zones:       0

Overall number of cells of each type:
    hexahedra:     1261492
    prisms:        52712
    wedges:        1
    pyramids:      0
    tet wedges:    550
    tetrahedra:    2
    polyhedra:     256572
    Breakdown of polyhedra by number of faces:
        faces   number of cells
            4   39626
            5   22129
            6   28566
            7   76408
            8   24811
```

```
              9    32867
             10    123
             12    20459
             15    11056
             18    495
             21    29
             24    3

Checking topology...
    Boundary definition OK.
    Cell to face addressing OK.
    Point usage OK.
    Upper triangular ordering OK.
    Face vertices OK.
    Number of regions: 1 (OK).

Checking patch topology for multiply connected surfaces...
                   Patch    Faces   Points                  Surface topology
            frontAndBack        0        0                        ok (empty)
                leftWall        0        0                        ok (empty)
               rightWall        0        0                        ok (empty)
               lowerWall        0        0                        ok (empty)
               upperWall        0        0                        ok (empty)
               aortaWall   247867   285740      ok (closed singly connected)

Checking geometry...
    Overall domain bounding box (0.0389332 -0.0443906 0.149293) (0.113807 0.131309
        0.183016)
    Mesh (non-empty, non-wedge) directions (1 1 1)
    Mesh (non-empty) directions (1 1 1)
    Boundary openness (-1.91619e-16 -3.42491e-17 1.49812e-16) OK.
    Max cell openness = 4.03527e-16 OK.
    Max aspect ratio = 13.4184 OK.
    Minimum face area = 2.63761e-09. Maximum face area = 9.76263e-07.  Face area
        magnitudes OK.
    Min volume = 4.52487e-13. Max volume = 9.14821e-10.  Total volume =
        6.96434e-05.  Cell volumes OK.
    Mesh non-orthogonality Max: 66.7028 average: 9.79509
    Non-orthogonality check OK.
    Face pyramids OK.
    Max skewness = 1.94323 OK.
    Coupled point location match (average 0) OK.

Mesh OK.

End
```

A.6 topoSetDict

```
/*--------------------------------*- C++ -*----------------------------------*\
| =========                 |                                                 |
| \\      /  F ield         | OpenFOAM: The Open Source CFD Toolbox           |
|  \\    /   O peration     | Version:  2.2.1                                 |
|    \\  /     A nd              | Web:         www.OpenFOAM.org                              |
|     \\/      M anipulation   |                                                            |
\*---------------------------------------------------------------------------*/
FoamFile
{
    version      2.0;
    format       ascii;
    class        dictionary;
    object       topoSetDict;
}

// * * * * * * * * * * * * * * * * * * * * * * * * * * * * * * * * * * * * * //

actions
(
   {
        name     allPatchSet;
        type     faceSet;
        action   new;
        source   boundaryToFace;
        sourceInfo
        {
        }
    }

   {
        name     c1;          //Inlet Set
        type     faceSet;
        action   new;
        source   boxToFace;
        sourceInfo
        {
        box (0.0425 0.0558 0.153) (0.0675 0.0708 0.177);
        }
    }

   {
        name     boxOutletSet;
        type     faceSet;
        action   new;
        source   boxToFace;
        sourceInfo
        {
        box (0.0825 0.129 0.16) (0.108 0.144 0.184);
        }
    }

   {
        name     s1;          //S01 Set
        type     faceSet;
        action   new;
        source   boxToFace;
        sourceInfo
        {
        box (0.04 -0.048 0.172) (0.05 -0.038 0.182);
        }
    }
```

```

  {
        name     boxS02Set;
        type     faceSet;
        action   new;
        source   boxToFace;
        sourceInfo
        {
        box (0.06 -0.0405 0.15) (0.07 -0.0305 0.16);
        }
    }

  {
        name     boxS03Set;
        type     faceSet;
        action   new;
        source   boxToFace;
        sourceInfo
        {
        box (0.071 -0.0515 0.15) (0.081 -0.0415 0.16);
        }
    }

);

// ************************************************************************* //
```

A.7 createPatchDict

```
/*--------------------------------*- C++ -*----------------------------------*\
| =========                 |                                                 |
| \\      /  F ield         | OpenFOAM: The Open Source CFD Toolbox           |
|  \\    /   O peration     | Version:  2.2.1                                 |
|   \\  /    A nd           | Web:      www.OpenFOAM.org                      |
|    \\/     M anipulation  |                                                 |
\*---------------------------------------------------------------------------*/
FoamFile
{
    version     2.0;
    format      ascii;
    class       dictionary;
    object      createPatchDict;
}

// * * * * * * * * * * * * * * * * * * * * * * * * * * * * * * * * * * * * //

// This application/dictionary controls:
// - optional: create new patches from boundary faces (either given as
//   a set of patches or as a faceSet)
// - always: order faces on coupled patches such that they are opposite. This
//   is done for all coupled faces, not just for any patches created.
// - optional: synchronise points on coupled patches.

// 1. Create cyclic:
// - specify where the faces should come from
// - specify the type of cyclic. If a rotational specify the rotationAxis
//   and centre to make matching easier
// - always create both halves in one invocation with correct 'neighbourPatch'
//   setting.
// - optionally pointSync true to guarantee points to line up.

// 2. Correct incorrect cyclic:
// This will usually fail upon loading:
//  "face 0 area does not match neighbour 2 by 0.0100005%"
//  " -- possible face ordering problem."
// - in polyMesh/boundary file:
//      - loosen matchTolerance of all cyclics to get case to load
//      - or change patch type from 'cyclic' to 'patch'
//        and regenerate cyclic as above


// Do a synchronisation of coupled points after creation of any patches.
// Note: this does not work with points that are on multiple coupled patches
//       with transformations (i.e. cyclics).
pointSync false;

// Patches to create.
patches
(
    {
        // Name of new patch
        name inlet;

        // Type of new patch
        patchInfo
        {
            type patch;
        }

        // How to construct: either from 'patches' or 'set'
        constructFrom set;

        // If constructFrom = patches : names of patches. Wildcards allowed.
        patches (aortaWall);

        // If constructFrom = set : name of faceSet
        set definitiveInletSet;
    }

  {
        // Name of new patch
        name outlet;

        // Type of new patch
        patchInfo
        {
            type patch;
        }

        // How to construct: either from 'patches' or 'set'
        constructFrom set;

        // If constructFrom = patches : names of patches. Wildcards allowed.
        patches (aortaWall);

        // If constructFrom = set : name of faceSet
        set definitiveOutletSet;
    }

  {
        // Name of new patch
        name S01;

        // Type of new patch
        patchInfo
        {
            type patch;
        }

        // How to construct: either from 'patches' or 'set'
        constructFrom set;

        // If constructFrom = patches : names of patches. Wildcards allowed.
        patches (aortaWall);

        // If constructFrom = set : name of faceSet
        set definitiveS01Set;
    }

{
        // Name of new patch
        name S02;

        // Type of new patch
        patchInfo
        {
            type patch;
        }

        // How to construct: either from 'patches' or 'set'
        constructFrom set;

        // If constructFrom = patches : names of patches. Wildcards allowed.
        patches (aortaWall);

        // If constructFrom = set : name of faceSet
        set definitiveS02Set;
    }

{
        // Name of new patch
        name S03;

        // Type of new patch
        patchInfo
        {
            type patch;
        }

        // How to construct: either from 'patches' or 'set'
        constructFrom set;

        // If constructFrom = patches : names of patches. Wildcards allowed.
        patches (aortaWall);

        // If constructFrom = set : name of faceSet
        set definitiveS03Set;
    }

);

// ************************************************************************* //
```

A.8 Script for patch definition

```

#!/bin/bash

#Requirements:

# -The 2 directories (createPatchScript and createPatchTemplates) must be at
    Desktop containing templates of the OpenFOAM files according to the
    instructions shown in the script
# -The AortaFoam case directory must be at Desktop
# -In the templates sheets there must be a space of 3 lines between the heading
    and the first "("
# -The last directory created by snappyHexMesh must be named "3" (if not, change
    it manually)

cp AortaFoam/3/polyMesh/sets/c1 createPatchScript/c1Intermediate #Copy data from
    topoSet

sed -i 1,+19d createPatchScript/c1Intermediate #Erase header

sed -i '$d' createPatchScript/c1Intermediate

sed -i '$d' createPatchScript/c1Intermediate

sed -i '$d' createPatchScript/c1Intermediate


cp AortaFoam/3/polyMesh/sets/allPatchSet createPatchScript/allPatchSetIntermediate
    #Copy data from topoSet

sed -i 1,+19d createPatchScript/allPatchSetIntermediate #Erase header

sed -i '$d' createPatchScript/allPatchSetIntermediate

sed -i '$d' createPatchScript/allPatchSetIntermediate

sed -i '$d' createPatchScript/allPatchSetIntermediate

sort createPatchScript/c1Intermediate > createPatchScript/c1Intermediate.sort
    #Sort (necessary for the comm instruction)
sort createPatchScript/allPatchSetIntermediate >
    createPatchScript/allPatchSetIntermediate.sort

comm -12 createPatchScript/c1Intermediate.sort
    createPatchScript/allPatchSetIntermediate.sort >
    createPatchScript/definitiveInletSetIntermediate #Compare to find common faces
    shearing the condition of external face and being inside the box

wc -w < createPatchScript/definitiveInletSetIntermediate >
    createPatchScript/WordCounter #Count the number of faces of the resulting file

ed -s createPatchScript/definitiveInletSet <<< $'20r
    createPatchScript/definitiveInletSetIntermediate\nw'

ed -s createPatchScript/definitiveInletSet <<< $'18r
    createPatchScript/WordCounter\nw'

> createPatchScript/c1Intermediate #Reinitialize to 0 all the files which were used
> createPatchScript/allPatchSetIntermediate
> createPatchScript/WordCounter
> createPatchScript/c1Intermediate.sort
> createPatchScript/allPatchSetIntermediate.sort
> createPatchScript/definitiveInletSetIntermediate

cp createPatchScript/definitiveInletSet
    AortaFoam/3/polyMesh/sets/definitiveInletSet
cp createPatchTemplates/definitiveInletSetTemplate
    createPatchScript/definitiveInletSet

####

cp AortaFoam/3/polyMesh/sets/boxOutletSet
    createPatchScript/boxOutletSetIntermediate

sed -i 1,+19d createPatchScript/boxOutletSetIntermediate

sed -i '$d' createPatchScript/boxOutletSetIntermediate

sed -i '$d' createPatchScript/boxOutletSetIntermediate

sed -i '$d' createPatchScript/boxOutletSetIntermediate


cp AortaFoam/3/polyMesh/sets/allPatchSet createPatchScript/allPatchSetIntermediate

sed -i 1,+19d createPatchScript/allPatchSetIntermediate

sed -i '$d' createPatchScript/allPatchSetIntermediate

sed -i '$d' createPatchScript/allPatchSetIntermediate

sed -i '$d' createPatchScript/allPatchSetIntermediate

```

```
sort createPatchScript/boxOutletSetIntermediate >
    createPatchScript/boxOutletSetIntermediate.sort
sort createPatchScript/allPatchSetIntermediate >
    createPatchScript/allPatchSetIntermediate.sort

comm -12 createPatchScript/boxOutletSetIntermediate.sort
    createPatchScript/allPatchSetIntermediate.sort >
    createPatchScript/definitiveOutletSetIntermediate

wc -w < createPatchScript/definitiveOutletSetIntermediate >
    createPatchScript/WordCounter

ed -s createPatchScript/definitiveOutletSet <<< $'20r
    createPatchScript/definitiveOutletSetIntermediate\nw'

ed -s createPatchScript/definitiveOutletSet <<< $'18r
    createPatchScript/WordCounter\nw'

> createPatchScript/boxOutletSetIntermediate
> createPatchScript/allPatchSetIntermediate
> createPatchScript/WordCounter
> createPatchScript/boxOutletSetIntermediate.sort
> createPatchScript/allPatchSetIntermediate.sort
> createPatchScript/definitiveOutletSetIntermediate

cp createPatchScript/definitiveOutletSet
    AortaFoam/3/polyMesh/sets/definitiveOutletSet
cp createPatchTemplates/definitiveOutletSetTemplate
    createPatchScript/definitiveOutletSet

####

cp AortaFoam/3/polyMesh/sets/s1 createPatchScript/s1Intermediate

sed -i 1,+19d createPatchScript/s1Intermediate

sed -i '$d' createPatchScript/s1Intermediate

sed -i '$d' createPatchScript/s1Intermediate

sed -i '$d' createPatchScript/s1Intermediate


cp AortaFoam/3/polyMesh/sets/allPatchSet createPatchScript/allPatchSetIntermediate

sed -i 1,+19d createPatchScript/allPatchSetIntermediate

sed -i '$d' createPatchScript/allPatchSetIntermediate

sed -i '$d' createPatchScript/allPatchSetIntermediate

sed -i '$d' createPatchScript/allPatchSetIntermediate

sort createPatchScript/s1Intermediate > createPatchScript/s1Intermediate.sort
sort createPatchScript/allPatchSetIntermediate >
    createPatchScript/allPatchSetIntermediate.sort

```

```
comm -12 createPatchScript/s1Intermediate.sort
    createPatchScript/allPatchSetIntermediate.sort >
    createPatchScript/definitiveS01SetIntermediate

wc -w < createPatchScript/definitiveS01SetIntermediate >
    createPatchScript/WordCounter

ed -s createPatchScript/definitiveS01Set <<< $'20r
    createPatchScript/definitiveS01SetIntermediate\nw'

ed -s createPatchScript/definitiveS01Set <<< $'18r
    createPatchScript/WordCounter\nw'

> createPatchScript/s1Intermediate
> createPatchScript/allPatchSetIntermediate
> createPatchScript/WordCounter
> createPatchScript/s1Intermediate.sort
> createPatchScript/allPatchSetIntermediate.sort
> createPatchScript/definitiveS01SetIntermediate

cp createPatchScript/definitiveS01Set AortaFoam/3/polyMesh/sets/definitiveS01Set
cp createPatchTemplates/definitiveS01SetTemplate createPatchScript/definitiveS01Set

####

cp AortaFoam/3/polyMesh/sets/boxS02Set createPatchScript/boxS02SetIntermediate

sed -i 1,+19d createPatchScript/boxS02SetIntermediate

sed -i '$d' createPatchScript/boxS02SetIntermediate

sed -i '$d' createPatchScript/boxS02SetIntermediate

sed -i '$d' createPatchScript/boxS02SetIntermediate


cp AortaFoam/3/polyMesh/sets/allPatchSet createPatchScript/allPatchSetIntermediate

sed -i 1,+19d createPatchScript/allPatchSetIntermediate

sed -i '$d' createPatchScript/allPatchSetIntermediate

sed -i '$d' createPatchScript/allPatchSetIntermediate

sed -i '$d' createPatchScript/allPatchSetIntermediate

sort createPatchScript/boxS02SetIntermediate >
    createPatchScript/boxS02SetIntermediate.sort
sort createPatchScript/allPatchSetIntermediate >
    createPatchScript/allPatchSetIntermediate.sort

comm -12 createPatchScript/boxS02SetIntermediate.sort
    createPatchScript/allPatchSetIntermediate.sort >
    createPatchScript/definitiveS02SetIntermediate

wc -w < createPatchScript/definitiveS02SetIntermediate >
    createPatchScript/WordCounter
```

```
ed -s createPatchScript/definitiveS02Set <<< $'20r
    createPatchScript/definitiveS02SetIntermediate\nw'

ed -s createPatchScript/definitiveS02Set <<< $'18r
    createPatchScript/WordCounter\nw'

> createPatchScript/boxS02SetIntermediate
> createPatchScript/allPatchSetIntermediate
> createPatchScript/WordCounter
> createPatchScript/boxS02SetIntermediate.sort
> createPatchScript/allPatchSetIntermediate.sort
> createPatchScript/definitiveS02SetIntermediate

cp createPatchScript/definitiveS02Set AortaFoam/3/polyMesh/sets/definitiveS02Set
cp createPatchTemplates/definitiveS02SetTemplate createPatchScript/definitiveS02Set

####

cp AortaFoam/3/polyMesh/sets/boxS03Set createPatchScript/boxS03SetIntermediate

sed -i 1,+19d createPatchScript/boxS03SetIntermediate

sed -i '$d' createPatchScript/boxS03SetIntermediate

sed -i '$d' createPatchScript/boxS03SetIntermediate

sed -i '$d' createPatchScript/boxS03SetIntermediate


cp AortaFoam/3/polyMesh/sets/allPatchSet createPatchScript/allPatchSetIntermediate

sed -i 1,+19d createPatchScript/allPatchSetIntermediate

sed -i '$d' createPatchScript/allPatchSetIntermediate

sed -i '$d' createPatchScript/allPatchSetIntermediate

sed -i '$d' createPatchScript/allPatchSetIntermediate

sort createPatchScript/boxS03SetIntermediate >
    createPatchScript/boxS03SetIntermediate.sort
sort createPatchScript/allPatchSetIntermediate >
    createPatchScript/allPatchSetIntermediate.sort

comm -12 createPatchScript/boxS03SetIntermediate.sort
    createPatchScript/allPatchSetIntermediate.sort >
    createPatchScript/definitiveS03SetIntermediate

wc -w < createPatchScript/definitiveS03SetIntermediate >
    createPatchScript/WordCounter

ed -s createPatchScript/definitiveS03Set <<< $'20r
    createPatchScript/definitiveS03SetIntermediate\nw'

ed -s createPatchScript/definitiveS03Set <<< $'18r
    createPatchScript/WordCounter\nw'
```

```

> createPatchScript/boxS03SetIntermediate
> createPatchScript/allPatchSetIntermediate
> createPatchScript/WordCounter
> createPatchScript/boxS03SetIntermediate.sort
> createPatchScript/allPatchSetIntermediate.sort
> createPatchScript/definitiveS03SetIntermediate

cp createPatchScript/definitiveS03Set AortaFoam/3/polyMesh/sets/definitiveS03Set
cp createPatchTemplates/definitiveS03SetTemplate createPatchScript/definitiveS03Set
```

A.9 p

```
/*--------------------------------*- C++ -*----------------------------------*\
| =========                 |                                                 |
| \\      /  F ield         | OpenFOAM: The Open Source CFD Toolbox           |
|  \\    /   O peration     | Version:  2.2.1                                 |
|   \\  /    A nd           | Web:      www.OpenFOAM.org                      |
|    \\/     M anipulation  |                                                 |
\*---------------------------------------------------------------------------*/
FoamFile
{
    version     2.0;
    format      ascii;
    class       volScalarField;
    object      p;
}
// * * * * * * * * * * * * * * * * * * * * * * * * * * * * * * * * * * * * * //

dimensions      [0 2 -2 0 0 0 0];

internalField   uniform 0;

boundaryField
{

    inlet
    {
        type            zeroGradient;
    }

    outlet
    {
        type            fixedValue;
        value           uniform 0;
    }

    S01
    {
        type            zeroGradient;
    }

    S02
    {
        type            zeroGradient;
    }

    S03
    {
        type            zeroGradient;
    }

    aortaWall
    {
        type            zeroGradient;
    }

    frontAndBack
    {
        type            slip;
    }

    leftWall
    {
        type            slip;
    }

    rightWall
    {
        type            slip;
    }

    lowerWall
    {
        type            slip;
    }

    upperWall
    {
        type            slip;
    }
}

// ************************************************************************* //
```

A.10 U

```
/*--------------------------------*- C++ -*----------------------------------*\
| =========                 |                                                 |
| \\      /  F ield         | OpenFOAM: The Open Source CFD Toolbox           |
|  \\    /   O peration     | Version:  2.2.1                                 |
|   \\  /    A nd           | Web:      www.OpenFOAM.org                      |
|    \\/     M anipulation  |                                                 |
\*---------------------------------------------------------------------------*/
FoamFile
{
    version     2.0;
    format      ascii;
    class       volVectorField;
    location    "0";
    object      U;
}
// * * * * * * * * * * * * * * * * * * * * * * * * * * * * * * * * * * * * //

dimensions      [0 1 -1 0 0 0 0];

internalField   uniform (0 0 0);

boundaryField
{
    inlet
    {
        type                fixedValue;
        value               uniform (-2.3407e-03 -0.6853 -9.674e-04);
    }

    outlet
    {
        type                inletOutlet;
        inletValue uniform  (0 0 0);
        value uniform       (0 0 0);
     }

    S01
    {
        type                flowRateInletVelocity;
        volumetricFlowRate  -2.713e-05;    //Negative because outgoing
        value uniform       (0 0 0);
    }

    S02
    {
        type                flowRateInletVelocity;
        volumetricFlowRate  -1.015e-05;   //Negative because outgoing
        value uniform       (0 0 0);
    }

    S03
    {
        type                flowRateInletVelocity;
        volumetricFlowRate  -1.8e-05;     //Negative because outgoing
        value uniform       (0 0 0);
    }

    aortaWall
    {
        type                fixedValue;
        value               uniform (0 0 0);
    }

    frontAndBack
    {
        type               slip;
    }

    leftWall
    {
        type            slip;
    }

    rightWall
    {
        type            slip;
    }

    lowerWall
    {
        type            slip;
    }

    upperWall
    {
        type            slip;
    }
}

// ************************************************************************* //
```

A.11 transportProperties

```
/*--------------------------------*- C++ -*----------------------------------*\
| =========                 |                                                 |
| \\      /  F ield         | OpenFOAM: The Open Source CFD Toolbox           |
|  \\    /   O peration     | Version:  2.2.1                                 |
|   \\  /    A nd           | Web:      www.OpenFOAM.org                      |
|    \\/     M anipulation  |                                                 |
\*---------------------------------------------------------------------------*/
FoamFile
{
    version     2.0;
    format      ascii;
    class       dictionary;
    object      transportProperties;
}
// * * * * * * * * * * * * * * * * * * * * * * * * * * * * * * * * * * * * * //

transportModel  Newtonian;

nu              nu [0 2 -1 0 0 0 0] 3.365e-06;

// ************************************************************************* //
```

A.12 RASProperties

```
/*--------------------------------*- C++ -*----------------------------------*\
| =========                 |                                                 |
| \\      /  F ield         | OpenFOAM: The Open Source CFD Toolbox           |
|  \\    /   O peration     | Version:  2.2.1                                 |
|   \\  /    A nd           | Web:      www.OpenFOAM.org                      |
|    \\/     M anipulation  |                                                 |
\*---------------------------------------------------------------------------*/
FoamFile
{
    version     2.0;
    format      ascii;
    class       dictionary;
    object      RASProperties;
}
// * * * * * * * * * * * * * * * * * * * * * * * * * * * * * * * * * * * * * //

RASModel            laminar;

turbulence          off;

printCoeffs         off;

// ************************************************************************* //
```

A.13 controlDict

```
/*--------------------------------*- C++ -*----------------------------------*\
| =========                 |                                                 |
| \\      /  F ield         | OpenFOAM: The Open Source CFD Toolbox           |
|  \\    /   O peration     | Version:  2.2.1                                 |
|   \\  /    A nd           | Web:      www.OpenFOAM.org                      |
|    \\/     M anipulation  |                                                 |
\*---------------------------------------------------------------------------*/
FoamFile
{
    version     2.0;
    format      ascii;
    class       dictionary;
    object      controlDict;
}
// * * * * * * * * * * * * * * * * * * * * * * * * * * * * * * * * * * * * * //

application     simpleFoam;

startFrom       latestTime;

startTime       0;

stopAt          endTime;

```

```
endTime         500;

deltaT          1;

writeControl    timeStep;

writeInterval   10;

purgeWrite      0;

writeFormat     binary;

writePrecision  6;

writeCompression uncompressed;

timeFormat      general;

timePrecision   6;

runTimeModifiable true;

// ************************************************************************* //
```

A.14 fvSchemes

```
/*--------------------------------*- C++ -*----------------------------------*\
| =========                 |                                                 |
| \\      /  F ield         | OpenFOAM: The Open Source CFD Toolbox           |
|  \\    /   O peration     | Version:  2.2.1                                 |
|   \\  /    A nd           | Web:      www.OpenFOAM.org                      |
|    \\/     M anipulation  |                                                 |
\*---------------------------------------------------------------------------*/
FoamFile
{
    version     2.0;
    format      ascii;
    class       dictionary;
    location    "system";
    object      fvSchemes;
}
// * * * * * * * * * * * * * * * * * * * * * * * * * * * * * * * * * * * * * //

ddtSchemes
{
    default         steadyState;
}

gradSchemes
{
    default         Gauss linear;
    grad(U)         cellLimited Gauss linear 1;
}
```

```

divSchemes
{
    default         none;
    div(phi,U)      bounded Gauss linearUpwindV grad(U);
    div((nuEff*dev(T(grad(U))))) Gauss linear;
}

laplacianSchemes
{
    default         Gauss linear corrected;
}

interpolationSchemes
{
    default         linear;
}

snGradSchemes
{
    default         corrected;
}

fluxRequired
{
    default         no;
    p               ;
}

// ************************************************************************* //
```

A.15 fvSolution

```
/*--------------------------------*- C++ -*----------------------------------*\
| =========                 |                                                 |
| \\      /  F ield         | OpenFOAM: The Open Source CFD Toolbox           |
|  \\    /   O peration     | Version:  2.2.1                                 |
|   \\  /    A nd           | Web:      www.OpenFOAM.org                      |
|    \\/     M anipulation  |                                                 |
\*---------------------------------------------------------------------------*/
FoamFile
{
    version     2.0;
    format      ascii;
    class       dictionary;
    location    "constant";
    object      fvSolution;
}
// * * * * * * * * * * * * * * * * * * * * * * * * * * * * * * * * * * * * * //

solvers
{
    p
    {
        solver          GAMG;
        tolerance       1e-7;
        relTol          0.01;
        smoother        GaussSeidel;
        nPreSweeps      0;
        nPostSweeps     2;
        cacheAgglomeration on;
        agglomerator    faceAreaPair;
        nCellsInCoarsestLevel 10;
        mergeLevels     1;
    }

    U
    {
        solver          smoothSolver;
        smoother        GaussSeidel;
        tolerance       1e-8;
        relTol          0.1;
        nSweeps         1;
    }
}

SIMPLE
{
    nNonOrthogonalCorrectors 2;
}

potentialFlow
{
    nNonOrthogonalCorrectors 10;
}

relaxationFactors
{
    fields
    {
        p               0.3;
    }
    equations
    {
        U               0.7;
    }
}

cache
{
    grad(U);
}

// ************************************************************************* //
```

Bibliography

[1] Mohamed Gad-el-Hak. Fluid mechanics from the beginning to the third millennium. *Int. J. Engng Ed.*, 1998.

[2] Josdo Parra Viol. Estudio e implementaci nuevas funcionalidades de deformaci malla en software de mecca de fluidos computacional. Technical report, ETSEIAT, 2011.

[3] *OpenFOAM, the open source CFD toolbox User Guide.* OpenFOAM, 2013.

[4] Jonas Lantz. On aortic blood flow simulations. Technical report, Linkping University, 2012.

[5] Wikipedia. Ascending aorta. `http://en.wikipedia.org/wiki/Ascending_aorta`, 2014.

[6] David Elad and Shmuel Einav. *Physical and flow properties of blood.* McGraw-Hill, 2004.

[7] Jones, Noble, Eichmann. What determines blood vessel structure? genetic prespecification vs. hemodynamics. `http://physiologyonline.physiology.org/content/21/6/388`, 2006.

[8] J Renner. Towards subject specific aortic wall shear stress. Technical report, Linkping University, 2011.

[9] P R Hoskins and D Hardman. Three-dimensional imaging and computational modelling for estimation of wall stresses in arteries. *The British Journal of Radiology, 82*, 2009.

[10] Eduardo Soudah, Jorge S. Ronda, Marcelino Rodriguez, Herkel Hervilla, Francesc Carreras and Eugenio O. Using 4d phase-contrast mri to determinate blood flow patterns in the aortic diseases. *2nd International Conference on Mathematical and Computational Biomedical Engineering - CMBE2011*, 2011.

[11] Wikipedia. Openfoam. `http://openfoamwiki.net/index.php/OpenFOAM#cite_note-1`, 2010.

[12] Eugene de Villiers. The potential of large eddy simulation for the modeling of wall bounded flows. Technical report, Imperial College of Science, 2006.

[13] Aleksandar Karac. Drop impact of fluid-filled polyethylene containers. Technical report, Imperial College of Science, 2003.

[14] Jennifer Katy Hutchings. On modelling the mass of arctic sea ice. Technical report, University College London, 2003.

[15] David Paul Hill. The computer simulation of dispersed two-phase flows. Technical report, Imperial College of Science, 1998.

[16] Ruth D Blum. Numerical simulations of aortic blood flow with a bicuspid aortic valve. Technical report, Emory University, 2010.

[17] Umberto Morbiducci. Visualization and quantification of blood flow in the human aorta. from in vivo 4d phase contrast mri to subject-specific computational hemodynamics. Technical report, Politecnico di Torino, 2011.

[18] Jonas Lantz, Johan Renner and Matts Karlsson. Wall shear stress in a subject specific human aorta. influence of fluid-structure interaction. *Internal Journal of Applied Mechanics, (3), 4, 759-778*, 2011.

[19] Eduardo Soudah, E. Y. K. Ng, T. H. Loong, Maurizio Bordone , Uei Pua and Sriram Narayanan. Cfd modelling of abdominal aortic aneurysm on hemodynamic loads using a realistic geometry with ct. *Journal of Computational and Mathematical Methods in Medicine, 472564, DOI:10.1155/2013/472564*, 2013.

[20] Auren F. Stalder, Alex Frydrychowicz, Max F. Russe, Jan G. Korvink, Jrgen Hennig, Kuncheng Li and Michael Markl. Assessment of flow instabilities in the healthy aorta using flow-sensitive mri. *Journal of Magnetic Resonance Imaging*, 2011.

[21] Eduardo Soudah, Riccardo Rossi, Sergio Idelsohn, and Eugenio O. A reduced order model based on coupled 1d/3d finite element simulations for an efficient analysis of hemodynamics problems. *Journal of Computational Mechanics, 54, 1013-1022*, 2014.

[22] Umberto Morbiducci. Visualization and quantification of blood flow in the human aorta. from in vivo 4d phase contrast mri to subject-specific computational hemodynamics. Technical report, Politecnico di Torino.